

**RENEWABLE ENERGY SYSTEMS FOR FORWARD
OPERATING BASES: A SIMULATIONS-BASED
OPTIMIZATION APPROACH**

Presented to
The Department of Electrical and Computer Engineering
Colorado State University

In Partial Fulfillment
of the Requirements for the Degree
Master of Engineering

by
Nathan C. McCaskey, 2d Lt, USAF
August 2010

Distribution A: Approved for Public Release; Distribution Unlimited

Report Documentation Page

Form Approved
OMB No. 0704-0188

Public reporting burden for the collection of information is estimated to average 1 hour per response, including the time for reviewing instructions, searching existing data sources, gathering and maintaining the data needed, and completing and reviewing the collection of information. Send comments regarding this burden estimate or any other aspect of this collection of information, including suggestions for reducing this burden, to Washington Headquarters Services, Directorate for Information Operations and Reports, 1215 Jefferson Davis Highway, Suite 1204, Arlington VA 22202-4302. Respondents should be aware that notwithstanding any other provision of law, no person shall be subject to a penalty for failing to comply with a collection of information if it does not display a currently valid OMB control number.

1. REPORT DATE AUG 2010		2. REPORT TYPE		3. DATES COVERED 00-00-2010 to 00-00-2010	
4. TITLE AND SUBTITLE Renewable Energy Systems for Forward Operating Bases: A Simulations-Based Optimization Approach				5a. CONTRACT NUMBER	
				5b. GRANT NUMBER	
				5c. PROGRAM ELEMENT NUMBER	
6. AUTHOR(S)				5d. PROJECT NUMBER	
				5e. TASK NUMBER	
				5f. WORK UNIT NUMBER	
7. PERFORMING ORGANIZATION NAME(S) AND ADDRESS(ES) Colorado State University, Department of Electrical and Computer Engineering, Fort Collins, CO, 80523				8. PERFORMING ORGANIZATION REPORT NUMBER	
9. SPONSORING/MONITORING AGENCY NAME(S) AND ADDRESS(ES)				10. SPONSOR/MONITOR'S ACRONYM(S)	
				11. SPONSOR/MONITOR'S REPORT NUMBER(S)	
12. DISTRIBUTION/AVAILABILITY STATEMENT Approved for public release; distribution unlimited					
13. SUPPLEMENTARY NOTES					
14. ABSTRACT The purpose of this paper is to quantify the impact of installing renewable energy sources on the fuel consumption, supply-line casualty rate, and operating cost of an Air Force forward operating base (FOB) through the use of computer simulations. This paper also discusses the potential of a leave-behind strategy (i.e. leaving renewable energy systems behind after US departure). Although FOBs are vital to the mission of today's expeditionary Air Force, current costs in terms of supply-line casualties and dollars are very high for sustaining these bases. Several tools are developed in this paper to aid in site-specific planning for installing renewable energy systems at FOBs. These tools are then applied to a hypothetical deployment in Afghanistan to develop a proposed system concept. According to the simulations used, the proposed system can reduce fuel consumption by 17%, supply-line casualties by 15%, and yearly operating costs by \$5.5 million. Finally, a test-bed and training site at Cannon AFB, NM is proposed and presented along with relevant statistics that would help validate the simulations used in this paper					
15. SUBJECT TERMS					
16. SECURITY CLASSIFICATION OF:			17. LIMITATION OF ABSTRACT	18. NUMBER OF PAGES	19a. NAME OF RESPONSIBLE PERSON
a. REPORT unclassified	b. ABSTRACT unclassified	c. THIS PAGE unclassified			

[This Page Intentionally Left Blank]

DISCLAIMER

The views expressed in this academic research paper are those of the author and do not reflect the official policy or position of the US government or the Department of Defense.

[This Page Intentionally Left Blank]

ABSTRACT

The purpose of this paper is to quantify the impact of installing renewable energy sources on the fuel consumption, supply-line casualty rate, and operating cost of an Air Force forward operating base (FOB) through the use of computer simulations. This paper also discusses the potential of a leave-behind strategy (i.e. leaving renewable energy systems behind after US departure). Although FOBs are vital to the mission of today's expeditionary Air Force, current costs in terms of supply-line casualties and dollars are very high for sustaining these bases. Several tools are developed in this paper to aid in site-specific planning for installing renewable energy systems at FOBs. These tools are then applied to a hypothetical deployment in Afghanistan to develop a proposed system concept. According to the simulations used, the proposed system can reduce fuel consumption by 17%, supply-line casualties by 15%, and yearly operating costs by \$5.5 million. Finally, a test-bed and training site at Cannon AFB, NM is proposed and presented along with relevant statistics that would help validate the simulations used in this paper.

[This Page Intentionally Left Blank]

ACKNOWLEDGEMENTS

I would like to thank Dr. Ron Sega for helping me to develop the topic for this paper. His advice and counsel helped provide direction to this study throughout the research, simulation, and writing process. Additionally, Daniel Zimmerle's knowledge of energy systems was crucial in the development of the models used for simulation in this paper. Without his assistance, I could have never completed the analysis presented here.

Several other people provided highly relevant information used in this analysis. I extend my thanks to: Dr. Daryl Hammond, Dr. Kamran Shahroudi, Capt. Timothy Scheffler, Mr. Richard Peck, and Mr. Rod Fisher.

[This Page Intentionally Left Blank]

TABLE OF CONTENTS

Disclaimer	iii
Abstract	v
Acknowledgements	vii
Table of Contents	ix
Table of Figures	xi
Introduction	1
Motivation	1
Literature Review	2
Paper Outline	4
System Concept Development	5
FOB Scenario	5
Simulation Methodology	7
Simulation Results	13
Economic Analysis	14
Casualty Analysis	20
Physical Footprint of Renewables	27
Multi-Objective Optimization Example: Casualties vs. Footprint	28
Proposed System Concept	32
Cannon AFB Test-Bed	39
Conclusions and Recommendations	41
Further Research	43
Appendix A – Resource Profiles	A-1
Appendix B – Load Profile	B-1
Appendix C – Equipment Models	C-1
Appendix D – Economic Model	D-1
Appendix E – Molten Salt Storage Analysis	E-1

[This Page Intentionally Left Blank]

TABLE OF FIGURES

Figure 1 - Example Leave-Behind Cash Flow.....	10
Figure 2 - Example Leave-Behind Cash Flow: Adjusted Capital Cost	10
Figure 3 - Four Year Economic Viability (Medium Shipping Cost)	15
Figure 4 - Four Year Economic Viability (Low Shipping Cost)	16
Figure 5 - Four Year Economic Viability (High Shipping Cost).....	16
Figure 6 - Two Year Economic Viability (Medium Shipping Cost)	17
Figure 7 - Four Year Economic Viability (Medium Shipping Cost) - Repeat.....	18
Figure 8 - Six Year Economic Viability (Medium Shipping Cost)	18
Figure 9 - Eight Year Economic Viability (Medium Shipping Cost).....	19
Figure 10 - Impact of Shipping Cost on Threshold FBCF	20
Figure 11 – Fuel Savings vs. Capacity for PV and Wind Energy (Independent)	21
Figure 12 - Fuel Savings vs. Capacity for PV and Wind Energy (Combined).....	22
Figure 13 – Lead-Acid Storage Fuel Savings	23
Figure 14 - Supply Casualties vs. Capacity for PV and Wind Energy (Independent).....	25
Figure 15 - Supply Casualties vs. Capacity for PV and Wind Energy (Combined).....	26
Figure 16 - Lead-Acid Storage Casualty Reduction	27
Figure 17 - Pareto Front for Casualties vs. Footprint (HOMER Simulations)	29
Figure 18 - Pareto Front for Casualties vs. Footprint (Linear Program)	31
Figure 19 - Generator 4 Load (Baseline System: Top; Renewable System: Bottom)	34
Figure 20 - Generator 5 Load (Baseline System: Top; Renewable System: Bottom)	35
Figure 21 - Generator 6 Load (Baseline System: Top; Renewable System: Bottom)	35
Figure 22 - Generator 7 Load (Baseline System: Top; Renewable System: Bottom)	36
Figure 23 - Cash Flow Diagram for Generator Only System (Four Year Timeframe)	38
Figure 24 - Cash Flow Diagram for Renewable System (Four Year Timeframe).....	38

[This Page Intentionally Left Blank]

INTRODUCTION

MOTIVATION

Today's US Air Force is organized as an expeditionary force. Airmen are prepared to deploy to any location around the globe in support of contingency operations at a moment's notice. Key to this expeditionary strategy is the forward operating base (FOB): a rapidly-established base in a forward location "capable of independently supporting and launching sustained combat operations with the same independence as fixed theater installations."¹ Although the use of FOBs is crucial to the projection of military power throughout the world, this strategy poses many logistical challenges, such as supplying materiel, water, and fuel.

In particular, supplying these bases with fuel needed to generate electrical power imposes "high costs in blood, treasure, and combat effectiveness."² Providing fuel to FOBs involves placing American troops at great risk while traveling along dangerous supply routes. For fiscal year (FY) 2007, one American soldier or contractor was wounded or killed, on average, for every 24 fuel supply convoys dispatched in Afghanistan.³ Reducing the fuel needed to provide electrical power in remote locations would result in the reduction of casualties incurred along the supply line.

The need to reduce fuel consumption at FOBs is not a new topic. In his journal article on energy challenges facing the Department of Defense (DoD), Amory Lovins highlights several benefits of reducing fuel consumption at FOBs. First and foremost, reducing the amount of fuel

¹"Basic Expeditionary Airfield Resources (BEAR)." *GlobalSecurity.org*. Web. 28 July 2010. <<http://www.globalsecurity.org/military/systems/aircraft/systems/bear.htm>>.

² Lovins, Amory B. "DOD's Energy Challenge as Strategic Opportunity." *Joint Forces Quarterly* 57 (2010): 33-42. National Defense University Press. Web. 28 July 2010.

³ *Sustain the Mission Project: Casualty Factors for Fuel and Water Resupply Convoys*. Tech. Arlington: Army Environmental Policy Institute, 2009, 6.

needed for electrification of FOBs can reduce cost in both dollars and casualties. Lovins notes that “fueling one FOB’s gensets might cost \$34 million per year – plus, at the FY07 casualty rate, nearly one casualty.”⁴ In addition, he asserts that reducing fuel consumption can improve combat effectiveness: “A lean or zero fuel logistics tail... increases mobility, maneuver, tactical and operational flexibility, versatility, and reliability.”⁵ The need to reduce fuel consumption has also attracted the attention of the Chief of Staff of the Air Force (CSAF). In his “CSAF’s Vector” published on 4 Jul 2010, General Norton Schwartz states the need to “substantially reduce fuel consumption through improved operational planning, alternative training concepts, and installation modernization and management.”⁶

LITERATURE REVIEW

Several authors have keyed in on a potential solution to the logistical challenge of transporting fuel to FOBs: renewable energy sources (“renewables”) such as photovoltaic (PV) arrays and wind turbines. In his paper on the use of renewable energy sources for contingency operations, Col. Gordon D. Kuntz (Army National Guard) outlines some advantages of these systems: “reducing the logistic footprint by decreasing the fuel requirement by as much as 20-30%, augmentation of power by up to 30%, a decrease in maintenance needs, and overall reduction in cost.”⁷ In addition, Kuntz states, “force protection and physical security are greatly improved by limiting soldier exposure to attack through significantly decreasing the number of convoys with less demand for fossil fuel.”⁸ His primary conclusion is that the Army (or more

⁴ Ibid, 37.

⁵ Ibid.

⁶ <<http://www.af.mil/information/viewpoints/csaf.asp?id=603>>

⁷ Kuntz, Gordon D. *Use of Renewable Energy in Contingency Operations*. Rep. Army Environmental Policy Institute, Apr. 2007. Web. 28 July 2010. <<http://www.aepi.army.mil/publications/sustainability/docs/use-of-renew-en-conting-ops.pdf>>.

⁸ Ibid, 15.

broadly the DoD) should place an emphasis on adopting renewable energy systems for contingency operations.

Whereas Kuntz focuses on the renewable energy policy within the Army, Maj. Randy L. Boswell (USAF) focuses on the fuel and cost savings of installing renewable energy systems at FOBs.⁹ In his paper, Boswell calculates the peak electrical load for a generic Air Force FOB of approximately 1,100 personnel. After identifying several criteria required for equipment used in the field, Boswell concludes that a fuel savings of 14% can be achieved by supplying airfield and base lighting, billeting, latrines, and chapels with dedicated renewable energy instead of power from the base electrical grid.¹⁰ In addition, he advocates the use of “a power generation station composed of solar arrays, small wind turbines, and... diesel engine-driven generators.”¹¹

Although Kuntz and Boswell provide a solid foundation for further research into the area of renewable energy sources for FOBs, both use relatively simple assumptions from which to draw their conclusions. Kuntz primarily uses efficiency values of various renewable energy sources to advocate their use.¹² Boswell develops a more sophisticated electrical model of a FOB by calculating the peak electrical demand at a typical Air Force forward installation.¹³ Neither has conducted analysis using time-varying electrical load at a specific bed-down location, which is crucial to understanding the costs and benefits associated with installing renewable energy sources in the field.

In addition, Kuntz and Boswell do not address the potential benefits of a leave-behind solution. Installing PV arrays and/or wind turbines at a forward location can have lasting benefits

⁹ Boswell, Randy L. *The Impact of Renewable Energy Sources on Forward Operating Bases*. Rep. Maxwell AFB: Air Command and Staff College, 2007. Print.

¹⁰ Boswell, 25.

¹¹ *Ibid*, 10.

¹² Kuntz, 14.

¹³ Boswell, 28-29.

for the local population in addition to the direct American benefit. One needs look no further than the current contingency operations in Iraq and Afghanistan for an example. After direct US involvement in each country ceases, a potential leave-behind renewable energy system that could provide limited electrification for use by police or service agencies would be highly beneficial to local development. Since restoring peace to each nation is obviously an objective of the DoD, leave-behind systems would hold real value for both the local government and the United States.

PAPER OUTLINE

The aim of this paper is to expand upon the research of Kuntz and Boswell in the area of renewable energy sources for FOBs. If one were to imagine this area of research as a systems development process (as described by Kossiakoff and Sweet¹⁴), one might consider Kuntz's work as satisfying the needs analysis phase and Boswell's work as satisfying the concept exploration phase. The goal of this paper, then, is to enter the concept definition phase. Specifically, this paper will address the following questions:

- What is the impact on casualty rate of installing renewables?
- What is the tradeoff between improved casualty rate and increased FOB footprint?
- What is the economic viability of the leave-behind strategy?
- What other analysis needs to be completed prior to implementation?

This paper will begin with a discussion of a hypothetical FOB situated in Marjah, Afghanistan. For this scenario, several computer simulations will be run based on an estimated, time-varying electrical load profile of the base. Based on the results of these simulations, the above questions will be addressed with regard to this scenario. The outputs of this analysis will

¹⁴ Kossiakoff, Alexander, and William N. Sweet. *Systems Engineering Principles and Practice*. Hoboken, NJ: Wiley-Interscience, 2003. Print.

be a proposed system concept for this hypothetical FOB and, more importantly, a method for analyzing the benefits of incorporating renewables at any potential FOB location.

The next section of this paper will focus on the potential construction of the system concept at Cannon AFB, New Mexico, for training and analysis purposes. The merits of the system concept, such as fuel savings, capital costs, and operating costs, will be presented in detail. In this way, should the system concept be constructed at Cannon AFB, the physical system can be used to validate the results of the computer simulations used for this analysis.

The final section of this paper will detail the implications for the Air Force, and more broadly the DoD, as a whole. Conclusions and recommendations will be presented to help guide decision making within the DoD regarding the application of renewables at FOBs.

SYSTEM CONCEPT DEVELOPMENT

FOB SCENARIO

The FOB scenario presented here describes a hypothetical base at a forward location established using Basic Expeditionary Airfield Resources (BEAR) mobile assets. This base is sized for one squadron of Air Force personnel, which consists of approximately 1,100 airmen; this represents a typical Air Force deployment at a forward location. To support the construction of this FOB, four modular deployment packages would be used: one 550 Initial Housekeeping Set, one 550 Follow-on Housekeeping Set, one Industrial Operations Set, and one Initial Flightline Set.¹⁵ The electrical distribution system for this base would consist of six to eight MEP-12A 750kW generators tied to a primary distribution system at 4.16 kV line-to-line.¹⁶ Although these generators would be placed at two physically separate power plants, they would

¹⁵ *AFH 10-222 Volume 1*, Table 1.1.

¹⁶ *AFH 10-222 Volume 5*, 13.

be paralleled together on a single primary distribution system.¹⁷ Transformers are then used to operate a secondary distribution system at 120/208 V which supplies the electrical load at the base.¹⁸ Additional smaller generators would be used for back-up power. Since these generators would only operate for a short time in an emergency situation, they are not included in the electrical model of the base for the purposes of this paper.

To aid in estimating the solar and wind resources available to PV arrays and wind turbines for this hypothetical base, a specific, typical FOB location was chosen. Marjah, Afghanistan was chosen as the site for this base for several reasons: it represents an area in which the DoD is already active; its solar and wind resources are representative of many similar locations in Afghanistan and Iraq; and it is an area that typifies the logistical challenges associated with supplying fuel for electrical generation. Marjah, situated in the North-central portion of Helmand province, has an average solar radiation of 5.74 kWh/m²/day and an average wind speed of 4.56 m/s at a height of 50m. This places Marjah in a slightly above-average location in terms of solar radiation compared with the remainder of Afghanistan; however, Marjah is in a region of relatively poor wind resource, which is typical of most of Afghanistan with the exception of the extreme southwest portion of the nation. For detailed information on the solar and wind resource values used for this analysis, see Appendix A.

In addition to aiding in estimates for solar and wind resources, selecting a specific location for this base allowed for a more detailed estimate of the electrical demand. The total electrical load of the base consists of two components: operational load and heating, ventilation, and air conditioning (HVAC) load. The operational load for this base is estimated as an average load of 1.61 MW that fluctuates around meal times due to increased cooking load. The HVAC

¹⁷ Ibid, 41. Referred to as a “looped distribution system,” shown in Figure 3.8.

¹⁸ Ibid, 17.

load, however, varies with ambient temperature. For Marjah, HVAC load is estimated to range from 0.9 to 3.3 MW; therefore, total load is 2.4 to 4.9 MW. The ratio of peak HVAC load to total peak load for this estimate, approximately 67%, is similar to Boswell's estimate for HVAC load: 59% of the total peak load.¹⁹ For detailed information on the load estimate used for this analysis, see Appendix B. It is important to note that these load values are still estimates. No data from an actual FOB exists with which to verify this estimate. Future study in this area would benefit greatly from actual time-series measurements of demand at a FOB.

SIMULATION METHODOLOGY

The analysis presented in this paper relies on computer simulations to calculate the cost and benefit of installing renewables at the hypothetical FOB described above. These simulations were run in a software package called HOMER. This program performs quasi-static hybrid power system simulations on an hour-by-hour basis over a project lifetime of a year or more. It simulates many different system configurations and calculates net present cost (NPC) for each alternative. The software also outputs all relevant non-monetary metrics for each alternative, for example fuel consumed, power generated by renewables, renewable penetration, and generator runtime. HOMER provides plotting tools for optimization based on system configuration and can show the sensitivity of the optimization results to changes in variables specified by the user (for example, fuel price or project lifetime). It is important to note that HOMER's simulation capabilities are advanced in that it can simulate energy scenarios for every hour of an 8,760 hour year, but limited in that it cannot model or simulate transient issues that have a timescale on the order of seconds. Because of this, HOMER is best used for analysis of different design alternatives and economic optimization.

¹⁹ Boswell, 6. Difference likely associated with very high summer temperatures in Marjah – up to 115°F.

Before using HOMER, however, a baseline simulation was developed in Matlab to clarify the generator dispatch algorithm utilized by HOMER. This very basic Matlab simulation modeled the base electrical system as it might be operated without any renewables installed. The model consisted of seven MEP-12A generators in parallel supplying power to the load described above and in Appendix B. For each week, the number of generators needed to supply power was determined based on the weekly peak load. This simulates an experienced operator who starts or stops generators as needed based on his prediction of the upcoming week. The load is then split evenly amongst the seven generators throughout the week. Fuel consumption is calculated from the fuel curve in Figure C – 1 in Appendix C. A similar scenario was also modeled in HOMER; the only difference was the generator dispatch strategy, which HOMER optimizes using its own dispatch scheme.

The results of this baseline simulation showed that the base consumed 1.92 million gallons of fuel per year based on the Matlab model and 1.93 million gallons per year based on the HOMER model. The HOMER model agreed very closely with the Matlab model, which indicates that the fuel consumption rates described by the generator-only HOMER model could likely be achieved by an experienced operator at a current-day FOB. For the remainder of this paper, all references to “baseline” or “generator-only” simulations will refer to the generator-only HOMER simulation described here.

Additionally, at a fully-burdened cost of fuel (FBCF) value of \$17.44/gal, these two models show a yearly cost of \$33.5 million and \$33.7 million, respectively; both agree closely with Lovins’ estimate of \$34 million per year for a typical Afghanistan FOB at this FBCF value. With the HOMER model in agreement with the basic Matlab model and Lovins’ calculations,

analysis could proceed by allowing HOMER to calculate results for many renewable energy scenarios.

Two sets of simulations were completed for the Marjah base. The first set of simulations, called “Marjah Leave-Behind” simulations, was designed to economically optimize the renewable system configuration based on costs associated with US involvement as well as the leave-behind timeframe. To do this, a monetary metric had to be established within the model to assess the benefit of leaving behind renewable energy after the departure of US troops. The monetary metric chosen was called “value of leave behind energy” in cents per kilowatt-hour. This metric represents how much value the DoD should place on the energy it leaves behind for the local government (Note that this metric may differ from the actual price of energy at the location. The intent is to quantify the combination of the traditional energy costs plus the additional value accrued by encouraging economic development.).

The following methodology was utilized to include the value of leave behind energy in the HOMER simulations. First, HOMER was used to calculate the *energy* in kWh left behind by the renewables for a particular configuration – a site-specific function of available resource and installed equipment. Then, this number was multiplied by the value of leave behind energy ($\text{\$/kWh}$) to find the total value of the leave behind solution (in dollars). Finally, the total value of the leave behind solution, discounted back to the present using an interest rate of 10%, was subtracted from the NPC for that particular alternative (simulated only over the timeframe of US involvement). The result adjusts the initial capital cost of the renewable installation to include the value of leave behind energy. Figures 1 and 2 below illustrate this concept for a hypothetical system with capital cost of \$6 million, operating cost of \$25 million/yr, and total value of leave behind energy of \$500,000/yr. In Figure 1, the capital cost is represented as a \$6 million cost in

year 0 and the total value of leave behind energy is represented as a \$500,000 yearly revenue from year 5 to year 20.

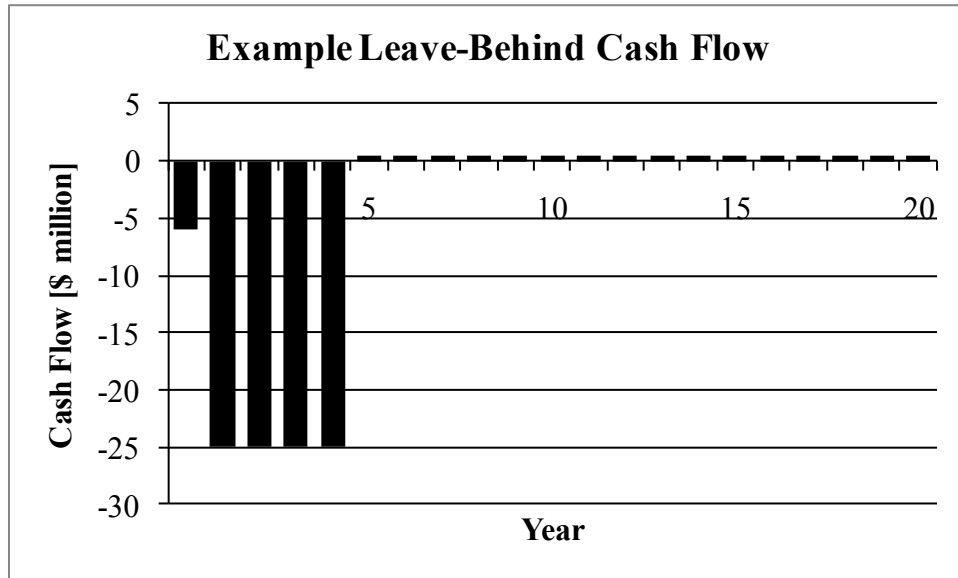


FIGURE 1 - EXAMPLE LEAVE-BEHIND CASH FLOW

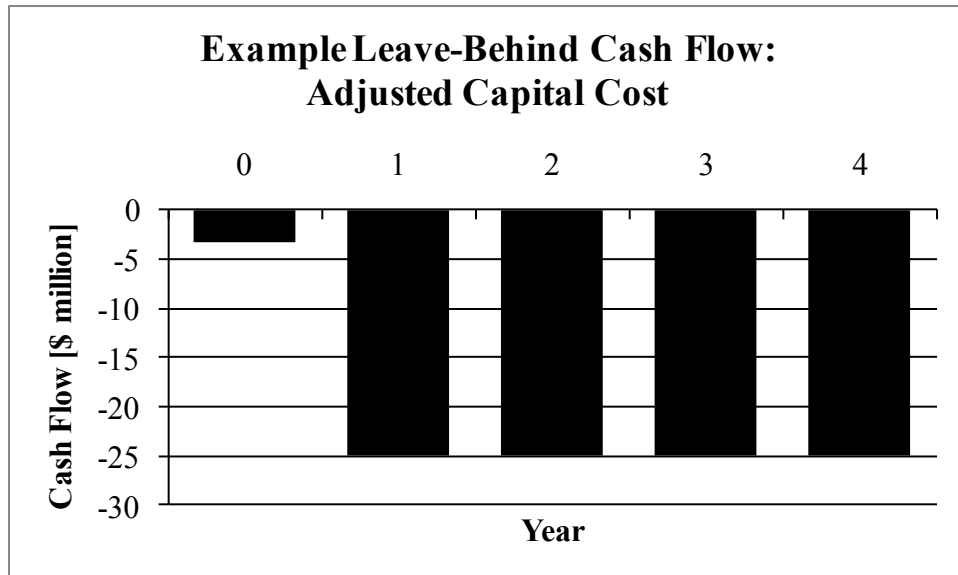


FIGURE 2 - EXAMPLE LEAVE-BEHIND CASH FLOW: ADJUSTED CAPITAL COST

Figure 2 shows the capital cost adjusted to include the total value of leave behind energy. The capital cost is now approximately \$3.3 million and the simulation timeframe is now only four years as the total value of leave behind energy is now accounted for in the adjusted capital

cost (discounted at a rate of 10%). For more information on this economic model, see Appendix D.

The second set of simulations, called “Marjah Actual Cost” simulations, considered only costs and benefits during the US operation of the FOB. These simulations were designed to determine the actual capital, operating, and net present costs associated with installing renewables at the Marjah FOB. In other words, these simulations reflect the true costs that the DoD would expect to pay for each alternative. As such, these simulations were run only over the timeframe of US involvement with no adjustment to the NPC based on the leave behind term. These simulations were also used to compute fuel consumption values for casualty analysis.

For each set of simulations, HOMER simulated alternatives from a predetermined set of equipment. This equipment set included eight MEP-12A 750 kW generators, with one assumed down for maintenance at all times; a range of 0 to 2000 kW of fixed PV panels in increments of 500 kW; 0, 10, or 20 wind turbines (100 kW each); 0, 4, or 8 strings of lead-acid batteries (2.16 kWh each) with 80 batteries per string (0, 320, or 640 batteries).²⁰ See Appendix C for more details on the equipment modeled.

A maximum of 2 MW total capacity for both PV arrays and wind turbines was used to keep the instantaneous renewable penetration at a reasonable level (e.g. a 4 MW PV array serving a 3 MW load could cause severe transient issues in the power distribution system should cloud cover develop rapidly). Renewable generation never exceeds load for any equipment combination with the exception of the maximum renewables case (2 MW PV array and 20 wind turbines); for this case, renewable generation exceeds load for one hour each year. Timeframes

²⁰ A hypothetical molten salt storage system was also considered for a portion of this analysis, but will not be discussed in the body of this paper. See Appendix E for details.

for US involvement were set at two, four, six, and eight years with leave-behind timeframes of eighteen, sixteen, fourteen, and twelve years, respectively (i.e. a total lifespan of twenty years).

Degradation of the leave-behind systems was not modeled; it is assumed that the local administration will be capable of effective operation and maintenance of the system after US departure. However, from previous experience in troubled areas – where most expeditionary deployments occur – this may be an optimistic assumption, and is a subject for additional study.

Estimates of capital and maintenance costs were developed for each type of equipment listed above. First, domestic estimates were established for the equipment used. Each MEP-12A generator was estimated at \$240,000 with maintenance costs of \$2.4/hr; PV arrays were estimated at \$5.70/W rated capacity with maintenance costs of \$12/kW-yr; wind turbines were estimated at approximately \$1800/kW with maintenance costs of 1.5¢/kWh; and lead-acid batteries were estimated at \$500/kWh.

Costs were increased by 20% to account for installation and maintenance in a remote environment. Additionally, capital costs were increased based upon an estimated shipping weight from the US to Marjah, Afghanistan. Shipping costs of \$1.00/lb, \$1.50/lb, and \$2.00/lb were used for purposes of comparison. For example, \$570/kW, \$855/kW, and \$1140/kW shipping costs were used for wind turbines and \$400/kW, \$600/kW, and \$800/kW were used for PV arrays (including inverters). Finally, fuel prices for these simulations, meant to reflect the fully-burdened cost of fuel, range from \$0/gal to \$24/gal in increments of \$4/gal with an additional value of \$17.44/gal to match Lovins' assumption. For more information on the economic model used and how it was derived, see Appendix D.

Casualty analysis was conducted outside of HOMER based on FY07 casualty rates in Afghanistan from *Sustain the Mission Project*. The casualty model included the expected supply-

line casualties incurred by shipping renewable energy equipment to the FOB as well as casualties resulting from fuel transportation. For this analysis, an average 16 truck fuel supply convoy capacity of 97,818 gallons was used.²¹ Additionally, an average materiel convoy (on which renewable equipment would be shipped) was estimated to carry 350,000 lbs. This estimate was based on the assumption that approximately 50% and 30% of the total volume shipped to FOBs was fuel and materiel, respectively.²² It was also assumed that shipping weight and volume are approximately synonymous (i.e. 50% and 30% of the total *weight* shipped to FOBs was fuel and materiel, respectively).

SIMULATION RESULTS

This section discusses the simulation results. The results presented here will focus on three primary metrics for evaluating each candidate system: the net present cost of the system, change in casualties associated with installing the system, and change in FOB land area (footprint) required for the renewables. The NPC of each solution will be quantified using the Marjah Leave-Behind simulations, which include US-operated cost as well as the value of leave behind energy. Then, the Marjah Actual Cost simulations, along with additional casualty analysis external to HOMER, will be used to explore the change in supply-line casualties that result from installing renewables. Next, estimates of land area needed to install PV arrays and wind turbines will be explored to help understand the impact on a typical FOB's defended perimeter. Finally, a multi-objective optimization technique called Pareto front analysis will be proposed as a potential method for defining the trade space between supply casualties reduced and the change in the defended perimeter of the FOB.

²¹ *Sustain the Mission Project*, 5.

²² *Ibid*, 3.

ECONOMIC ANALYSIS

This section addresses the installation of renewable energy systems at FOBs from an economic perspective. The results presented in this section are not meant to identify a specific solution; instead, they are meant to articulate the sensitivity of the solution to the VLBE, FBCF, shipping cost, and timeframe of US involvement. The following plots will show the economically optimal system type as a function of VLBE and FBCF. A series of plots will be used to show additional sensitivities to shipping cost and timeframe of US involvement.

Figure 3 shows a plot of the optimal system type for the Marjah FOB versus VLBE and FBCF (note that “Diesel Price” here is meant to represent FBCF). For this “typical” case of a four year US involvement with a medium shipping cost of \$1.50/lb, lead-acid batteries are monetarily beneficial (i.e. reduce NPC) above FBCF values of ~\$2.5/gal, regardless of VLBE. PV arrays and wind turbines are monetarily beneficial starting at fuel prices of ~\$16/gal, neglecting the VLBE. A “monetary threshold” for each technology can be defined by varying both VLBE and FBCF (shown in the figure as the transition from one color region to another). Below this threshold (toward the bottom left of the plot), the technology is not economically beneficial to install; above this threshold, the technology is economical. For both wind energy and solar energy, the threshold fuel price decreases as the VLBE increases: about \$10/gal at a VLBE of 25¢/kWh and about \$4/gal at a VLBE of 50¢/kWh.

Also note that the threshold for wind turbines occurs at slightly lower fuel prices than for PV arrays (by ~\$0.50/gal), even though Marjah is situated in an area with a better solar resource than wind resource. This is attributable to the large capital cost difference for the two technologies (approximately 2.6:1).

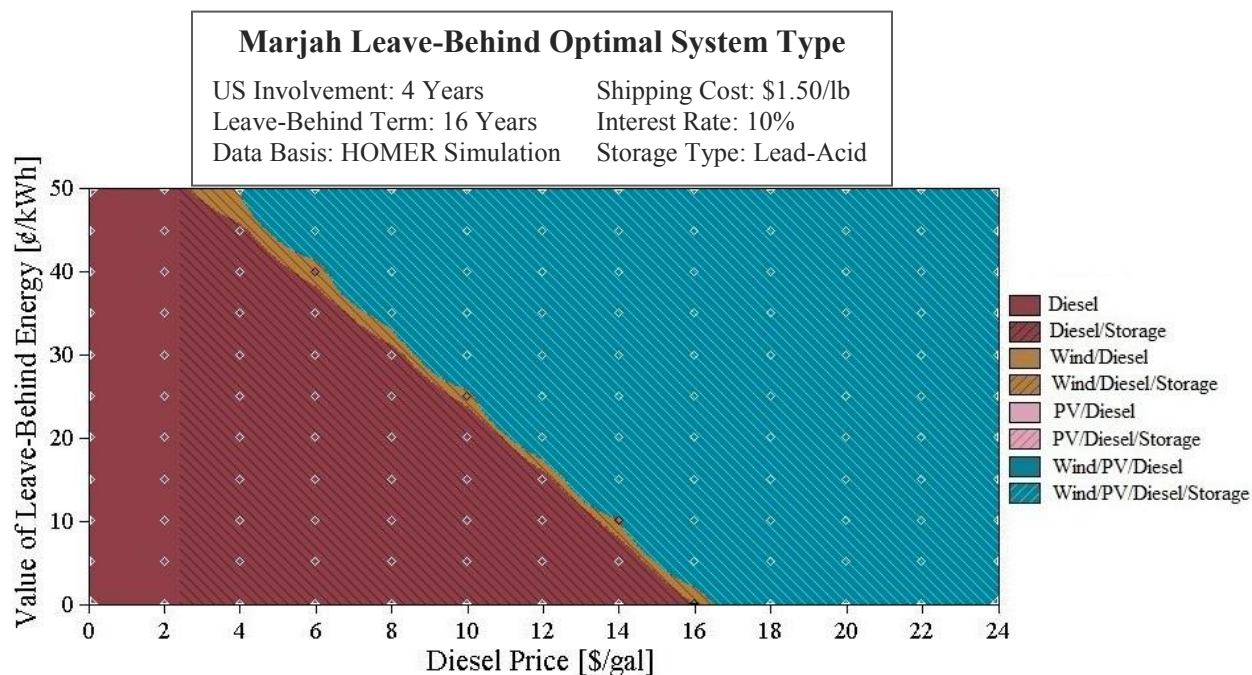


FIGURE 3 - FOUR YEAR ECONOMIC VIABILITY (MEDIUM SHIPPING COST)

Additionally, it is important to understand the amount of renewable equipment that is monetarily beneficial. For both wind turbines and PV arrays, the optimal capacity (for lowest NPC) increases abruptly across the threshold. For the assumptions used in this paper, the lowest NPC results from either no wind turbines or 20 wind turbines, depending on the FBCF and VLBE. Likewise, the lowest NPC results from either no PV array or a 2 MW PV array.

The next two optimal system type plots (Figures 4 and 5) illustrate the difference in NPC introduced by varying the shipping cost for each component. With shipping costs at \$1.00/lb, the threshold shifts to the left, indicating that renewables reduce NPC at lower fuel prices. For example, wind energy is now monetarily beneficial at about \$8/gal at a VLBE of 25¢/kWh (versus \$10/gal at the same VLBE for a shipping cost of \$1.50/lb). For higher shipping costs (\$2.00/lb), solar energy becomes economical at a slightly lower fuel price than wind energy; however, both types require higher fuel prices to be monetarily beneficial when compared with the original \$1.50/lb shipping cost.

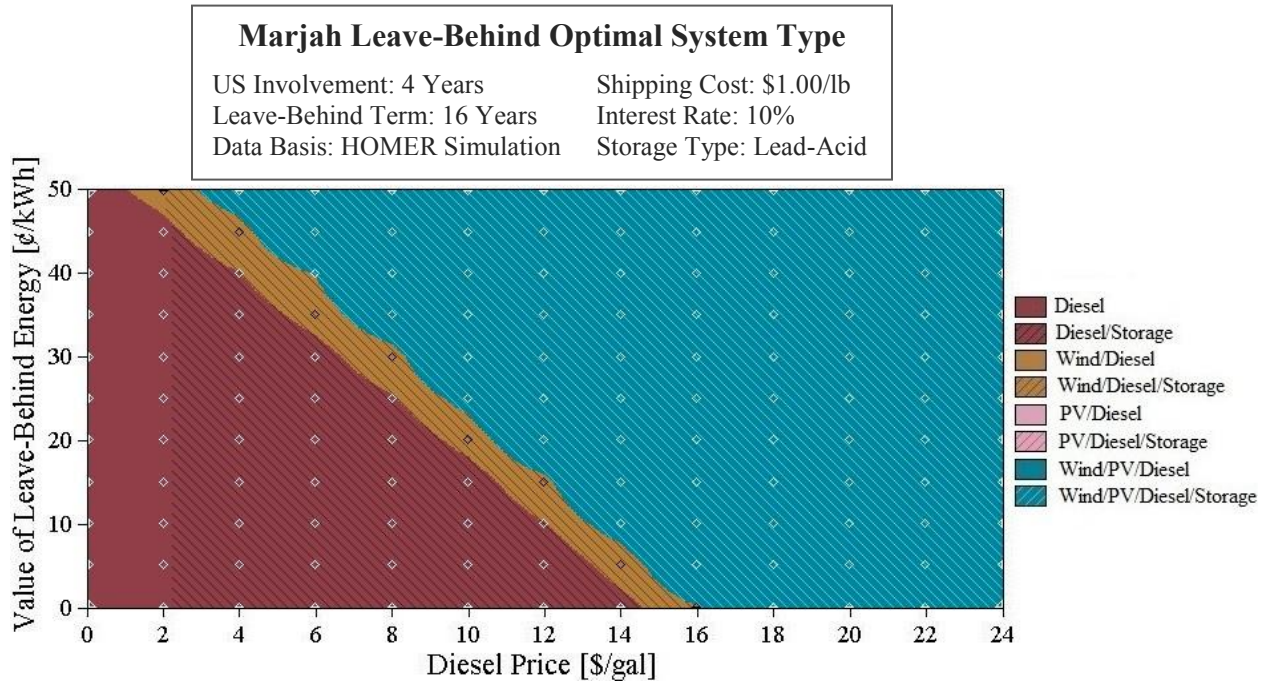


FIGURE 4 - FOUR YEAR ECONOMIC VIABILITY (LOW SHIPPING COST)

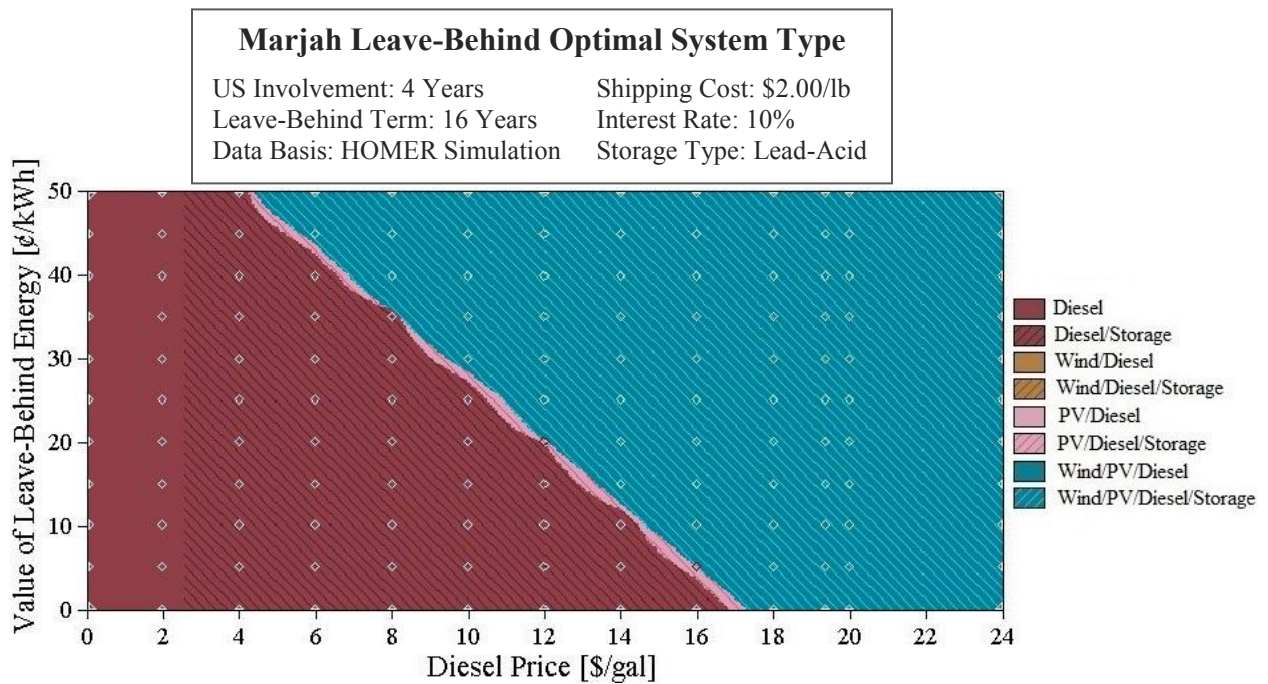


FIGURE 5 - FOUR YEAR ECONOMIC VIABILITY (HIGH SHIPPING COST)

The previous plots illustrated how the threshold for each technology varied with shipping cost; the next set of plots will illustrate how these thresholds vary with the timeframe of US

involvement. Figures 6 – 9 show the optimal system type for various values of FBCF and VLBE for the two, four, six, and eight year timeframes of US involvement with a fixed shipping cost of \$1.50/lb. The total timeframe (US involvement plus leave behind) is 20 years in each case. Note that Figure 7 is a repeat of Figure 3, shown for clarity. For the shorter timeframes (two and four years), the thresholds vary significantly with the VLBE. This is due to the fact that the longer leave-behind timeframe for these scenarios (18 and 16 years, respectively) allows for a more significant amount of total leave-behind energy. One important result shown on these plots is that even at a VLBE of only 25¢/kWh (compared to an approximate US operating cost of \$1.19/kWh²³), renewable energy systems still pay for themselves in less than two years at a FBCF of \$17.44/gal.

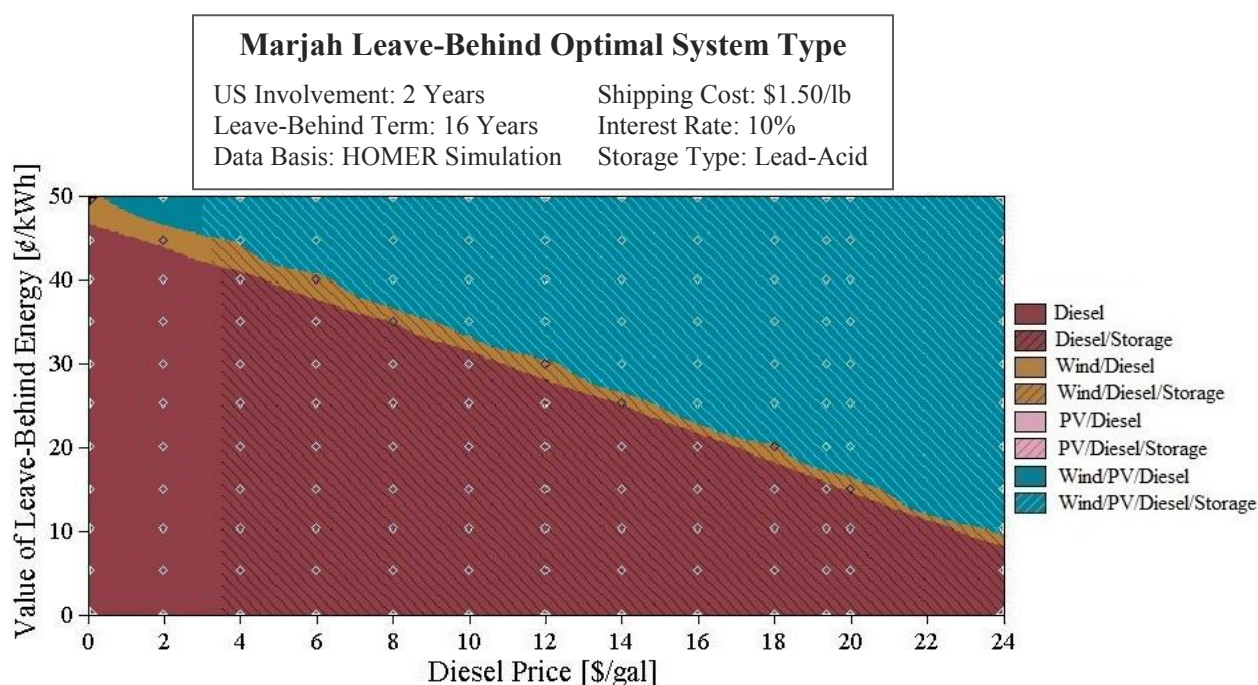


FIGURE 6 - TWO YEAR ECONOMIC VIABILITY (MEDIUM SHIPPING COST)

²³ Based on a current-day base with seven MEP-12A generators, FBCF of \$17.44/gal, fuel consumption of 1.93 million gallons per year, and an average load of 77.69 MWh/day.

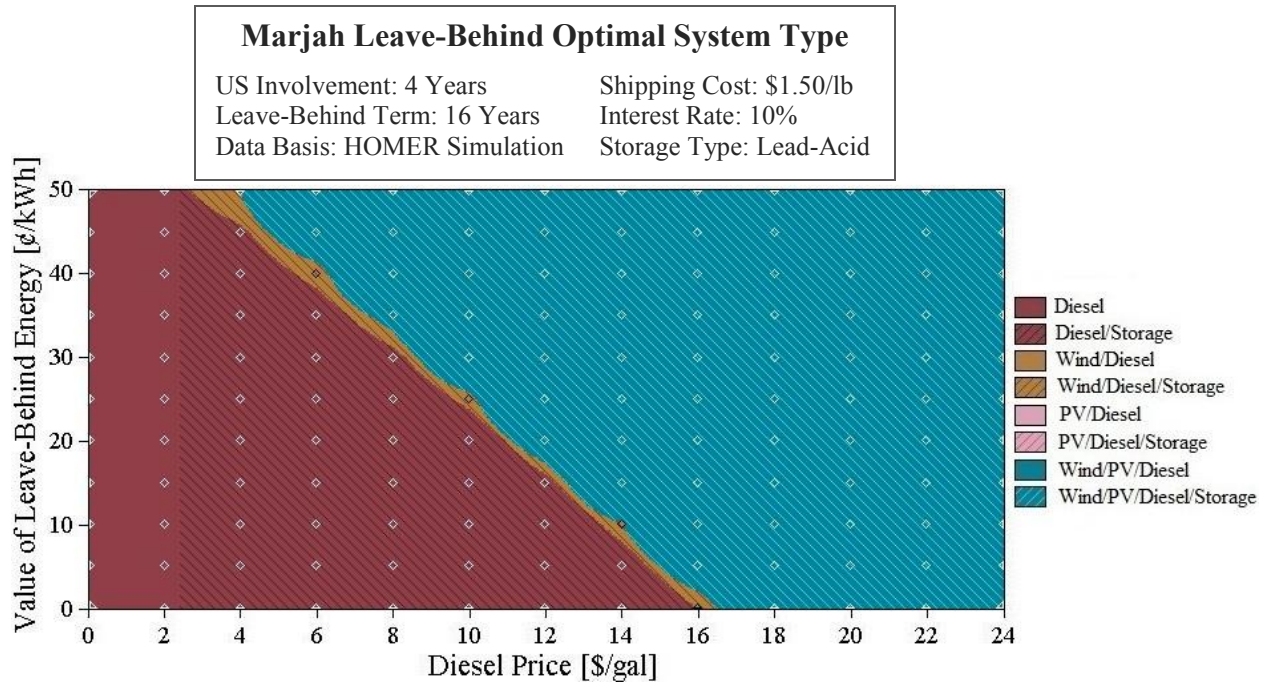


FIGURE 7 - FOUR YEAR ECONOMIC VIABILITY (MEDIUM SHIPPING COST) - REPEAT

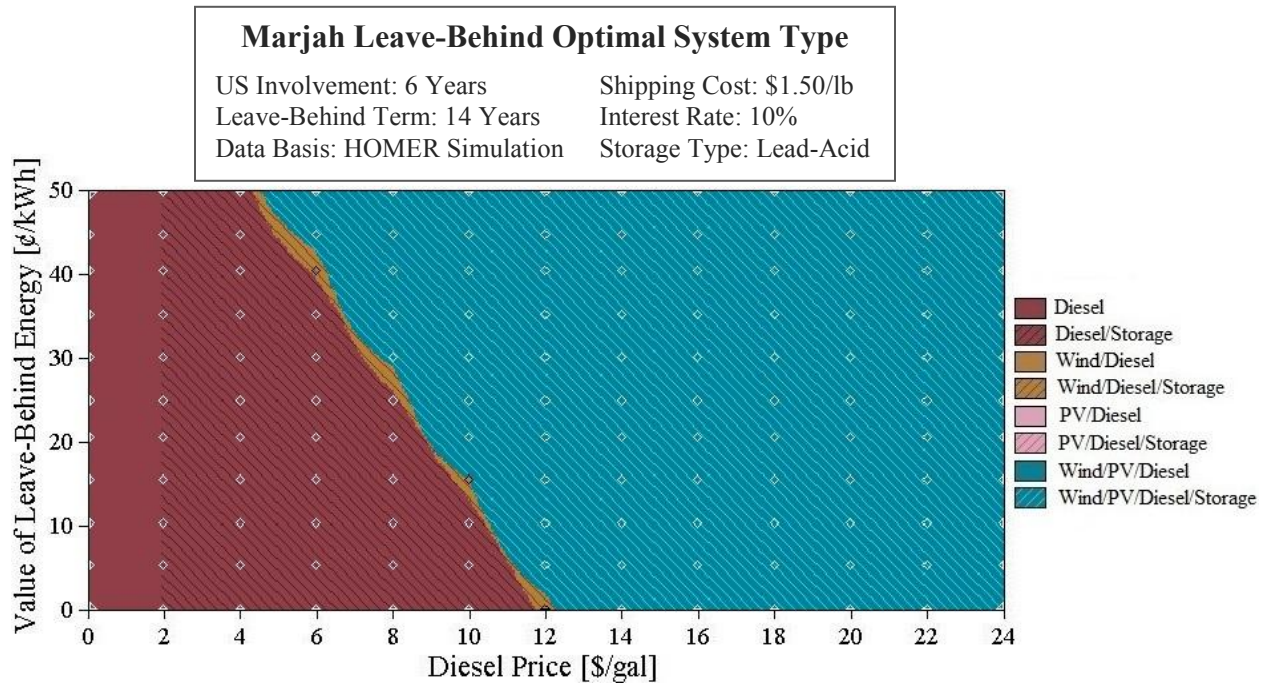


FIGURE 8 - SIX YEAR ECONOMIC VIABILITY (MEDIUM SHIPPING COST)

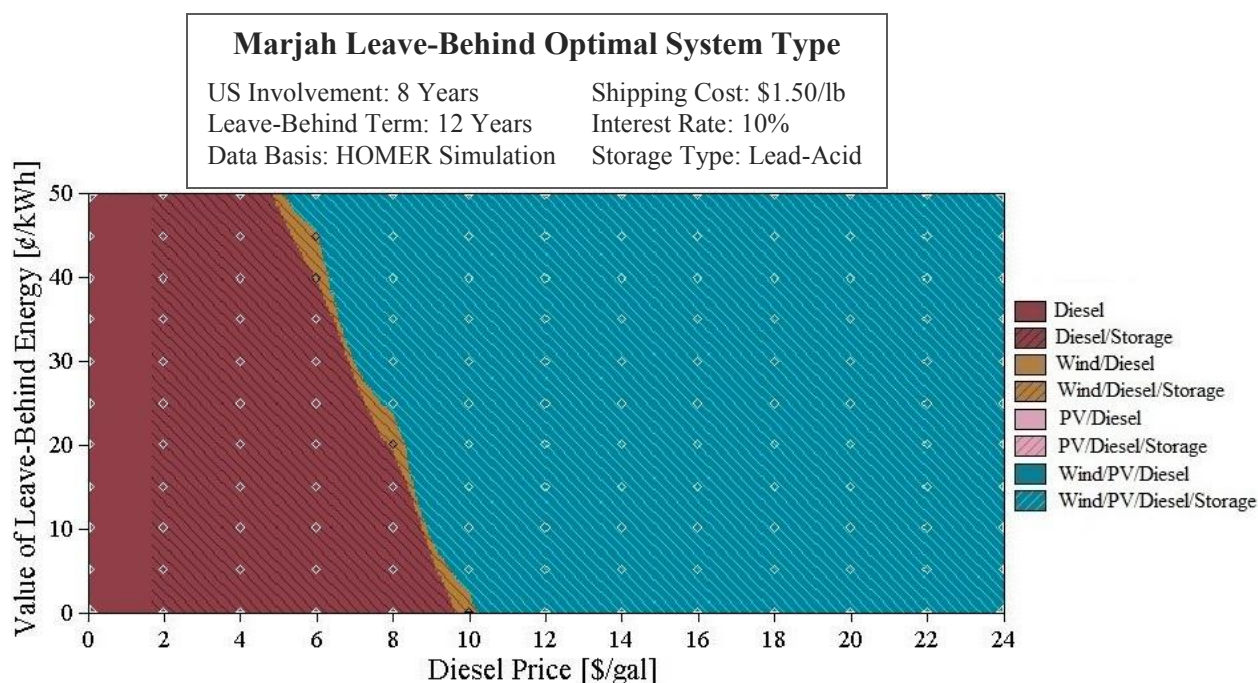


FIGURE 9 - EIGHT YEAR ECONOMIC VIABILITY (MEDIUM SHIPPING COST)

In summary, the sensitivity analysis presented in this section highlights two relationships: the impact of different timeframes on the economic thresholds for wind and solar energy and the impact of shipping cost on which technology is more favorable in terms of NPC. The timeframe of US involvement has a substantial impact on the thresholds for both technologies. For the eight year timeframe, the threshold FBCF varies little with VLBE; however, for the two year timeframe, the threshold varies dramatically. This indicates that the expected term of US involvement is an important consideration when determining the appropriate mix of diesel generation and renewables.

The second relationship highlighted by this analysis is the impact of shipping cost on which technology becomes monetarily beneficial at a lower FBCF. For shipping costs of \$1.00/lb and \$1.50/lb, wind turbines have a lower threshold FBCF (gold section in Figures 3 and 4). However, at a shipping cost of \$2.00/lb, the PV array has a lower threshold (pink section in Figure 5). This is primarily due to the difference in shipping weight versus capacity for each technology (~400 lb/kW for PV; ~570 lb/kW for wind turbines). Figure 10 shows the threshold

FBCF values for each technology as a function of shipping cost at a fixed VLBE of 25 ¢/kWh (for the four year scenario).

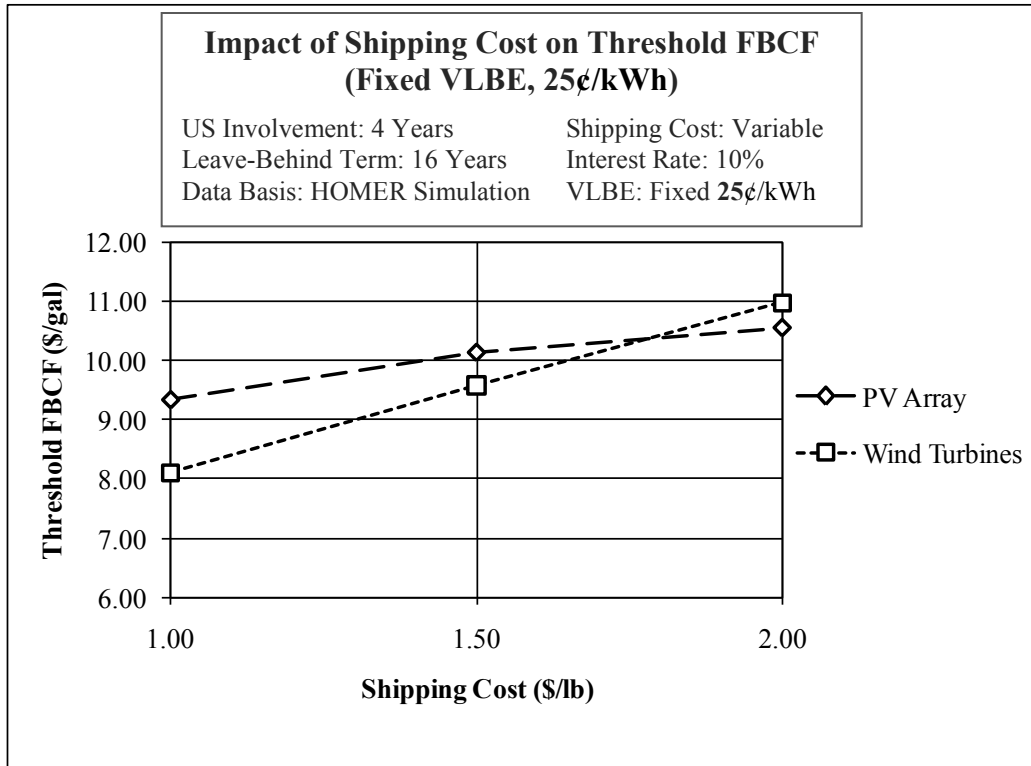


FIGURE 10 - IMPACT OF SHIPPING COST ON THRESHOLD FBCF

This figure shows that the optimal mix of renewables is sensitive to shipping cost. For shipping costs below ~\$1.80/lb, the NPC-based threshold is lower for wind turbines; however, above this shipping cost, the PV array has a lower threshold FBCF value.

CASUALTY ANALYSIS

Although economic analysis such as net present cost is important to consider in the design of a renewable energy system for FOBs, what is of more importance is reducing the resupply casualty rate by reducing fuel consumption at these bases. The analysis in this section will begin with the fuel savings associated with installing PV arrays, wind turbines, and energy storage systems (from the Marjah Actual Cost simulations). Then, these fuel savings values will be related directly to the change in the number of supply-line casualties. This analysis will

include the expected supply-line casualties incurred by shipping renewable system components to the FOB.

Figure 11 shows the fuel saved (in percent) for various installations of both PV arrays and wind turbines. For this analysis, four strings of lead-acid batteries (320 batteries total) were used. Note that the batteries alone account for a 1.4% reduction in fuel consumption, which explains why the intercept of each plot is not 0%. For this range of capacity values, fuel savings is almost perfectly linear with slopes of 6.7% per MW and 3.0% per MW for solar and wind energy, respectively.

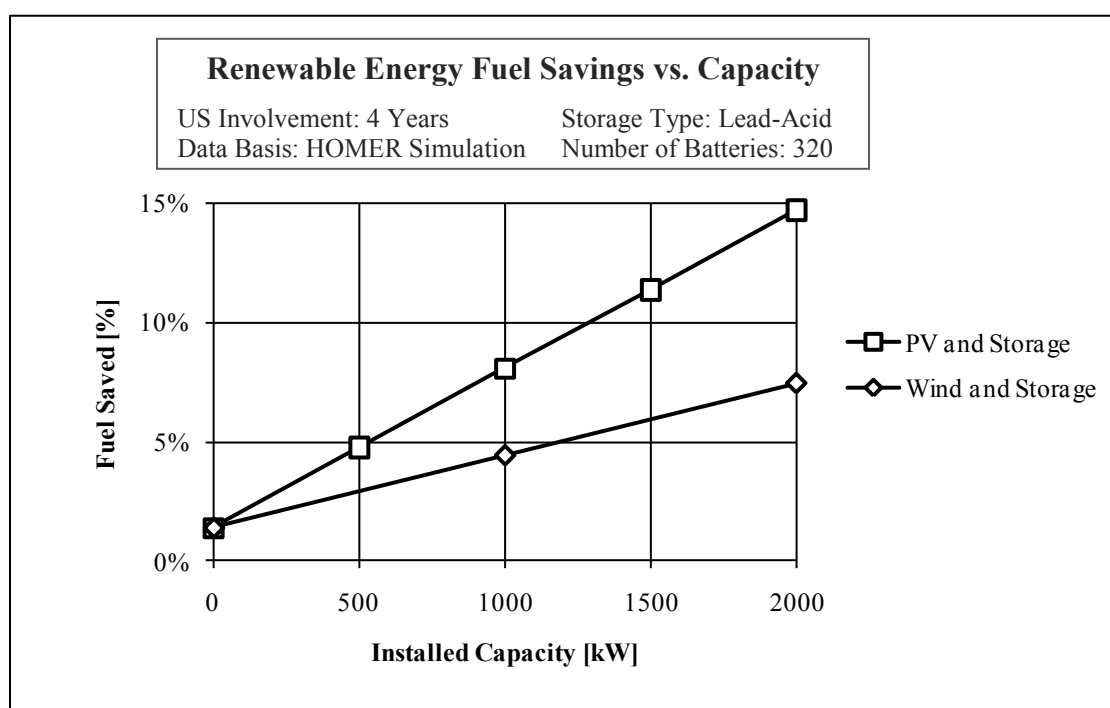


FIGURE 11 – FUEL SAVINGS VS. CAPACITY FOR PV AND WIND ENERGY (INDEPENDENT)

Solar energy saves more fuel per kilowatt hour rated capacity, which is consistent with the solar and wind resources available in Marjah.

Although Figure 11 shows the fuel savings for each type of energy source independently, it does not show the fuel savings that can be achieved when combining these systems. Figure 12 provides this information in the form of a surface plot. The resulting surface is a plane, which

indicates that the fuel savings is linear even for combined PV and wind energy systems (with the same slopes as described previously). This result is reasonable for two reasons: the two energy sources are independent and renewable generation never exceeds load (so all generation is used).²⁴ The latter is partially a result of the fact that the PV array and wind turbines tend to provide maximum power at different times during the day (e.g. PV during early afternoon and wind turbines in the evening). The maximum fuel savings value is approximately 21%.

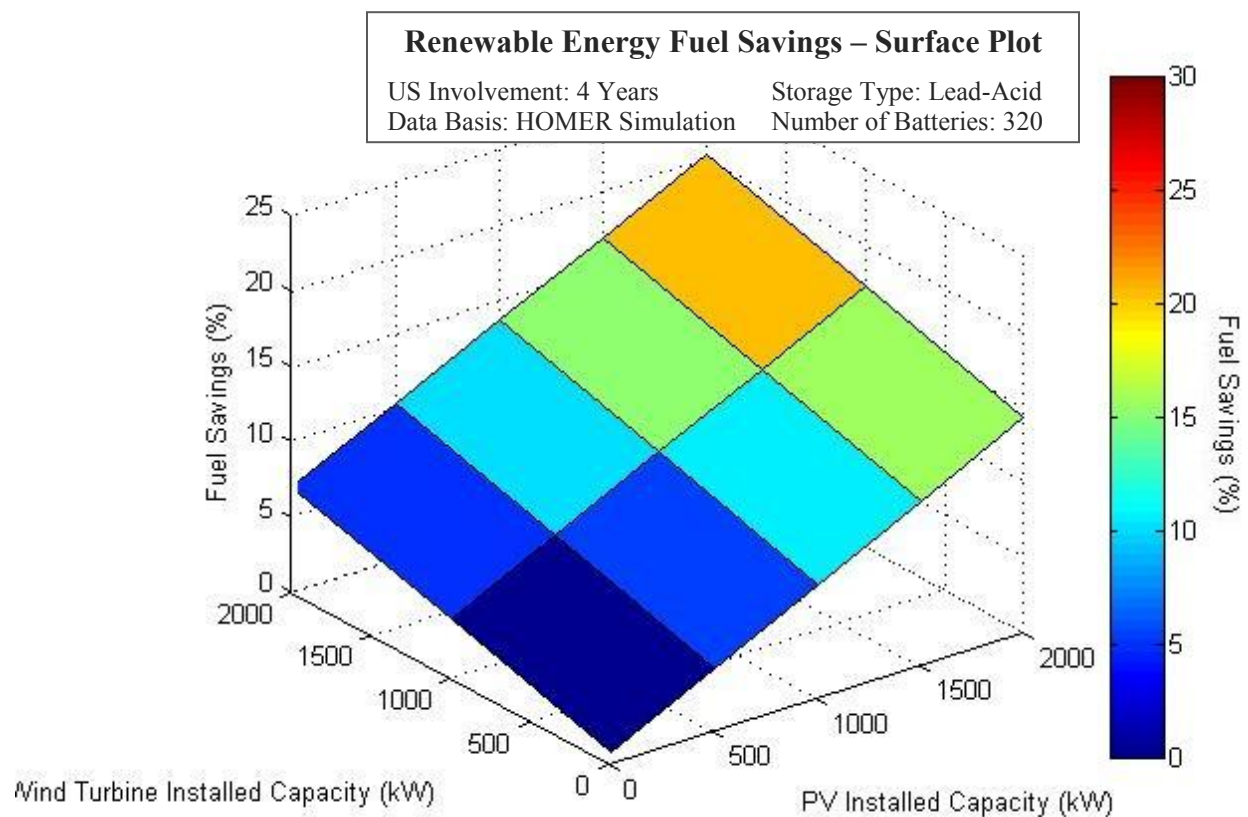


FIGURE 12 - FUEL SAVINGS VS. CAPACITY FOR PV AND WIND ENERGY (COMBINED)

Also of interest is the impact of lead-acid battery storage on fuel savings, shown in Figure 13.

²⁴ Recall the exception noted earlier: for the 2 MW PV array and 20 wind turbine case, renewable generation exceeds load for one hour each year.

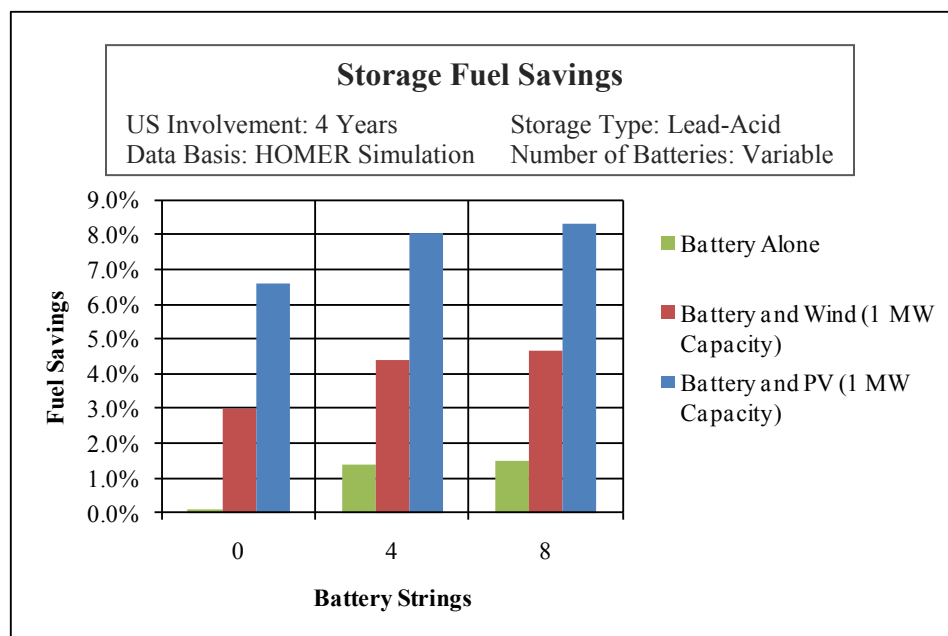


FIGURE 13 – LEAD-ACID STORAGE FUEL SAVINGS

Figure 13 shows the fuel savings resulting from the use of four and eight strings (320 and 640 total) of lead-acid batteries in three cases: only batteries used, batteries used with 1 MW rated capacity of wind turbines, and batteries used with a 1 MW rated capacity PV array. For all three cases, the first four strings of batteries provide a significant fuel savings, whereas the second four strings have only a slight benefit. For example, when a 1 MW PV array is installed the marginal fuel savings of the first four strings of batteries is 1.5%, but the marginal benefit of the second four strings is only 0.3%. Note that installing a 1 MW PV array or 10 wind turbines with zero storage is ill-advised due to transient/stability issues; the zero storage case is shown only to highlight the impact of the batteries on fuel savings.

Reducing fuel consumption, as described by the previous plots, can significantly reduce casualties resulting from attacks on resupply convoys; however, the analysis to show the actual expected casualty reduction must be all-inclusive. In other words, the question that must be raised is: Does the reduced amount of fuel that must be supplied to the FOB offset the initial transportation of the renewable energy system to the FOB in terms of supply-line casualties?

Based on FY07 convoy casualty rates in Afghanistan,²⁵ the following casualty factor model was created for the Marjah, Afghanistan scenario.

$$C_0 = 2.88 \times 10^{-2} W_{PV} + 4.10 \times 10^{-3} N_{WT} + 9.49 \times 10^{-6} N_{BATT} \quad (1)$$

$$C_i = 0.4294f \quad (2)$$

Equation 1 quantifies the Year 0 (up-front) casualties expected as a result of shipping PV, wind turbine, and battery equipment to the FOB. W_{PV} is the rated capacity of the PV array in MW; N_{WT} and N_{BATT} are the number of wind turbines and lead-acid batteries installed; and C_0 is the expected Year 0 supply casualties. This equation was developed using the following assumptions: average materiel convoy capacity of 350,000 lbs; materiel shipments responsible for 30% of supply-line casualties at FY07 casualty rates;²⁶ and shipping weights of 400 lb/kW for the PV array, 57,000 lb per wind turbine, and 10,540 lb per battery string (including inverter). For example, as a result of installing 1 MW of PV, 10 wind turbines, and 320 batteries, one would expect to incur 0.073 casualties. Equation 2 quantifies the yearly casualties expected as a result of supplying fuel to the FOB. f represents the fuel consumption in millions of gallons per year and C_i represents the expected supply casualties in year i . The total expected casualties associated with a particular system concept are:

$$C_T = N \times C_i + C_0 \quad (3)$$

Here, N is the number of years of US involvement.

Using the above analysis, Figures 11, 12, and 13 can all be recast in terms of casualty reduction as opposed to fuel savings. The result is Figures 14, 15, and 16.

²⁵ *Sustain the Mission Project: Casualty Factors for Fuel and Water Resupply Convoys*. Tech. Arlington: Army Environmental Policy Institute, 2009.

²⁶ *Sustain the Mission Project*, 3.

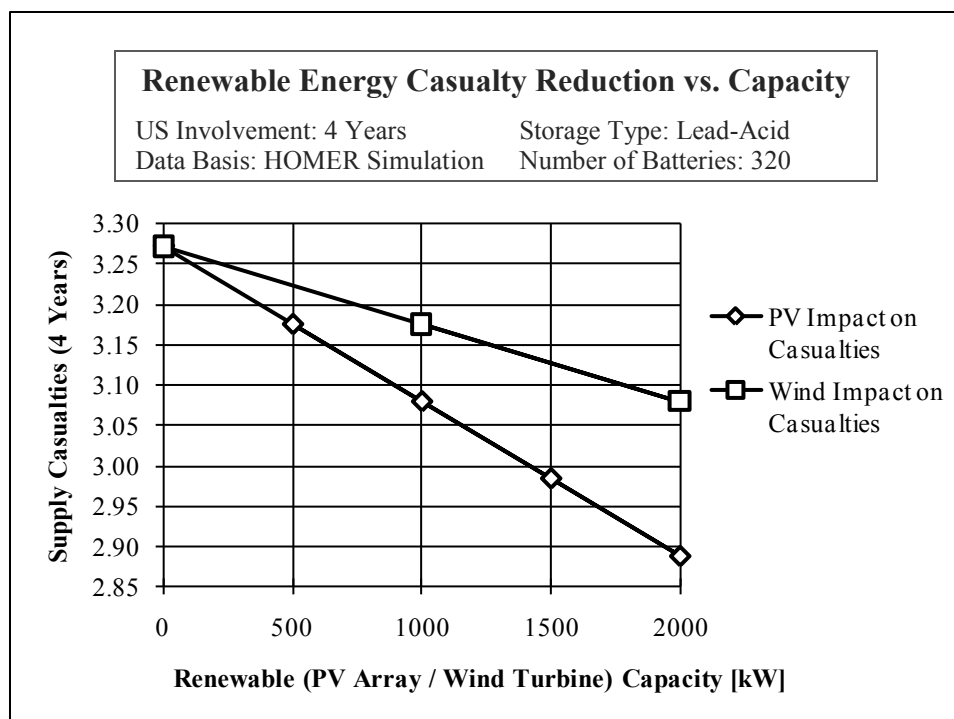


FIGURE 14 - SUPPLY CASUALTIES VS. CAPACITY FOR PV AND WIND ENERGY (INDEPENDENT)

Using the generator-only simulations as a baseline, approximately 3.3 casualties are expected over a period of four years for a current-day (genset-only) FOB. Figure 14 shows the expected casualties for various independent installations of PV and wind turbines with a fixed storage installation of 320 batteries. When related to rated capacity, solar energy reduces casualties significantly more effectively than does wind energy. Installing a PV array 2 MW in size can reduce expected supply casualties from 3.3 to 2.9 total casualties (a reduction of 12%). Additionally, casualty reductions are linear for each type of equipment: PV arrays and wind turbines reduce casualties by 0.19/MW (5.8%/MW) and 0.10/MW (2.9%/MW) respectively. Note that 320 batteries alone reduce expected casualties by 0.04 (1.3%), which accounts for the intercept slightly below the baseline value of 3.3 casualties.

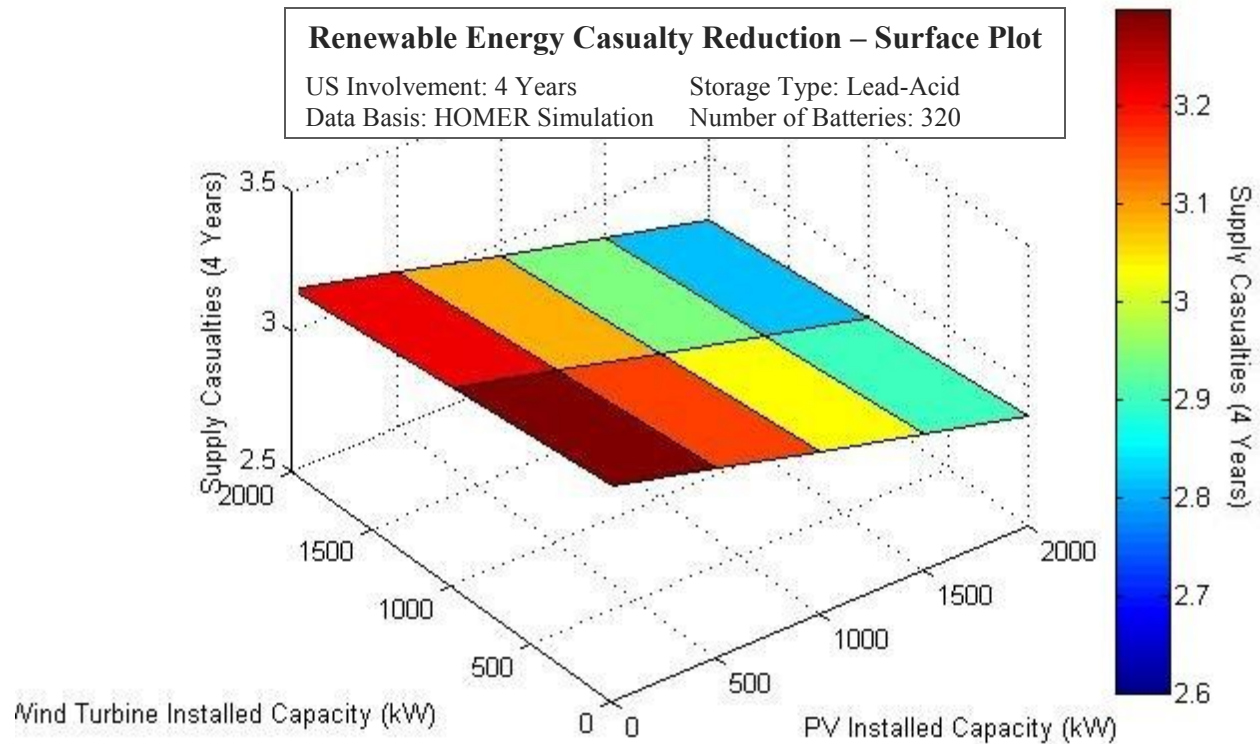


FIGURE 15 - SUPPLY CASUALTIES VS. CAPACITY FOR PV AND WIND ENERGY (COMBINED)

Figure 15 displays the expected casualties for several combinations of PV and wind energy in the form of a surface plot. Note that the relationship is still linear with the same slopes as described previously. The minimum expected casualty value is 2.8 casualties, a reduction of 15%.

Figure 16 illustrates the impact of installing zero, four, and eight strings of lead-acid batteries in terms of percent casualty reduction. Note that in the absence of renewables, installing the second four strings of batteries (for a total of eight strings) actually *increases* the casualty rate compared with the four string case. This is due to the fact that the additional batteries provide limited fuel savings while requiring more equipment to be shipped initially. However, the additional four strings of batteries continue to reduce the casualty rate when coupled with 1 MW capacity of either PV or wind energy.

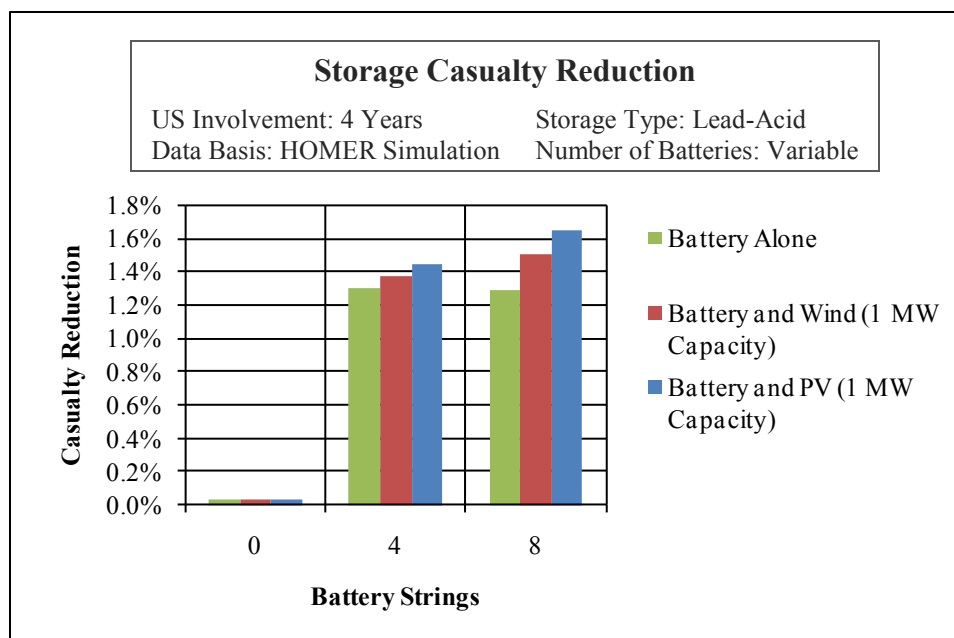


FIGURE 16 - LEAD-ACID STORAGE CASUALTY REDUCTION

PHYSICAL FOOTPRINT OF RENEWABLES

This section will address the issue of physical footprint required to install renewables (i.e. how much land area these systems occupy). To understand the footprint needed to install these systems, a basic model of land area used versus capacity was developed. For wind turbines, an estimated area of 10 m² per kilowatt rated capacity was used.²⁷ The estimate used for the PV array was a slightly more compact 9.29 m² per kilowatt rated capacity.²⁸ Another way to express the footprint of these systems is by comparing the land area needed for their installation to a relevant reference; footprint can be expressed relative to the land area set aside for a typical FOB's runway, taxiways, and parking aprons. Table 1 shows the land area needed to install several renewable systems based on an approximate reserved area for a runway of two miles by half a mile (one square mile) sorted in order of increasing footprint.

²⁷ Denholm, Paul, Maureen Hand, Maddalena Jackson, and Sean Ong. *Land-Use Requirements of Modern Wind Power Plants in the United States*. Tech. no. NREL/TP-6A2-45834. National Renewable Energy Laboratory, 2009.

²⁸ "Fast Solar Energy Facts." *Solarbuzz*. 2002. Web. 29 July 2010.
<<http://www.solarbuzz.com/Consumer/FastFacts.htm>>.

TABLE 1 – FOOTPRINT REQUIRED FOR VARIOUS RENEWABLE SYSTEMS

PV Array Capacity (MW)	Wind Turbines	Footprint (m ²)	Percent of Runway Area
0.0	0	-	0.0%
0.5	0	5,000	0.2%
1.0	0	9,000	0.3%
0.0	10	10,000	0.4%
1.5	0	14,000	0.5%
0.5	10	15,000	0.6%
2.0	0	19,000	0.7%
1.0	10	19,000	0.7%
0.0	20	20,000	0.8%
1.5	10	24,000	0.9%
0.5	20	25,000	1.0%
2.0	10	29,000	1.1%
1.0	20	29,000	1.1%
1.5	20	34,000	1.3%
2.0	20	39,000	1.5%

MULTI-OBJECTIVE OPTIMIZATION EXAMPLE: CASUALTIES VS. FOOTPRINT

This section presents a possible method for developing the trade space between supply-line casualty reduction and renewables footprint that could be applicable for future work. The tradeoff between supply-line casualty reduction and base footprint is a classic multi-objective optimization problem. The two objectives are to minimize casualties while simultaneously minimizing the renewables footprint. This situation naturally lends itself to Pareto front analysis²⁹. This analysis does not identify a single optimal solution, but rather a curve demonstrating the optimum solution for varying objective priorities (as seen in Figure 17). Figure 17 shows all of the alternatives simulated (“x” marks) against axes of footprint and supply-line casualties. Sub-optimal solutions are displayed in blue with the optimal solutions in red. The Pareto front is defined by the red line.

²⁹ A detailed description of this method is beyond the scope of this paper but can be found in most graduate-level optimization textbooks, for example: Edwin K.P. Chong, and Stanislaw H. Żak. "Chapter 23: Multiobjective Optimization." *An Introduction to Optimization*. Hoboken, NJ: Wiley-Interscience, 2008. 542-48. Print.

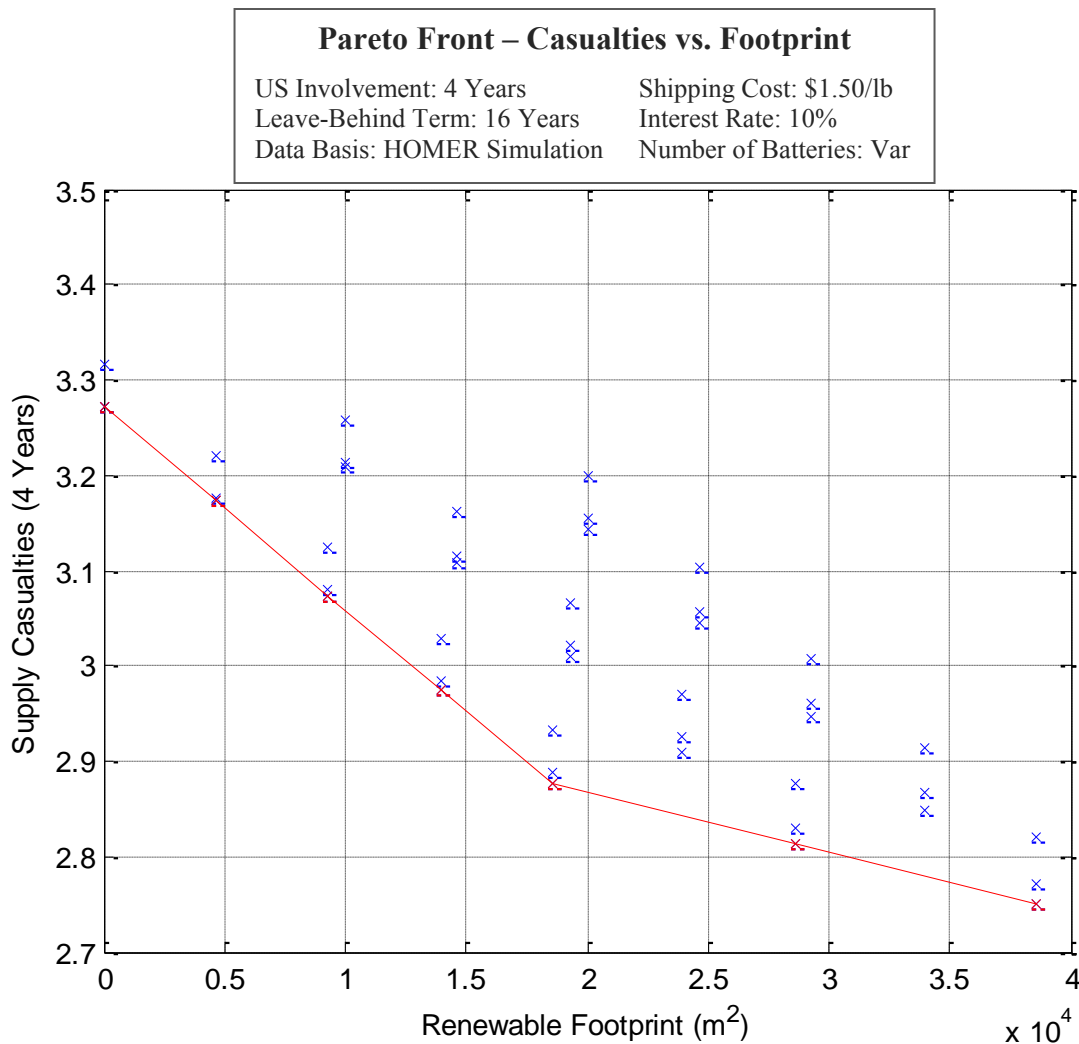


FIGURE 17 - PARETO FRONT FOR CASUALTIES VS. FOOTPRINT (HOMER SIMULATIONS)

Table 2 shows the optimal system alternatives sorted in order of decreasing casualties (increasing footprint). This table shows that the steeper portion of the Pareto front develops as the PV array size increases from 0 to 2 MW. The remainder of the front shows the impact of adding wind turbines once the maximum 2 MW of PV has already been installed. Note that 640 batteries is the optimal amount for all solutions except the zero-renewable alternative.

TABLE 2 - CASUALTY/FOOTPRINT OPTIMAL SOLUTIONS

PV (kW)	Wind Turbines	Batteries	Footprint (m ²)	Supply Casualties
0	0	320	0	3.3
500	0	640	5,000	3.2
1000	0	640	9,000	3.1
1500	0	640	14,000	3.0
2000	0	640	19,000	2.9
2000	10	640	29,000	2.8
2000	20	640	39,000	2.8

Due to the computational time required to run the HOMER models used, it would be difficult to conduct Pareto front analysis for the entire set of system alternatives (i.e. all PV array capacities from 0 to 2 MW and all integer number of wind turbines from 0 to 20). However, since both supply-line casualties and footprint vary linearly with PV array capacity and number of wind turbines (recall this result from Figures 14 and 15), a multi-objective linear program can be developed for a fixed number of batteries (in this case, 320):

$$\min \bar{f}(\bar{x}) = \begin{bmatrix} 0 & 9.29 & 10 \\ 3.272 & -1.91 \times 10^{-4} & -9.6 \times 10^{-5} \end{bmatrix} \begin{bmatrix} 1 \\ x_1 \\ x_2 \end{bmatrix}$$

$$st \begin{cases} 0 \leq x_1 \leq 2000 \\ 0 \leq x_2 \leq 2000 \end{cases}$$

For this linear program, x_1 is the PV array capacity in kW, x_2 is the wind turbine capacity in kW, the first objective function is the renewable footprint, and the second objective function is the supply-line casualty value. Using this linear program, the complete set of alternatives can be described with Pareto front analysis.

Figure 18 shows similar results to those from the actual HOMER simulations (Figure 17). However, it illustrates that the Pareto front is in fact piecewise-linear across the entire solution space. The linear program model allows for casualty/footprint tradeoff analysis for sizes not covered in the original HOMER simulations (for example, 1.3 MW of PV or 3 wind turbines). The steeper portion of the front is again indicative of the tradeoff between casualty reduction and footprint for PV array installations from 0 to 2 MW; the shallower portion again represents wind turbine installation in addition to a 2 MW capacity PV array.

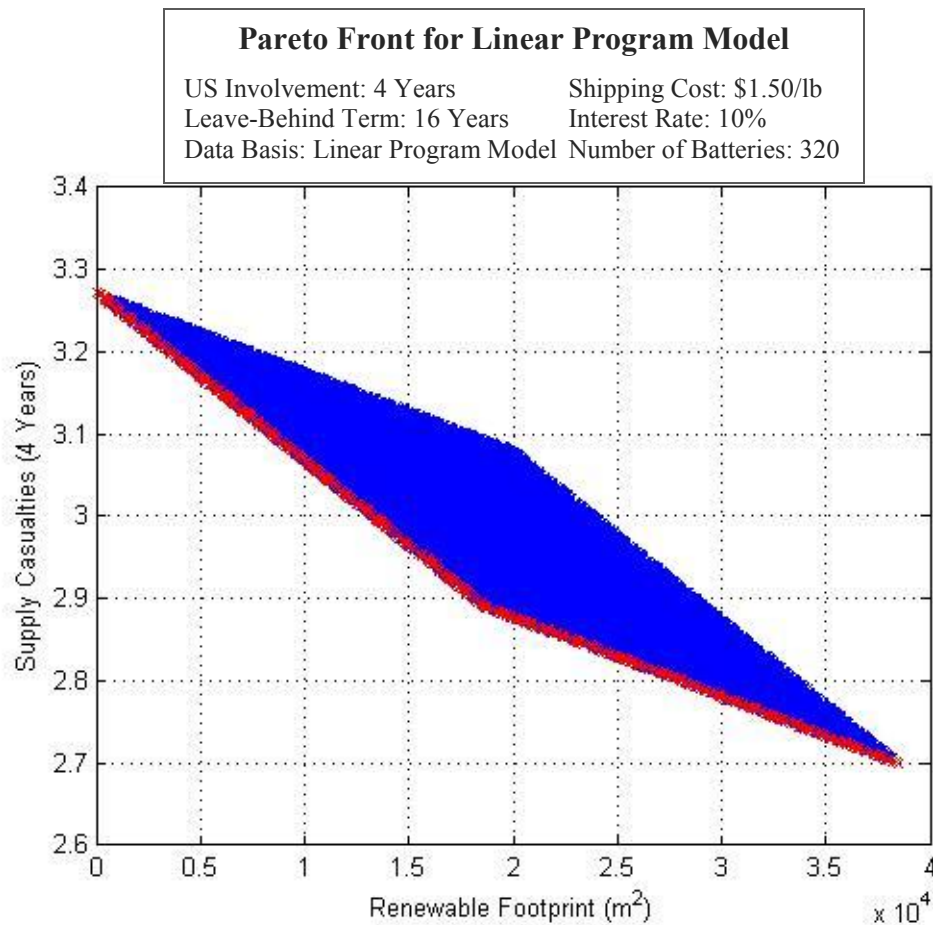


FIGURE 18 - PARETO FRONT FOR CASUALTIES VS. FOOTPRINT (LINEAR PROGRAM)

Recognizing that the PV array is more desirable in terms of the casualty/footprint tradeoff leads to an important question: If utilizing solar energy allows for a more significant decrease in casualties for the same footprint as wind energy, why not continue to install more PV panels past the 2 MW maximum imposed on the simulation (instead of beginning to install wind turbines)? The answer is a matter of implementation. The PV array and wind turbines provide their maximum power at different times during the day. This temporal diversity reduces the maximum instantaneous renewable penetration for a given average renewable penetration. The higher the instantaneous (peak) renewable penetration, the more difficult renewable systems become to implement in terms of transient issues in the power distribution system. Table 3 shows that when wind turbines are installed alongside a 2 MW PV array, the result is a higher ratio of average to peak renewable penetration.

TABLE 3 - RENEWABLE PENETRATION FOR VARIOUS ALTERNATIVES (640 BATTERIES)

PV (kW)	Wind Turbines	Peak Penetration	Average Penetration	Avg/Peak Ratio
2000	0	86%	16%	0.18
2000	10	99%	19%	0.19
2000	20	104%	22%	0.21

The result is an increase in the total renewable energy supplied for a given peak penetration value. In other words, using both technologies decreases both fuel consumption and supply-line casualties for a given difficulty of system implementation.

PROPOSED SYSTEM CONCEPT

The previous section identified several relationships that can be used as tools for designing a renewable energy system for FOBs; in this section these tools will be used to develop a system concept for a hypothetical deployment. For example, consider a future FOB at a location similar to that of Marjah, Afghanistan. For this location, the FBCF is estimated at \$15/gal, shipping costs are estimated at \$1.50/lb, the value of leave behind energy is assessed at 20¢/kWh, the base is expected to be in operation for four years, and no more than 29,000 m² is available for renewable installation.

After consulting Figure 3, it is clear that PV arrays, wind turbines, and lead-acid batteries all reduce NPC when the VLBE is included. To reduce supply-line casualties, the highest capacity renewable system within the physical footprint requirement should be chosen (see Figure 15). Table 1 shows two options with a footprint of 29,000 m²: a 1 MW PV array with 20 wind turbines or a 2 MW PV array with 10 wind turbines. Recall from Figure 14 that solar energy is more effective at reducing casualties per kilowatt rated capacity; therefore, a 2 MW PV array with 10 wind turbines should be selected. Also recall from Figure 16 that eight strings of batteries reduce casualties more than four strings, so eight strings should be selected. For these reasons, the proposed system concept presented here consists of a 2 MW PV array, 10 wind

turbines, and 640 lead-acid batteries. The remainder of this section will be devoted to a comparison of the performance of this proposed system concept with the performance of the baseline, genset-only power system.

Tables 4 and 5 show the electrical production across each component for the baseline (MEP-12 generators only) and proposed system concept. Note that for the baseline case four generators operate as base load machines, one operates as a swing machine, two operate as reserve machines during peak load hours only, and the final generator is on maintenance standby. Seven generators are required to operate at peak load for a total of 975 hours per year.

TABLE 4 - BASELINE ELECTRICAL PRODUCTION

Component	Production	Fraction
	(kWh/yr)	
MEP-12 (1)	6,570,000	23%
MEP-12 (2)	6,570,000	23%
MEP-12 (3)	6,570,000	23%
MEP-12 (4)	5,023,264	18%
MEP-12 (5)	2,553,752	9%
MEP-12 (6)	847,012	3%
MEP-12 (7)	222,460	1%
MEP-12 (8)	0	0%
Total	28,356,488	100%

TABLE 5 - SYSTEM CONCEPT ELECTRICAL PRODUCTION

Component	Production	Fraction
	(kWh/yr)	
PV array	4,450,949	15%
Wind turbines	938,262	3%
MEP-12 (1)	6,552,930	23%
MEP-12 (2)	6,374,508	22%
MEP-12 (3)	5,698,668	20%
MEP-12 (4)	3,676,114	13%
MEP-12 (5)	1,017,685	4%
MEP-12 (6)	99,785	0%
MEP-12 (7)	450	0%
MEP-12 (8)	0	0%
Total	28,809,352	100%

For the system concept, approximately 18% of the power generated comes from renewable sources. Note that the renewable system produces ~450 MWh/yr more than the genset-only baseline. This is attributable to the roundtrip losses incurred as power is cycled through the lead-acid batteries. Actual excess energy production for the renewable system is only 380 kWh/yr. Load on the generators is significantly reduced, particularly for generators 4 – 7.

Figures 19 – 22 show a side-by-side comparison of the load on these generators across an entire typical year for the generator-only baseline (top) and renewable system (bottom).

When renewables are used, seven generators are required to meet peak load for only two hours each year. In terms of generator hours, the renewables offset approximately 1.6 generators (on average).³⁰ This leads to significantly less maintenance on the generators: average time between overhauls increases from 1.5 years to 2.0 years.

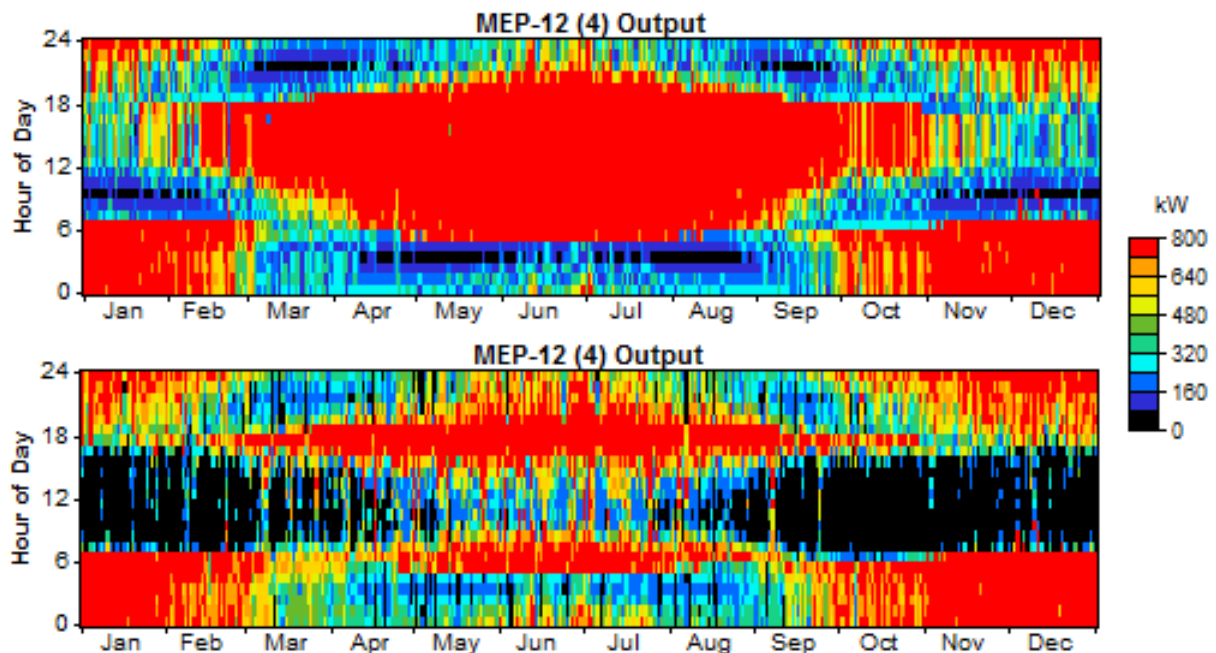


FIGURE 19 - GENERATOR 4 LOAD (BASELINE SYSTEM: TOP; RENEWABLE SYSTEM: BOTTOM)

³⁰ 46,000 generator-hours for baseline system; 35,000 generator-hours for renewable system.

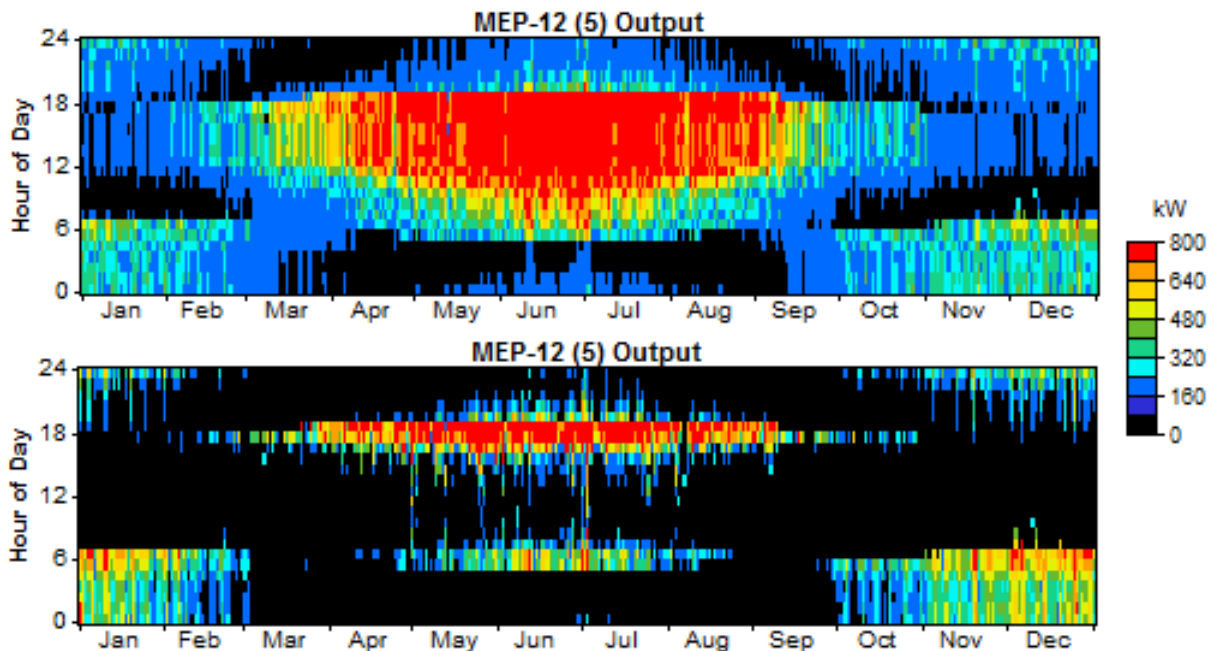


FIGURE 20 - GENERATOR 5 LOAD (BASELINE SYSTEM: TOP; RENEWABLE SYSTEM: BOTTOM)

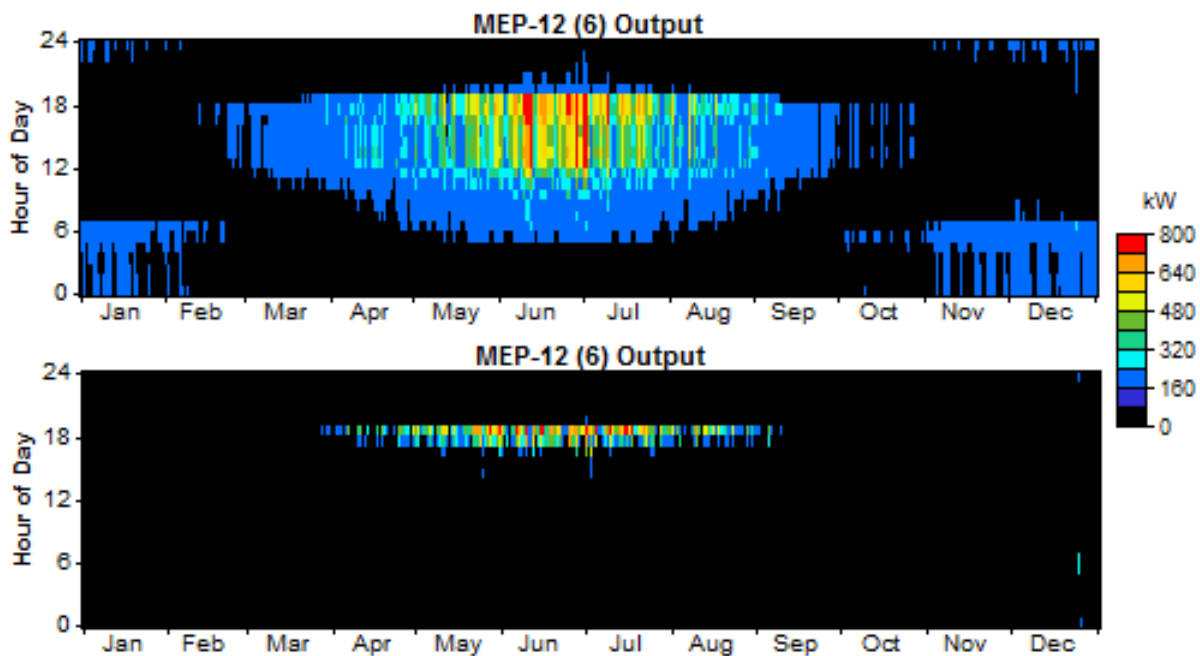


FIGURE 21 - GENERATOR 6 LOAD (BASELINE SYSTEM: TOP; RENEWABLE SYSTEM: BOTTOM)

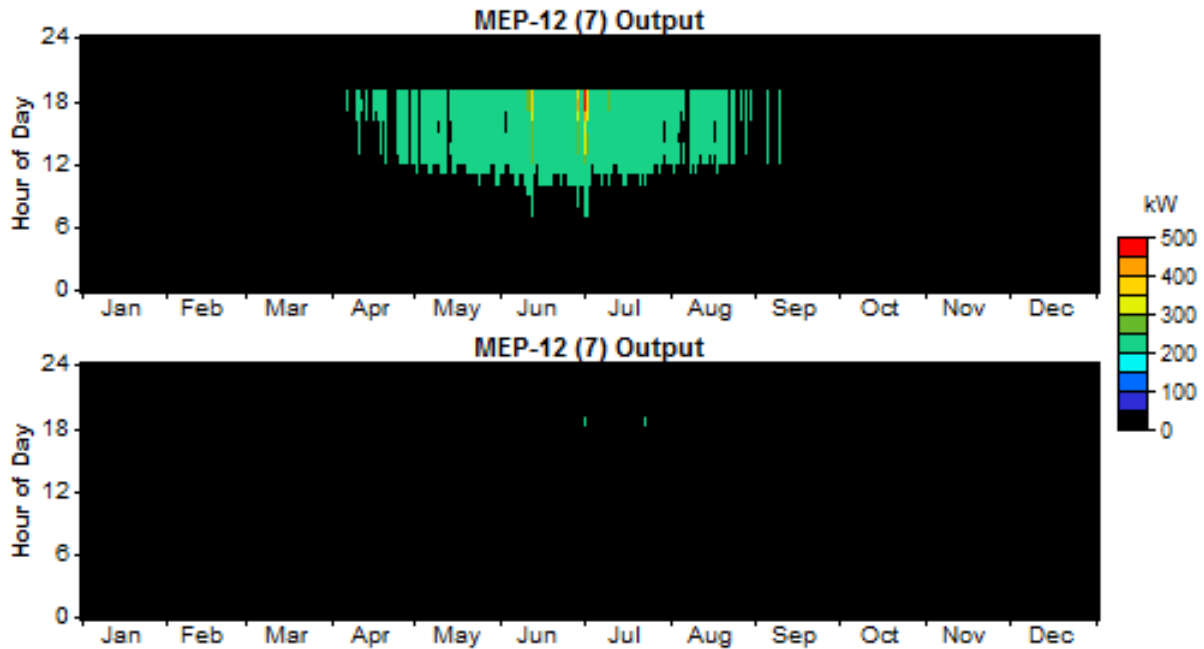


FIGURE 22 - GENERATOR 7 LOAD (BASELINE SYSTEM: TOP; RENEWABLE SYSTEM: BOTTOM)

The reduction in diesel generation needed has a significant benefit in terms of fuel consumption, casualty reduction, and operating costs. Table 6 shows a summary of the costs and benefits associated with installing this renewable system for the hypothetical deployment discussed in this section. This table shows that by investing less than one percent of NPC, a casualty can be saved every eight years with a 17% reduction in fuel consumption. In addition, this solution is monetarily beneficial (reduced NPC) when considering the value of leaving behind renewable energy. The total land area required for the installation of this system is approximately 29,000 m², or 5.4 football fields.

TABLE 6 - SUMMARY OF COST AND BENEFIT FOR HYPOTHETICAL DEPLOYMENT

Marjah Actual Cost			
	Baseline	Renewable System	Difference
Total net present cost	\$95,600,000	\$96,300,000	\$700,000
Levelized cost of energy	\$ 1.06/kWh	\$ 1.07/kWh	1.0 c/kWh
Additional Footprint	0 m ²	29,000 m ²	29,000 m²
Operating cost	\$ 29.3 million/yr	\$ 23.8 million/yr	\$5.5 million/yr
Expected Casualties	3.3	2.8	0.5
Fuel Consumption	1.9 million gal	1.6 million gal	17%
Average Generator Overhaul	Every 1.5 years	Every 2.0 years	6 months
Energy from Diesel	100%	82%	18%

Recall that this analysis is for a single hypothetical FOB. If similar renewable systems had been installed theater-wide for FY07, fuel-related supply-line casualties for all operations in Afghanistan could have been reduced from 38 to approximately 33.³¹

Figures 23 and 24 are included for clarification regarding the “total net present cost” row in Table 6. For the renewable system, capital costs are much higher than the generator-only baseline (~\$21 million versus ~\$2.5 million), but fuel costs are much lower (~\$23.5 million versus ~\$29 million). This results in a difference in NPC (at an interest rate of 10%) of only \$700,000. Table 7 illustrates the sensitivity of this result to interest rate. At interest rates of 8% and below, the renewable system has a lower NPC than the generator-only system. In the range of interest rates from 0% - 20%, the NPC values differ by no more than \$3.9 million.

³¹ Total casualties from *Sustain the Mission Project*, 5; based on a blanket 15% casualty reduction consistent with values from Table 5.

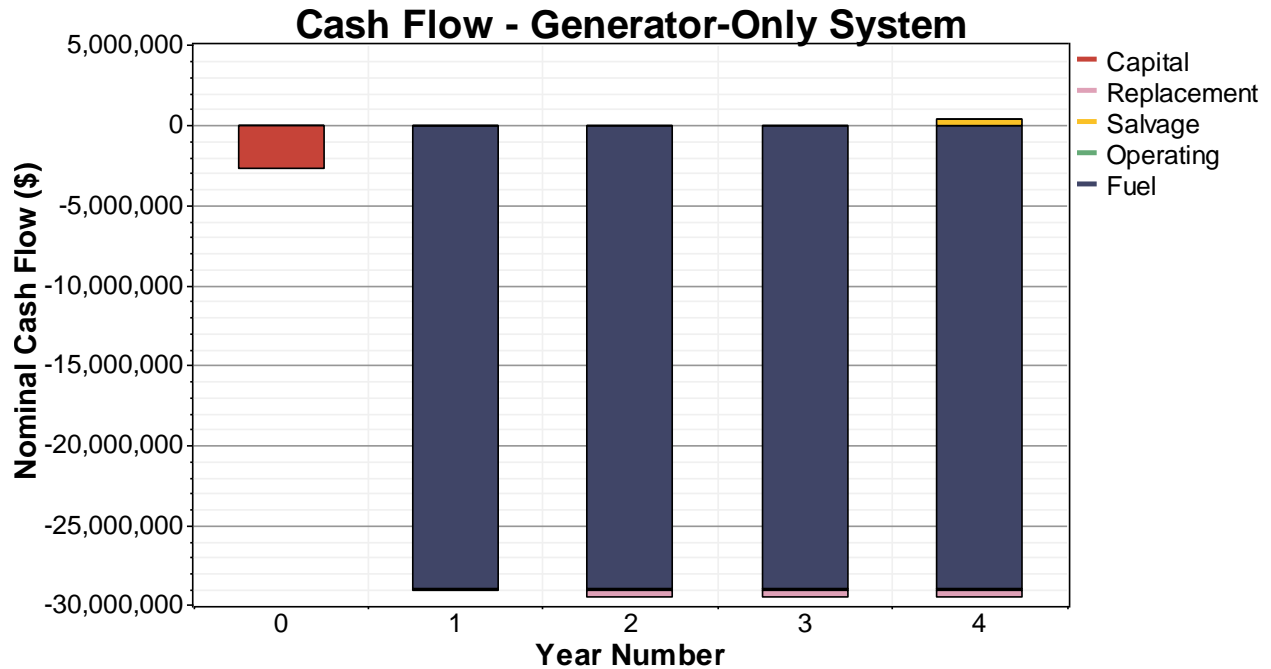


FIGURE 23 - CASH FLOW DIAGRAM FOR GENERATOR ONLY SYSTEM (FOUR YEAR TIMEFRAME)

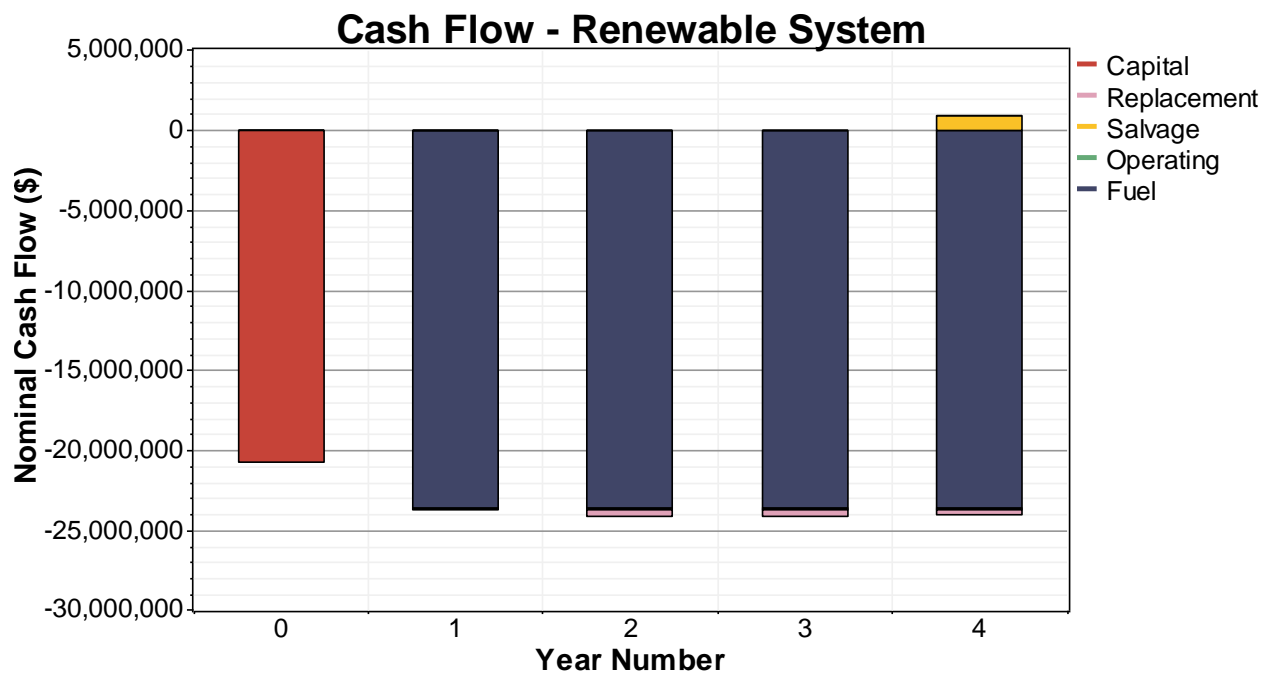


FIGURE 24 - CASH FLOW DIAGRAM FOR RENEWABLE SYSTEM (FOUR YEAR TIMEFRAME)

TABLE 7 - INTEREST RATE SENSITIVITY OF NET PRESENT COSTS

Interest Rate	Baseline NPC (\$M)	Renewable NPC (\$M)	Difference (\$M)
0%	119.9	115.9	3.9
2%	114.2	111.4	2.9
4%	109.0	107.2	1.9
6%	104.2	103.2	1.0
8%	99.7	99.6	0.1
10%	95.5	96.2	0.7
12%	91.7	93.1	1.4
14%	88.0	90.2	2.1
16%	84.7	87.4	2.8
18%	81.5	84.9	3.4
20%	78.5	82.4	3.9

CANNON AFB TEST-BED

Now that a proposed system concept has been established based on HOMER simulation results, the next step in the design process would be to construct a test-bed to verify the simulation results. Additionally, developing a stateside test-bed would be highly beneficial in terms of training personnel to maintain and operate such a system. This section will detail the performance of the proposed system concept (2 MW PV array, 10 wind turbines, and 640 lead-acid batteries) at a hypothetical test-bed/training site at Cannon AFB, NM.

The simulation parameters used for the Cannon AFB site were identical to those used in the Marjah Actual Cost simulations with the exception of HVAC load and resource profiles. Since Cannon AFB (near Clovis, NM) summer high temperatures are slightly lower than those in Marjah, the HVAC load is slightly lower. For Cannon AFB, HVAC load is estimated to range from 0.9 to 2.9 MW; therefore, total load is 2.4 to 4.5 MW, with an average of 3.2 MW. The ratio of peak HVAC load to total peak load for this estimate is approximately 64%. For more detailed information, see Appendix B. Additionally, estimates of solar and wind resource for Clovis, NM, were used for the Cannon AFB site. Average solar radiation in this area is estimated

at 5.32 kWh/m²/day, which is about 7% less than Marjah. Average wind speed for Cannon AFB is 7.87 m/s at a height of 100 m, which is about 59% greater than Marjah (after correction for height difference). Cannon AFB is thus much better situated for wind energy than Marjah. For more information on the development of these estimates, see Appendix A.

After importing the different load and resource profiles into HOMER, a simulation was run for the proposed system concept at Cannon AFB. Note that this system is not optimized for the Cannon AFB site; however, this analysis serves to illustrate how the Marjah-optimized system would perform at Cannon AFB. This information could be used to validate the simulation methodology used in this paper. Table 8 shows the performance of the proposed system concept at the Cannon AFB site.

TABLE 8 - PERFORMANCE OF SYSTEM CONCEPT AT CANNON AFB

Cannon Actual Cost			
	Baseline	Renewable System	Difference
Additional Footprint	0 m ²	29,000 m ²	29,000 m ²
Additional Capital Cost	\$0	\$15.2 million	\$15.2 million
Fuel Consumption	1.9 million gal	1.5 million gal	16%
Energy from Diesel	100%	78%	22%

Note that the fuel consumption reduction is comparable to, but slightly lower than, that of the Marjah case. This result is reasonable since the system is not optimized for the solar and wind resources available at Cannon AFB.

CONCLUSIONS AND RECOMMENDATIONS

The economic sensitivity analysis presented in this paper shows two trends. First, the impact of the value of leave behind energy (VLBE) metric depends heavily on the timeframe. Since the economically optimal system type varies greatly with timeframe for a fixed VLBE, special attention must be paid in estimating the time horizon of US operations at a FOB for VLBE to be used as a planning tool. Second, the technology favored in terms of net present cost depends upon the cost of shipping materiel to the FOB. For shipping costs below ~\$1.80/lb, wind turbines are favored, whereas PV arrays are favored above this value. Since this result is due to a difference in shipping weight between the two technologies, this argues for a focus on lightweight, easily transportable renewable energy sources – a potential topic for future research.

The fuel consumption and casualty analysis presented in this paper show that reducing fuel consumption by installing renewables can reduce total supply-line casualties. The additional risk to troops associated with transporting renewable equipment to a FOB is more than offset by the fuel savings provided by this technology. Casualty reductions in the range of 10% - 15% are possible using the systems considered. Additionally, these systems can be installed in relatively small physical areas: in the range of 0.2% - 1.5% of the area set aside for a typical runway.

Although any renewable installation must be considered on a site-specific basis, several metrics and tools presented in this paper can be used to quantify this analysis. Specifically, approximate casualty reduction ratios (e.g. per MW installed capacity), physical footprint values, and the value of leave behind energy can be used to determine the appropriate mix of renewables for a given deployment. For a typical, one-squadron Air Force FOB in Afghanistan, a combination of a 2 MW PV array with ten 100 kW wind turbines and 640 lead-acid batteries is one viable and highly beneficial system concept. This system could reduce fuel consumption by 17%, casualties by 15%, and operating cost by \$5.5 million per year. In addition, a system test-

bed could be established at a domestic Air Force base, such as Cannon AFB, to validate the simulations used here as well as to train personnel in system operations and maintenance.

Installing similar renewable systems at FOBs theater-wide could reduce the fuel required to produce electrical power by 15-20%. As fuel consumption is directly related to supply-line casualties, reducing the amount of fuel that must be transported across dangerous supply routes reduces the number of soldiers wounded or killed in action. Therefore, installing renewables at FOBs is justified from the standpoint of casualty reduction alone. Additional benefits, such as reduced operating costs, reduced generator maintenance, and the value of energy left behind after US departure, serve to highlight the attractiveness of incorporating renewable energy into bases in forward locations.

FURTHER RESEARCH

Time constraints necessitated a limited scope for this paper. Far short of final, conclusive analysis, this paper is intended to be a jumping-off point for further study that will hopefully result in the production of a functioning renewable energy system for FOBs. To achieve this goal, further research is needed into the best physical placement of the renewable energy components. For example, using PV arrays to shade shelters at FOBs could reduce HVAC load as well as provide power for the base.³² Additionally, further research into developing lightweight, transportable renewable energy systems would be beneficial in the effort to reduce shipping costs and supply-line casualties associated with delivering renewable equipment to remote locations.

Certain tactical issues also arise with the installation of renewables: potential targeting of renewable equipment by the enemy and placement of equipment (specifically of wind turbines) near aircraft flight paths, among others. A detailed study of these issues would help substantially in the effort to field the systems described in this paper. Additionally, instantaneous renewable penetration values in the 90% range require significant care in design for system stability. A study of the information and control architecture required to field such a system is also needed.

³² Some of this research and development is already underway: specifically “solar flies” under development by HQ AFCEA/CEXX.

[This Page Intentionally Left Blank]

APPENDIX A – RESOURCE PROFILES

SOLAR RESOURCE

The simulations described in this paper require values for the solar radiation (in kWh/m²) at each hour of a typical year in Marjah, Afghanistan and Cannon AFB, NM. In the case of Marjah, no measured data set exists; however, the National Renewable Energy Laboratory (NREL) has developed numerical estimates for all of Afghanistan, with 10km resolution, based on satellite photos of cloud cover.³³ NREL has compiled these estimates into a Geospatial Toolkit for Afghanistan which allows hourly time series solar radiation values to be exported directly to the HOMER software.³⁴ Table A – 1 shows the monthly average estimates for solar radiation used for Marjah based on the values from the Geospatial Toolkit.

TABLE A - 1: MARJAH SOLAR RADIATION AVERAGES (ESTIMATE)

Month	Daily Radiation (kWh/m ² /d)
January	3.221
February	4.328
March	5.141
April	6.327
May	7.373
June	8.177
July	7.874
August	7.438
September	6.625
October	5.456
November	3.838
December	3.010

Figure A – 1 shows the hourly time series solar radiation estimates. Each day of the year is represented on the x-axis with the time of day on the y-axis. Color indicates the solar radiation

³³ Perez, Richard, Jim Schlemmer, Kathleen Moore, and Ray George. *Satellite-Derived Resource Assessment in Afghanistan & Pakistan in Support of the USAID South Asia Regional Initiative*. Rep. National Renewable Energy Laboratory. Web. 19 July 2010. <http://www.nrel.gov/international/pdfs/solar_documentation.pdf>.

³⁴ "NREL: International Activities - Geospatial Toolkits." *National Renewable Energy Laboratory (NREL) Home Page*. Web. 19 July 2010. <http://www.nrel.gov/international/geospatial_toolkits.html>.

for each of the 8,760 hours of the year with a maximum of approximately 1.15 kW/m². Note that peak solar radiation is concentrated in the summer with very few cloudy days throughout the year.

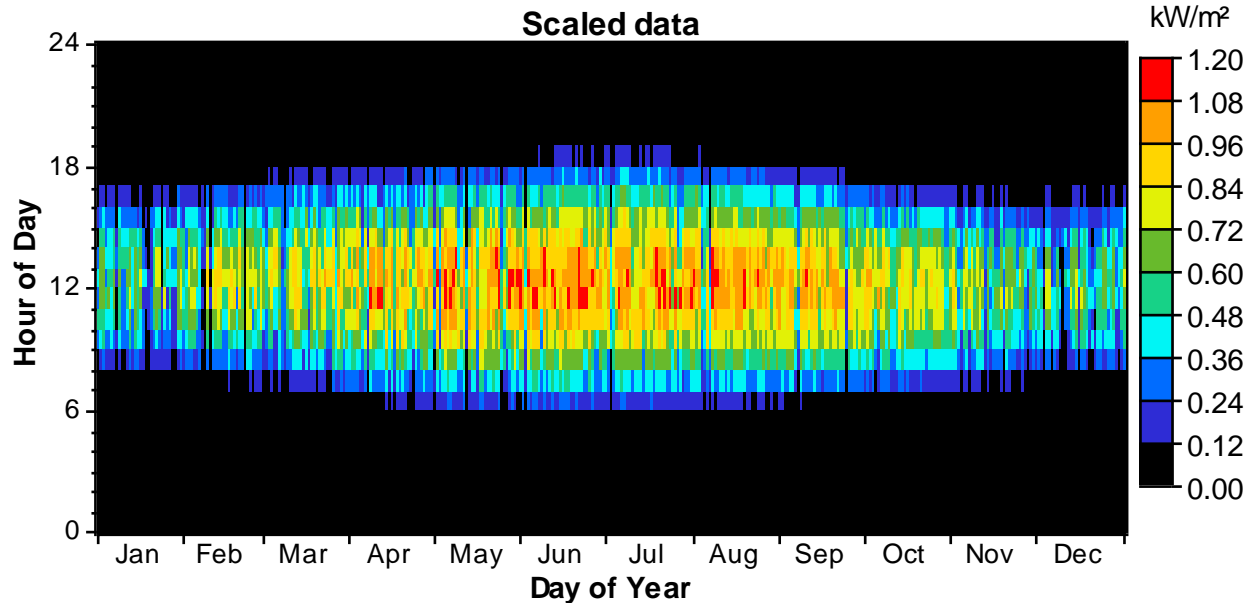


FIGURE A - 1: MARJAH HOURLY SOLAR RADIATION (ESTIMATE)

Similar estimates from NREL’s National Solar Radiation Data Base (NSRDB) were used to populate the solar radiation profile for Cannon AFB, NM. NREL developed these hourly estimates using Geostationary Operational Environmental Satellite (GOES) imagery with a resolution of 10 km.³⁵ Solar radiation values for site 722686 (Clovis Cannon AFB, NM) for the year 2005 were used for the Cannon AFB simulations. NREL lists these estimated values as “Low Uncertainty.”³⁶ Table A – 2 shows the monthly average estimates for solar radiation used for Cannon AFB based on the values from the NSRDB.

³⁵ *National Solar Radiation Database 1991–2005 Update: User’s Manual*. Tech. National Renewable Energy Laboratory, Apr. 2007. Web. 20 July 2010. <<http://www.nrel.gov/docs/fy07osti/41364.pdf>>.

³⁶ *Ibid*, A-244.

TABLE A - 2: CANNON SOLAR RADIATION AVERAGES (ESTIMATE)

Month	Daily Radiation (kWh/m ² /d)
January	3.163
February	3.754
March	5.297
April	6.795
May	6.508
June	7.938
July	7.815
August	5.906
September	5.899
October	3.986
November	3.788
December	2.944

Figure A – 2 shows the hourly time series solar radiation estimates. Each day of the year is represented on the x-axis with the time of day on the y-axis. Color indicates the solar radiation for each of the 8,760 hours of the year with a maximum of approximately 1.05 kW/m². Note that peak solar radiation is concentrated in the summer with several cloudy days throughout the year.

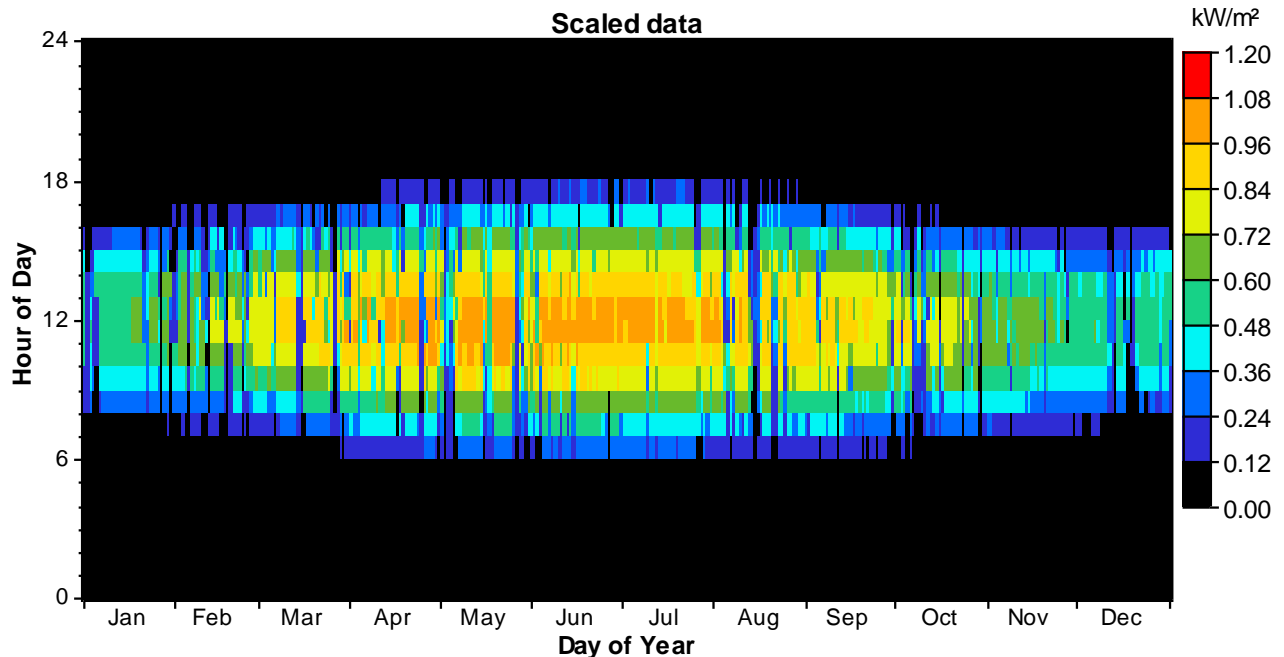


FIGURE A - 2: CANNON HOURLY SOLAR RADIATION (ESTIMATE)

WIND RESOURCE

The simulations described in this paper also require values for wind speed (in m/s) at each hour of a typical year in Marjah, Afghanistan and Cannon AFB, NM. NREL has developed wind speed estimates for all of Afghanistan, with 1 km resolution at 50 m height, based on a compilation of several data sources and numerical models.³⁷ NREL has also compiled these estimates into a Geospatial Toolkit for Afghanistan which allows hourly time series wind speed values to be exported directly to the HOMER software.³⁸ Table A – 3 shows the monthly average estimates for wind speed used for Marjah based on the values from the Geospatial Toolkit.

TABLE A - 3: MARJAH WIND SPEED AVERAGES (ESTIMATE AT 50M HEIGHT)

Month	Wind Speed (m/s)
January	4.021
February	4.391
March	4.391
April	4.431
May	5.002
June	5.552
July	5.092
August	5.022
September	5.062
October	4.231
November	3.621
December	3.901

Figure A – 3 shows the variation in wind speed estimates across each month. The box plots show the minimum, daily average low, mean, daily average high, and maximum wind speeds for each month. Wind speeds in Marjah are modest, with speeds of less than 10 m/s accounting for more than 95% of the hourly estimates (Figure A – 4); however, maximum wind speeds are in the 20 m/s range across the summer months.

³⁷ Elliot, Dennis. *Wind Resource Assessment and Mapping for Afghanistan and Pakistan*. Rep. National Renewable Energy Laboratory, June 2007. Web. 20 July 2010.

<http://www.nrel.gov/international/pdfs/afg_pak_wind_june07.pdf>.

³⁸ NREL: International Activities - Geospatial Toolkits.

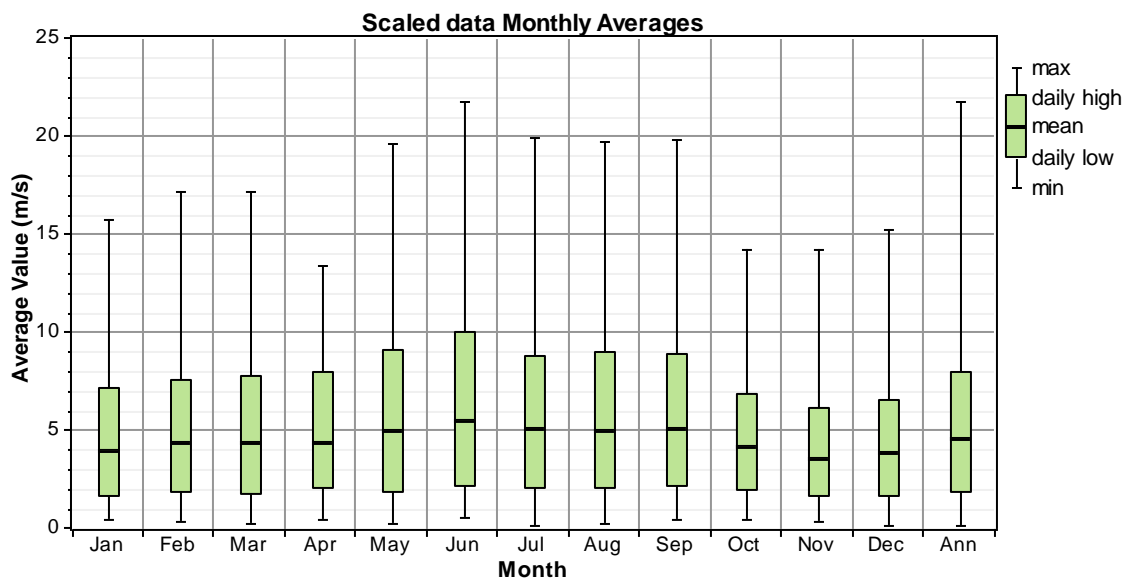


FIGURE A - 3: MARJAH MONTHLY WIND SPEEDS (ESTIMATE AT 50M HEIGHT)

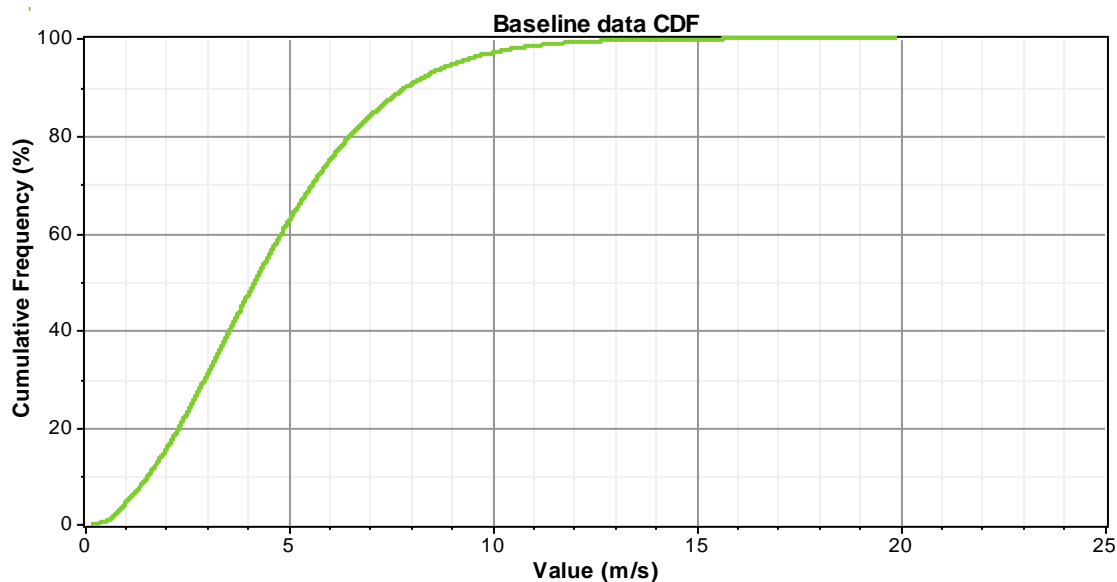


FIGURE A - 4: MARJAH WIND SPEED CUMULATIVE DISTRIBUTION FUNCTION (ESTIMATE AT 50M HEIGHT)

Similar estimates from NREL’s Western Wind Resources Dataset were used to populate the wind resource for Cannon AFB, NM. NREL developed these estimates for wind speed and power using numerical weather prediction models. These models use boundary conditions from “spatially and temporally coarse global datasets” along with “conservation equations that model the physical interactions in the atmosphere” to compute wind speed every ten minutes at more

than 30,000 sites throughout Western America.³⁹ Wind speed values at 100 m height for site 1990 (approximately 15 miles east of Cannon AFB) for the year 2005 were used for the Cannon AFB simulations.⁴⁰ Table A – 4 shows the monthly average estimates for wind speed used for Cannon AFB based on the values from the Western Wind Resources Dataset.

TABLE A - 4: CANNON WIND SPEED AVERAGES (ESTIMATE AT 100M HEIGHT)

Month	Wind Speed (m/s)
January	8.876
February	7.656
March	9.185
April	9.021
May	7.881
June	7.636
July	6.734
August	5.762
September	7.199
October	7.241
November	8.685
December	8.552

Figure A – 5 shows the variation in wind speed estimates across each month. The box plots show the minimum, daily average low, mean, daily average high, and maximum wind speeds for each month. Wind speeds at Cannon AFB are significantly more favorable for generation than in Marjah. Speeds are consistently in the 5 – 12 m/s range with maximum values in the 20 – 25 m/s range for much of the winter and spring.⁴¹

³⁹ Potter, Cameron W., Debra Lew, Jim McCaa, Sam Cheng, Scott Eichelberger, and Eric Gruit. *Creating the Dataset for the Western Wind and Solar Integration Study (U.S.A.)*. Rep. 7th International Workshop on Large Scale Integration of Wind Power and on Transmission Networks for Offshore Wind Farms. Web. 20 July 2010. <http://www.nrel.gov/wind/systemsintegration/pdfs/2008/lew_creating_dataset_wwsis.pdf>.

⁴⁰ "NREL: Western Wind Resources Dataset." *National Renewable Energy Laboratory*. Web. 20 July 2010. <http://wind.nrel.gov/Web_nrel/>.

⁴¹ These values must be reduced by approximately 8% to compare directly to the Marjah estimates due to the height difference (100m versus 50m).

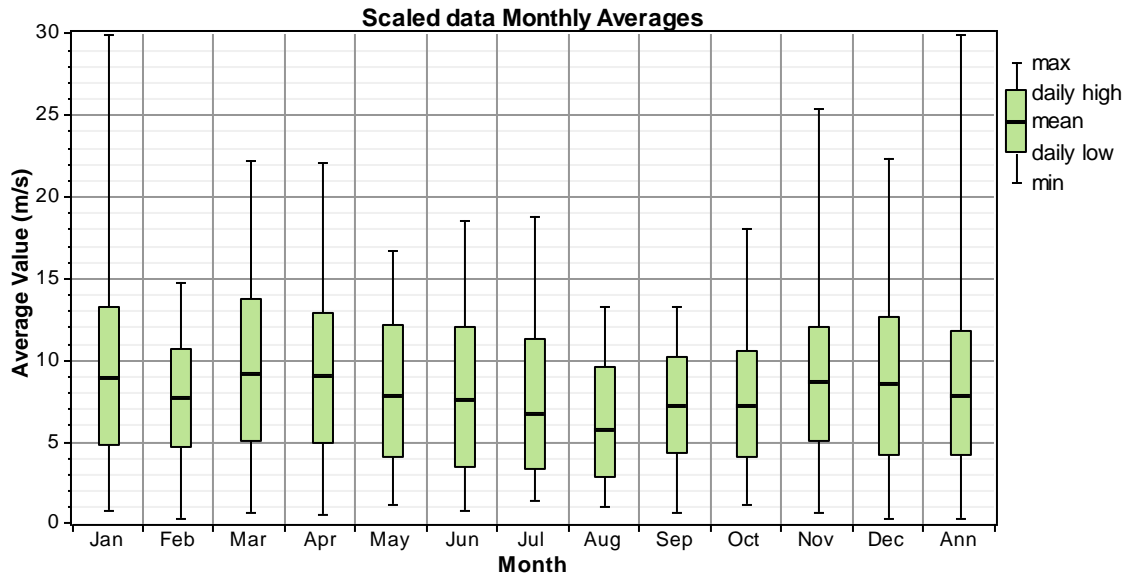


FIGURE A - 5: CANNON MONTHLY WIND SPEEDS (ESTIMATE AT 100M HEIGHT)

Since wind speed decreases with a decrease in wind turbine hub height, a logarithmic profile was used to compute wind speed at heights other than 50m (for Marjah) and 100m (for Cannon AFB). The same profile was used for both locations. Equation A.1 describes the logarithmic profile used.⁴²

$$\frac{U_{hub}}{U_{anem}} = \frac{\ln(z_{hub}/z_0)}{\ln(z_{anem}/z_0)} \quad (A.1)$$

Here, U_{hub} is wind speed at hub height (m/s), U_{anem} is wind speed at anemometer (estimation) height (m/s), z_{hub} is hub height (m), z_{anem} is anemometer (estimation) height (m), and z_0 is the surface roughness length (m). The surface roughness length used for both Marjah and Cannon AFB was 0.01m, which corresponds to “rough pasture.”⁴³ Figure A – 6 illustrates this logarithmic profile.

⁴² Lambert, Tom. *Wind Shear Inputs*. HOMER Help. October 8, 2009.

⁴³ HOMER Wind Speed Variation with Height window.

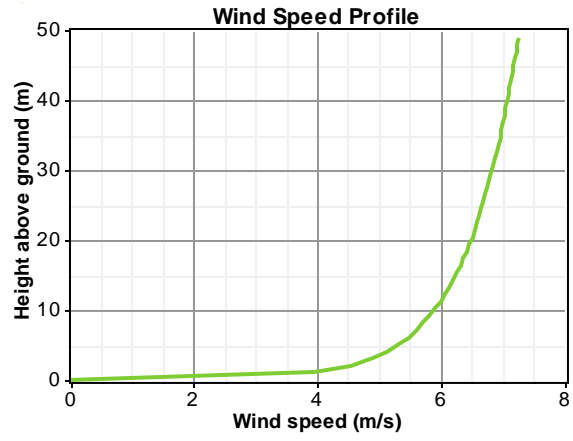


FIGURE A - 6: LOGARITHMIC WIND SPEED PROFILE (SURFACE ROUGHNESS LENGTH OF 0.01M)

APPENDIX B – LOAD PROFILE

OPERATIONAL LOAD

For the purposes of this simulation, the operational load is defined as all power required for the operation of the base with the exception of heating, ventilation, and air conditioning (HVAC) loads. The estimated average operational load for a base of 1,100 personnel is approximately 1.61 MW. The breakdown of this load by structure is shown below in Tables B – 1, B – 2, and B – 3 provided by HQ AFCEA/CEXX.

TABLE B - 5: OPERATIONAL LOAD SUMMARY (1)

ITEM	QUANTITY	POWER DEMAND (kW)
FDECU-5	207	See Detail Below
Shelters – SSS billeting (4.5 Kw)	96	432
SSS other (TOTAL)	67	
• Admin	8	
Wing HQ CC/Staff/Admin	1	5.7
Spt Gp Contr/Legal	1	4.9
Spt Gp Finance/PERSCO	1	4.5
Spt Gp Admin	1	5
Services Admin	1	5
LRS Admin	1	5
BCE/Admin/EOD Readiness	1	5
Security Forces	1	4.5
• CE Ind – Utilities	1	5.8
• CE Ind – Structures	1	11.6
• CE Ind - Refrigeration	1	7.8
• CE Ind – Liquid Fuels	1	7.2
• CE Ind – Electrical	1	7.3
• CE Ind – Tool Crib	1	4.5
• CE Maintenance	1	4.6
• Power Pro/Supply (7.5 Kw)	3	22.5
• Engineering Mgt (6 Kw)	2	12
• Chaplain	1	7.8
• CAF Add On		
AMU		
• CAF Follow-on	4	
Mx Backshop/Avionics	1	15
Mx Backshop/Electrical	1	15
Mx Backshop/Pneudraulics	1	15
Mx Backshop/Propulsion	1	15
• CAF Initial Support	8	
POL	3	15
Mx/CTK	1	5
SMO/MOC/Staff	1	4.5
AMU	1	6.3
General Maint Support (8 Kw)	2	16
• Combat Supply (8.25Kw)	4	33
• Fire Ops/Crash Rescue (4.5Kw)	4	18

TABLE B - 6: OPERATIONAL LOAD SUMMARY (2)

ITEM	QUANTITY	POWER DEMAND (kW)
• Mobility AF Support	8	
POL (5Kw)	3	15
Aerial Port	1	5
Ops/Classified Briefing	1	6
Ops/OG/Planning/Staff	1	5
Ops/OSS	1	5
Ops/Life Spt/Survival	1	5
• Mortuary Support	1	6.3
• Munitions Support	1	14.7
• SHL (included with SHL)	2	
• Shower/Shave/Latrine (included with SSL)	12	
• TFE	1	6
• Vehicle Ops/Maint	1	27.5
Medium Shelters (total)	20	
• Barrier Maint	1	7
• CE Ind – Pavements	1	6.9
• CAF Add-On		
Ops/Intel/Mission Planning		
Mx/AGE?		
• CAF Initial Support	8	
Ops/Intel/Mission Planning	1	15
Ops/Weather/Airfield Manager	1	15
Ops/Life Support	1	10
Mx AGE	1	8.2
Mx/Fuel Cell	1	10
Mx/Armament	1	10
Mx/Egress	1	10
Mx/Structures	1	10
• Mobility AF Support	6	
Ops/Aircrew Briefing	1	10
Ops/Life Spt/Survival (10 Kw)	2	20
Mx/CTK	1	9
Mx/AGE (9Kw)	2	18
• Munitions (Included in Munitions)	1	
• Postal	1	6.5
• SPEK (Included in SPEK)	2	
4K Dome	3	
Vehicle Ops/Maint* (15Kw)	2	30
MAF	1	15

TABLE B - 7: OPERATIONAL LOAD SUMMARY (3)

ITEM	QUANTITY	POWER DEMAND (kW)
8K Dome	5	
Combat Supply (Included in CS)	1	
Traffic Management	1	12
CAF Initial	1	15
Community Center	1	20
Gym	1	15
LAMS (15 Kw)	4	60
ADR-300s (includes mortuary) (4.7Kw)	11	51.7
Water Production, 1500 ROWPU (Or 600)	1	45
Water Production, 600 ROWPU (Or 1500)	1	
Water Distribution – initial (36Kw)	1	36
Follow-on (7 Kw)	1	7
Source Run	1	
Extension Package	1	2.1
SPEK (1.5 Kw)	2	3
9-2 Kitchen(187 Kw) 125Kw + 62Kw for 4 FDECU's	2	374
Self Help Laundry (172 Kw)	2	344
Shower/Shave/Latrine (12 Kw)	6	72
RALS (2.1 Kw)	6	12.6
EMEDS	1	200
FACILITY LOAD SUBTOTAL		2296
.7 Demand Factor		1607.2

The total connected load is estimated at 2.30 MW. After applying a demand factor of 70%, the average operational load is estimated at 1.61 MW. Since a base of this size would be in operation twenty four hours per day, the operational load varies as little as $\pm 5\%$ of the average value over the course of the day. The highest load is likely to be at meal times (set at 0000, 0600, 1200, and 1800) due to the high power demand of the kitchen. Lower loads are expected between these times.⁴⁴ For the purposes of this simulation, the operational load is modeled as a sinusoid with average value 1.61 MW, amplitude of 80.5 kW, and period of six hours. The equation for this load model is shown below:

$$L_{op}(t) = 80.5 \cos(\pi t/3) + 1607.2 \text{ kW} \quad (\text{B.1})$$

⁴⁴ Scheffler, Timothy D, Capt, USAF. *AFIT Civil Engineer School*. Telephone interview. 11 June 2010.

where t is the number of hours past 0000 on 1 Jan. This load estimate is used for base locations in both Marjah, Afghanistan and Cannon AFB, NM.

HVAC LOAD

Recent studies of USAF expeditionary power show that environmental control units (ECUs) make up more than half of the power demand at forward operating bases (FOBs).⁴⁵ As a result, a reliable estimate of the heating and air conditioning needs at a FOB is necessary for an accurate simulation. The model of the ECU loads must start with an estimate of the ambient temperature in Marjah and at Cannon AFB for each hour across an entire typical year. This temperature estimate can then be used to construct a model of the ECU load for the entire base for each hour of the year.

TEMPERATURE MODEL DEVELOPMENT - MARJAH

In the case of Marjah, Afghanistan, two main obstacles must be overcome in the construction of an accurate temperature model: climate data for the region is limited and temperature must be correlated to solar radiation. The first obstacle is simply a matter of record-keeping. The best climate data this author could find were monthly average low and high temperatures recorded in a paper released in 1959.⁴⁶ The same paper also noted that “there is little doubt that the most analogous area in the United States for the Helmand Valley [where Marjah lies] is that of southern Arizona or southeastern California, especially when comparable elevations are selected.” For some of the analysis presented here, where noted, the city of Tucson, AZ (elev. 728m) is used as an analogue for Marjah (elev. 775m).

⁴⁵ Boswell, Randy L. *The Impact of Renewable Energy Sources on Forward Operating Bases*. Rep. Air University: Air Command and Staff College, 2007. Print.

⁴⁶ Michel, Aloys A. *The Kabul, Kunduz, and Helmand Valleys and the National Economy of Afghanistan*. Publication. Washington, DC: National Academy of Sciences - National Research Council, 1959. Print, pg 144.

With regard to the second obstacle, this simulation involves the use of photovoltaic (PV) arrays to convert sunlight into useful power for the base. The amount of power generated by the PV arrays is approximately proportional to the amount of solar radiation incident on the panels. However, the temperature, and thus the ECU load, will also vary with solar radiation as days with more direct sunlight tend to be warmer than cloudy days. Therefore, to improve simulation accuracy, the temperature estimates presented here must be driven by the solar radiation estimates presented in Appendix A. To accomplish this, an hour-by-hour Matlab simulation of temperature across an entire typical year was implemented. The underlying model for this simulation was the equations:

$$\frac{\Delta T}{\Delta t} = -k_1(T - T_{min}) + k_2\sqrt[4]{R} \quad (\text{B.2})$$

$$T_{n+1} = T_n + \Delta T \quad (\text{B.3})$$

where T is the temperature in degrees Fahrenheit, T_{min} is the low temperature for a particular day in degrees Fahrenheit, R is the solar radiation in kW/m^2 , t is the time in hours, n is the current hour of the year, and k_1 and k_2 are positive proportionality factors. Since this model was run on an hourly time scale, Δt is always one hour, and B.2 becomes:

$$\Delta T = -k_1(T - T_{min}) + k_2\sqrt[4]{R} \quad (\text{B.4})$$

Before discussing the mechanics of calculating the entire year's hourly temperatures, it is first important to understand each term of equation B.4. This climate model is admittedly very simple as it only consists of two terms: a heating term and a cooling term. The first term, $-k_1(T - T_{min})$, is essentially an exponential decay cooling term. At night, when there is no solar radiation, this term leads to an exponential decay in temperature until $\Delta T \cong 0$ and $T \cong T_{min}$. Thus it is clear that T_{min} will be approximately the night time low temperature. The scaling factor k_1 is used to change the rate of decay.

The second term, $k_2\sqrt[4]{R}$, is a solar radiation heating term. From some very simple mathematical temperature models, it has been established that temperature is approximately proportional to the fourth-root of solar radiation.⁴⁷ This term implements this effect; however, it acts on the change in temperature rather than the temperature itself. The daily high temperature in most locations lags peak solar radiation by two hours or more, which is an important effect to model with regard to PV production and ECU load. This term intentionally introduces a similar lag in the model temperature with respect to the solar radiation. It is also important to note that the relationship between the factors k_1 and k_2 determines the maximum temperature that can be achieved each day. During the day time, the maximum temperature is achieved when $\Delta T = 0$ or (from B.4):

$$k_1(T_{max} - T_{min}) = k_2\sqrt[4]{R_{max}} \quad (\text{B.5})$$

From this analysis, the model can be completed and run through the following four-step process:

STEP 1: APPROXIMATING k_1

An approximation for the proportionality factor k_1 can be determined by observing the night time cooling pattern for Tucson, AZ. An approximate value of $k_1 = 1/7$ was determined through trial and error based on forecast data for Tucson.⁴⁸ This value, which appears to be a good match for the actual night time cooling profile, is assumed constant throughout the year. This value is also assumed applicable to Marjah. The following plot shows the actual forecast data along with the model data using $k_1 = 1/7$ for a typical summer night in Tucson with a sunset temperature of 89°F and a low temperature of 68°F.

⁴⁷ "Zero-Dimensional Energy Balance Model." *New York University, Courant Institute, Department of Mathematics*. Web. 30 June 2010.

⁴⁸ "Hour by Hour Weather Forecast for Tucson, AZ - Weather.com." *The Weather Channel*. Web. 08 July 2010. <<http://www.weather.com/outlook/recreation/outdoors/hourbyhour/USAZ0247>>.

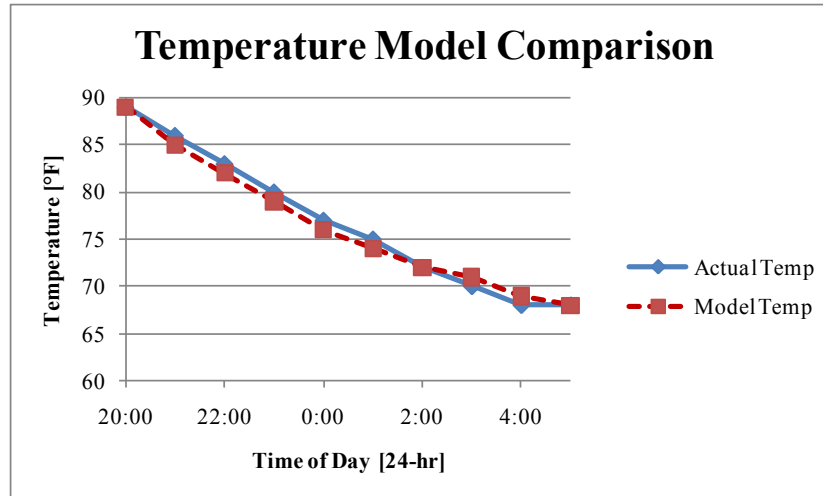


FIGURE B - 1: COMPARISON BETWEEN TEMPERATURE MODEL AND ACTUAL FORECAST COOLING

STEP 2: DETERMINING T_{MIN}

Daily low temperatures can be generated using a probability distribution about the monthly average low temperatures. First, an average daily low temperature curve is generated using a linear approximation between the monthly average lows. Then, a random value from a normal distribution with mean zero and standard deviation four degrees Fahrenheit is added to each average daily low temperature. This introduces variation in the low temperatures which would be caused by effects not included in the model itself (humidity, night time cloud cover, etc). These values are then reduced by an additional factor of 11% of the average daily low (determined through trial and error). This factor compensates for the fact that the exponential decay in temperature never actually reaches the value of T_{min} . To achieve the low temperatures desired T_{min} is set 11% lower than the actual low temperature. The final result is a vector of 365 values for T_{min} that tracks the monthly average low temperatures with some daily variation and an offset of 11%.

STEP 3: DETERMINING K_2

An approximation for the proportionality factor k_2 can then be found from equation B.5. Since k_1 and T_{min} are now known, the only values needed to solve for k_2 are T_{max} and R_{max} . In

addition, since T_{min} is a vector of daily low temperatures, daily values for T_{max} and R_{max} are also required to solve for daily values of k_2 . In other words, k_2 is not strictly a constant; it has a value for each day of the year. To determine T_{max} , or the maximum temperature possible on a cloudless day, the maximum deviation above the mean high temperature for each month must be known for Marjah. Since this data is not available, the following table from 2005 data for Tucson, AZ is used⁴⁹.

TABLE B - 8: PEAK TEMPERATURE DEVIATION FOR TUCSON, AZ (2005)

Month	Mean Hi (°F)	Deviation(°F)
January	69.1	14
February	72.5	7
March	77.9	14
April	82.1	13
May	94.9	14
June	96.8	9
July	102.5	7
August	101.9	8
September	96.5	9
October	83.7	10
November	78.7	12
December	63.4	13

This table shows, for example, that the peak temperature recorded in May of 2005 for Tucson was approximately 109°F, or about 14°F above the mean high temperature for that month. Using Tucson as an analogue for Marjah, the peak temperature deviations are assumed the same for both cities. Therefore, the following table based on the mean high temperatures for Marjah⁵⁰ and the deviations from Tucson was generated:

⁴⁹ "Monthly Climate Reports." *National Weather Service - Western Region Headquarters*. Web. 07 July 2010. <<http://www.wrh.noaa.gov/twc/climate/monthly/2009.php>>.

⁵⁰ Michel, 144.

TABLE B - 9: SYNTHESIZED MONTHLY PEAK TEMPERATURES FOR MARJAH, AFGHANISTAN

Month	Mean Hi (°F)	Peak (°F)
January	58.4	72.4
February	64.8	71.8
March	72.0	86.0
April	88.2	101.2
May	99.1	113.1
June	106.4	115.4
July	108.5	115.5
August	103.1	111.1
September	97.2	106.2
October	81.9	91.9
November	72.0	84.0
December	62.8	75.8

These monthly peak temperatures can be used to create a daily peak temperature profile using a linear interpolation between the points. This generates a vector of 365 daily peak temperatures – i.e. the highest temperature one would expect on that day if it were totally cloudless. These values, once increased by a factor of 10% (determined through trial and error), become the daily values for T_{max} . The 10% factor, similar to that used for T_{min} , is necessary because the model temperature never rises to exactly T_{max} over the course of one day.

To determine R_{max} , it is assumed that the peak solar radiation across an entire month is very close to the solar radiation that would be present on a cloudless day. In other words, it is assumed that at least one day a month is cloudless. Under this assumption, the peak solar radiation across each month can be determined from the solar radiation estimates for Marjah. A linear approximation can then be applied to form a daily radiation index – i.e. the maximum radiation one would expect on that day if it were totally cloudless. These daily radiation index values are the daily R_{max} values needed to solve for k_2 on a daily basis. With all other parameters known for equation B.5, daily values for k_2 are calculated from this simple algebraic equation.

STEP 4: RUNNING THE MODEL

Once all the parameters have been calculated, the model can be used to calculate a temperature profile for an entire typical year on an hourly basis using equations B.3 and B.4. Starting with an initial seed temperature of 45°F for 0000 on 1 Jan, the model calculates the temperature at the next hour by finding ΔT at the current hour (B.4) and adding it to the temperature at the current hour (B.3). It runs in this manner until a temperature has been calculated for all 8,760 hours of the year.

TEMPERATURE MODEL RESULTS - MARJAH

The following plots show the results of the temperature model for Marjah, Afghanistan.

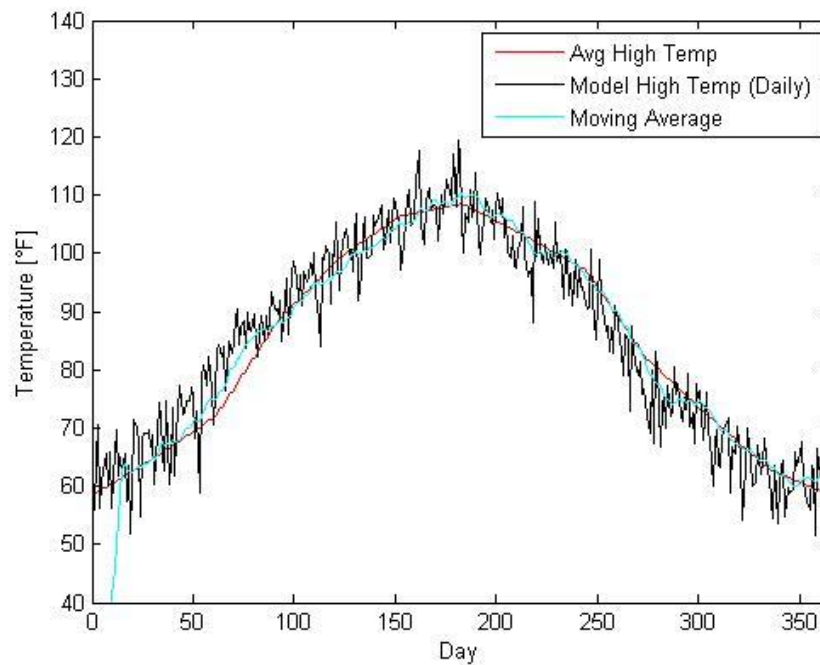


FIGURE B - 2: MARJAH MODEL DAILY HIGH TEMPERATURES

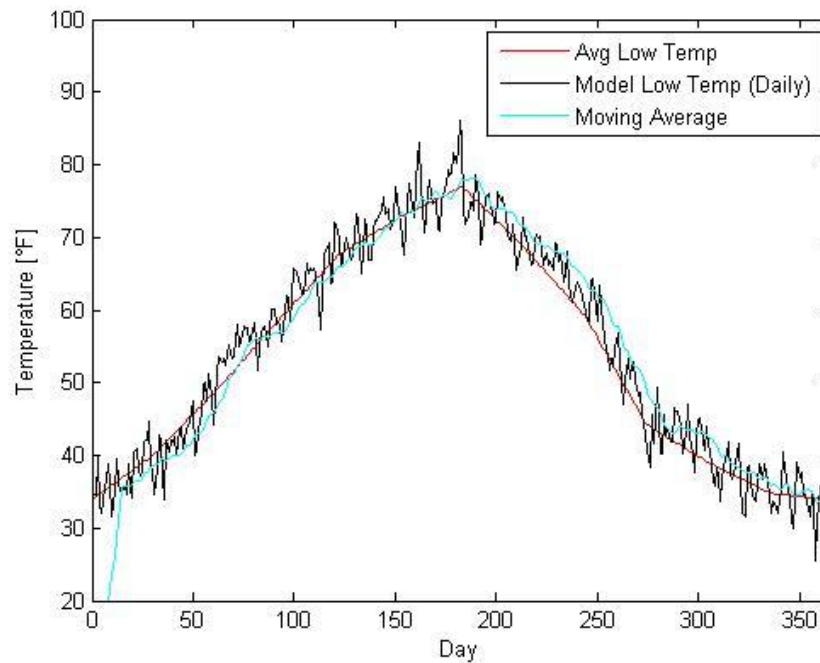


FIGURE B - 3: MARJAH MODEL DAILY LOW TEMPERATURES

Figure B – 2 shows the daily mean high temperatures based on a linear interpolation of the monthly mean high temperatures (red)⁵¹, the daily high temperatures generated by the model for Marjah (black), and a 15-day moving average of the model high temperatures (cyan). Considering the simplicity of the model, it appears to fit the measured monthly averages very closely.

Figure B – 3 shows the daily mean low temperatures based on a linear interpolation of the monthly mean low temperatures (red)⁵², the daily low temperatures generated by the model for Marjah (black), and a 15-day moving average of the model low temperatures (cyan). Again, considering the simplicity of the model, it appears to fit the measured monthly averages very closely.

⁵¹ Michel, 144.

⁵² Ibid.

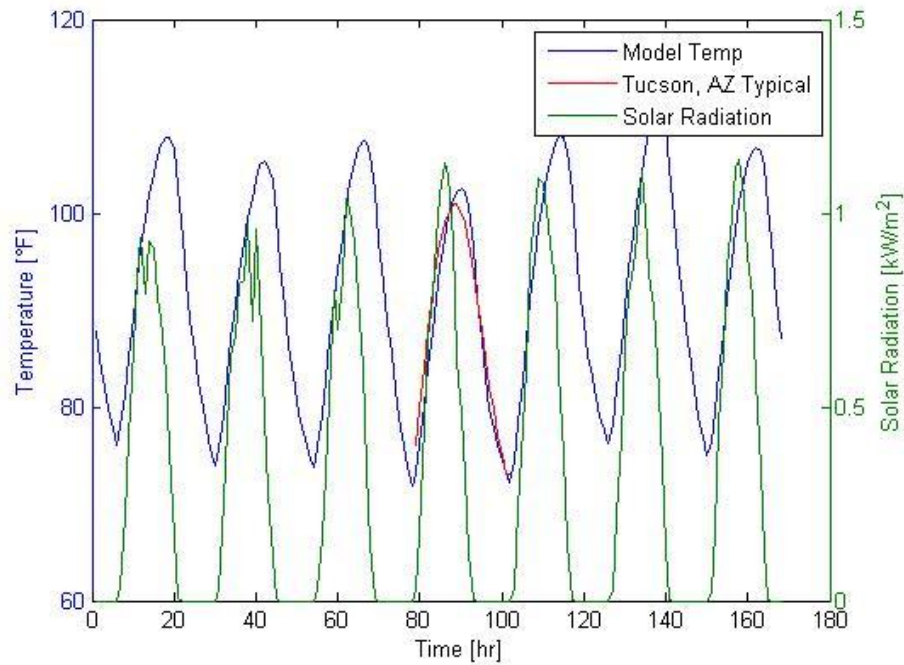


FIGURE B - 4: MARJAH MODEL WEEKLY PROFILE

Figure B-4 shows a typical week in June for the Marjah temperature model. Note that the peak temperature lags peak solar radiation by approximately 2-3 hours. Additionally, the daily heating and cooling profile appears to fit very well with a typical summer day in Tucson⁵³.

TEMPERATURE MODEL DEVELOPMENT – CANNON AFB

Although hourly temperature data for an entire typical year may exist, the above model was also used to synthesize temperature estimates for Cannon AFB for three reasons. First, it is still important to ensure that the daily temperatures are correlated with the solar radiation estimates used. Second, using the temperature model for both scenarios allows for an equal comparison between the simulations for both Marjah and Cannon AFB. Finally, the author was unable to obtain reliable hourly temperature data for Cannon AFB in the timeframe of this project.

⁵³ *The Weather Channel.*

The model was used as described above for the Marjah location with only two primary differences: the monthly average temperature values used and the factor applied to T_{max} . The following table shows the monthly average high, average low, and peak temperatures used for the Cannon AFB temperature model.⁵⁴

TABLE B - 10: ACTUAL MONTHLY AVERAGE HIGH, AVERAGE LOW, AND PEAK TEMPERATURES FOR CANNON AFB, NM

Month	Mean Hi (°F)	Peak (°F)	Mean Lo (°F)
January	51.2	65.2	23.5
February	56.0	63.0	26.9
March	62.8	76.8	32.1
April	72.2	85.2	41.1
May	80.8	94.8	50.6
June	89.4	98.4	59.5
July	92.0	99.0	63.5
August	90.1	98.1	62.1
September	83.7	92.7	55.0
October	73.2	83.2	43.9
November	60.5	72.5	32.1
December	52.0	65.0	25.0

Additionally, through trial and error, it was determined that a 5% increase to T_{max} allowed for a more appropriate fit than the 10% factor used with the Marjah model.

TEMPERATURE MODEL RESULTS – CANNON AFB

The following plots show the results of the temperature model for Cannon AFB, NM.

⁵⁴ "CLOVIS, NEW MEXICO - Climate Summary." *Western Regional Climate Center*. Web. 08 July 2010. <<http://www.wrcc.dri.edu/cgi-bin/cliMAIN.pl?nmclov>>.

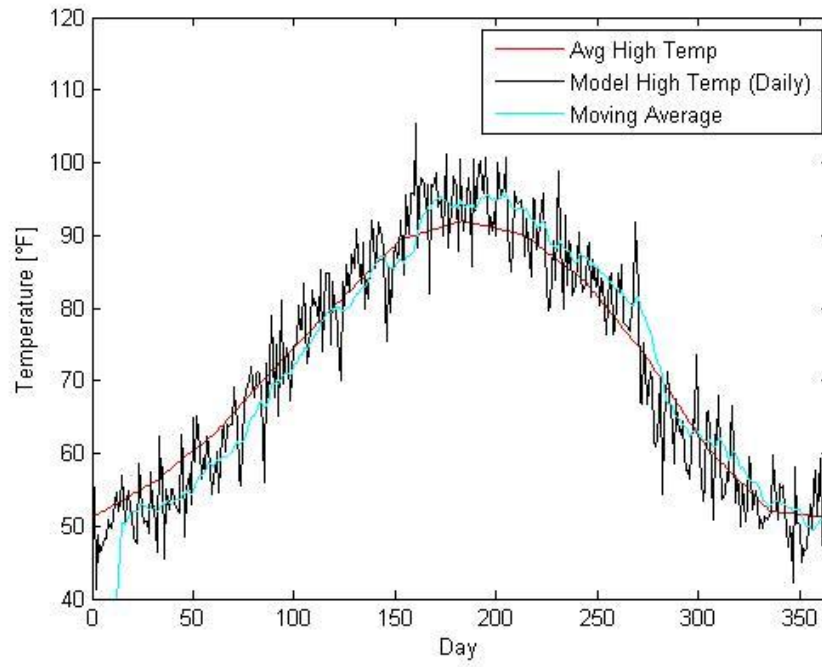


FIGURE B - 5: CANNON MODEL DAILY HIGH TEMPERATURES

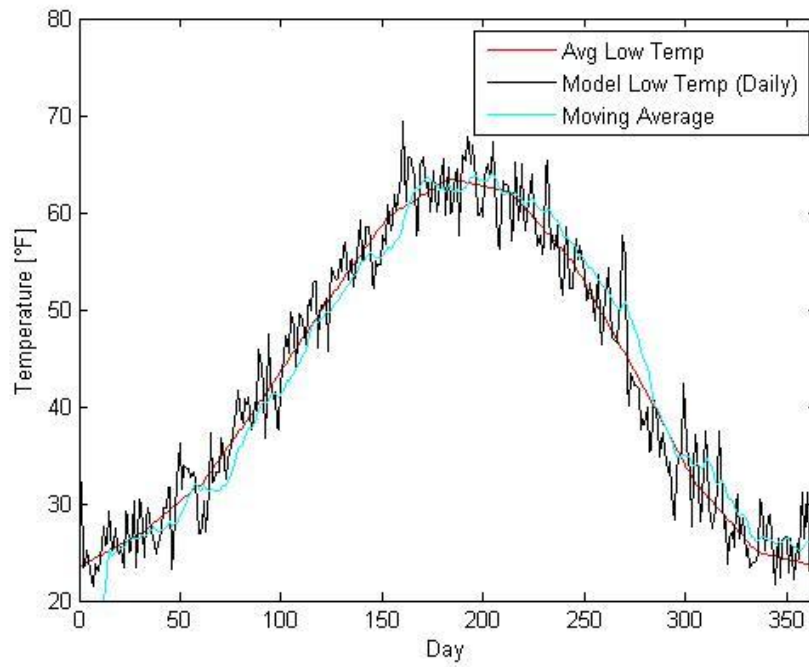


FIGURE B - 6: CANNON MODEL DAILY LOW TEMPERATURES

Figure B – 5 shows the daily mean high temperatures based on a linear interpolation of the monthly mean high temperatures (red)⁵⁵, the daily high temperatures generated by the model for Cannon AFB (black), and a 15-day moving average of the model high temperatures (cyan). The model does not fit quite as well for Cannon AFB as it does for Marjah. This is probably due to the effects of higher humidity and afternoon thunderstorms at Cannon AFB, particularly in the summer months, that are not accounted for in this model. One must keep in mind that the results of this simulation are based on a relatively cool winter and warm summer for Cannon AFB, on the order of two degrees below and four degrees above average, respectively.

Figure B – 6 shows the daily mean low temperatures based on a linear interpolation of the monthly mean low temperatures (red)⁵⁶, the daily low temperatures generated by the model for Cannon (black), and a 15-day moving average of the model low temperatures (cyan). Considering the simplicity of the model, it appears to fit the measured monthly averages very closely.

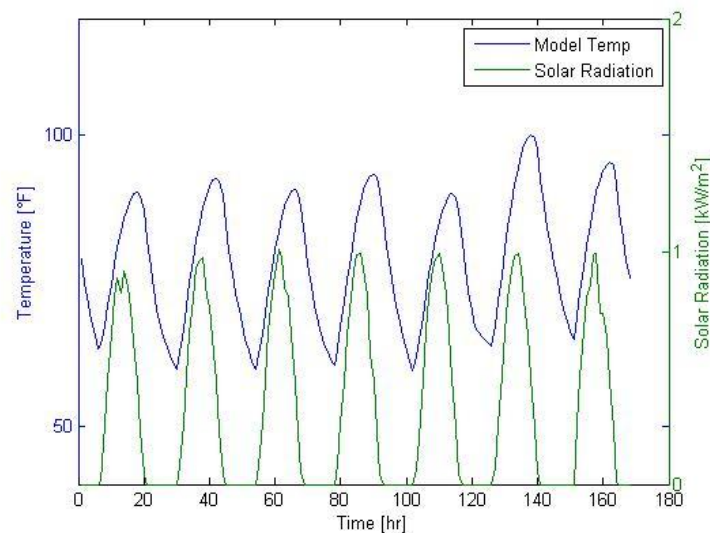


FIGURE B - 7: CANNON MODEL WEEKLY PROFILE

⁵⁵ *Western Regional Climate Center.*

⁵⁶ *Ibid.*

Figure B-7 shows a typical week in June for the Cannon temperature model. Note that the peak temperature lags peak solar radiation by approximately two hours.

ECU LOAD MODEL

The Field Deployable Environmental Control Units (FDECUs or simply ECUs) used by the Air Force in contingency operations are essentially heat pump-operated air conditioning and heating units.⁵⁷ The ECUs are not in continuous operation, but instead are activated by an automatic control system set to maintain a desired shelter temperature. Typical temperature set points for these units are around 75°F.⁵⁸ Limited data for the power consumption of a single unit at different ambient, day time temperatures are listed in the table below.⁵⁹ Note that these values are average loads rather than instantaneous loads.

TABLE B - 11: ECU AVERAGE LOAD

Ambient Temperature (°F)	ECU Load (kW)
85	10.5
95	11.8
105	13.6
115	15.5
125	15.5

In order to accurately model the ECU load of an entire FOB, these data must be extrapolated to determine the approximate load for ambient temperatures in the range of 20°F – 115°F for both day time and night time operation.

To extrapolate the data in the day time case, several assumptions were made. First, 30% of the peak ECU power is assumed to be consumed by the internal and cooling coil fans and other fixed loads. The rest of the load (approximately 10.9 kW at the peak of operation) is

⁵⁷ Army Technical Manual TM-9-4120-411-14, Chapter 1.

⁵⁸ Ibid, §2.1.4.

⁵⁹ Provided by HQ AFCESA/CEXX.

assumed to be the power required to operate the heat pump. Additionally, the average load of the heat pump is assumed to vary linearly with ambient temperature with a slope of approximately 0.168 kW/°F, averaged over cycling of the compressor, etc. The shelters themselves are assumed to be capable of 10°F of passive heating or cooling by opening or closing tent flaps and/or doors (with the ECU fan still running). Finally, heating is assumed to be equally efficient as cooling – i.e. heat pump load is linear with a slope of -0.168 kW/°F when heating is needed. For night time operation, it is assumed that the lack of radiative heating from the sun accounts for a drop in cooling demand (or increase in heating demand) of 4.05 kW.⁶⁰ The equations used to calculate average ECU load from ambient temperature are as follows:

$$P_{day}(T) = \begin{cases} -0.168T + 11.47, & T < 40.9 \\ 4.6, & 40.9 \leq T \leq 50.9 \\ 0.168T - 3.95, & T > 50.9 \end{cases} \quad (\text{B.6})$$

$$P_{night}(T) = \begin{cases} -0.168T + 15.57, & T < 65 \\ 4.6, & 65 \leq T \leq 75 \\ 0.168T - 8.00, & T > 75 \end{cases} \quad (\text{B.7})$$

In these equations, P_{day} and P_{night} are the average loads of a single ECU unit in kW and T is the ambient temperature in degrees Fahrenheit. The following plot illustrates the average ECU load for temperatures from 20°F – 115°F for both day time and night time operation. Note that only the fan load is required between approximately 40.9°F - 50.9°F during the day and 65°F – 75°F at night. This is admittedly quite an extrapolation based on the limited data set available; however, this author believes these assumptions to be reasonable in the absence of more specific information.

⁶⁰ Based on a linear approximation, the total average day-time load at 75°F would be approximately 8.65 kW. The heat pump load is therefore approximately 4.05 kW. In this case, the ambient temperature is equal to the shelter set point at 75°F, which means that the 4.05 kW is attributed to radiative heating from the sun.

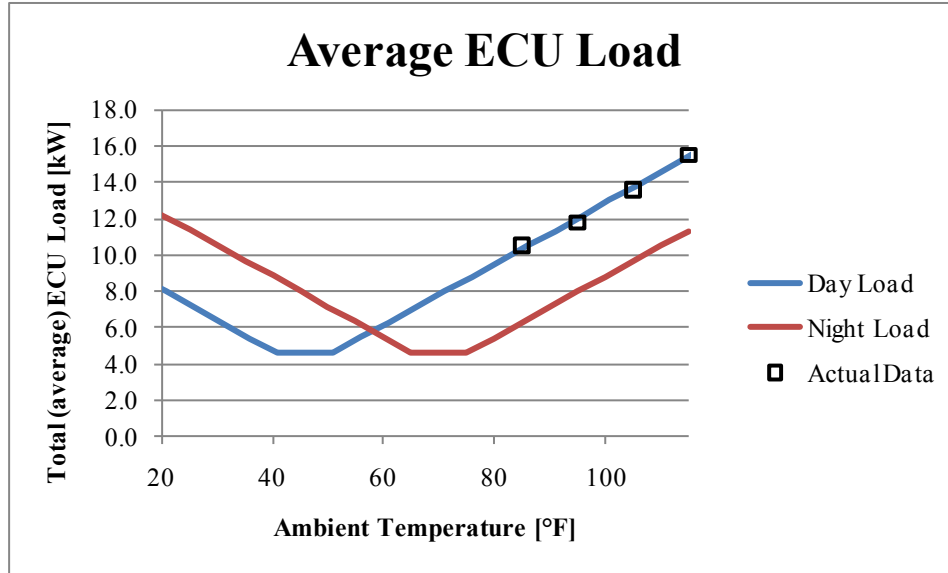


FIGURE B - 8: AVERAGE ECU LOAD VS. AMBIENT TEMPERATURE

These average load values can be used as an approximation for the base ECU load. For each hour of the year, the power consumption of a single unit is calculated from equations B.6 and B.7 with ambient temperature input from the temperature model described previously.⁶¹ The average load across that hour of a single ECU is then multiplied by the total number of units at the base (207 ECUs⁶²) to form the total base HVAC load for that hour of simulation.

TOTAL LOAD

Once the operational and HVAC loads have been calculated for both the Marjah, Afghanistan and Cannon AFB, NM scenarios, the addition at each hour of these two load components forms the total load.

$$P_{total} = P_{operational} + P_{HVAC} \quad (B.8)$$

The following plots illustrate the total load profile for the Marjah, Afghanistan site⁶³.

⁶¹ An hour of simulation is considered “night” if the solar radiation is less than 0.01 kW/m².

⁶² HQ AFCESA/CEXX.

⁶³ Plots generated by HOMER.

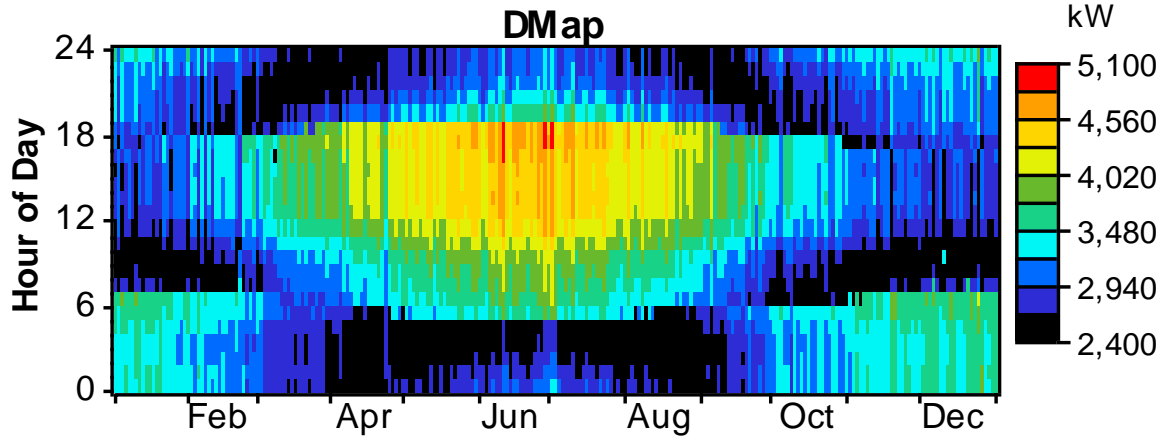


FIGURE B - 9: MARJAH YEARLY LOAD PROFILE

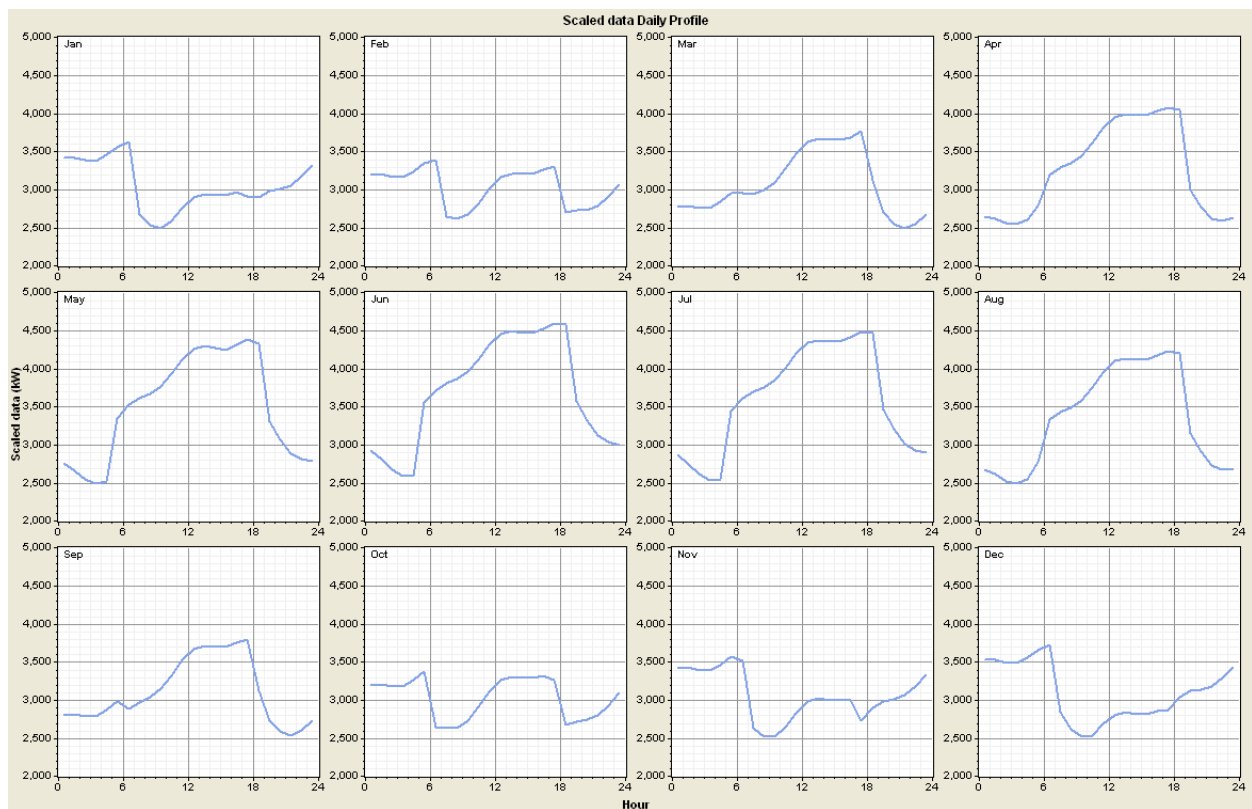


FIGURE B - 10: MARJAH "AVERAGE DAY" LOAD PROFILE BY MONTH

Figure B – 9 shows the load profile for each hour across the entire year. On the x-axis is the day of the year; on the y-axis is the hour of the day; and on the z-axis (color) is the load at that particular time. Figure B – 10 shows an average day’s load profile for each month of the year with the hour of the day on the x-axis and the load on the y-axis. The Marjah load profile

peaks at 4.98 MW with an average load across the entire year of 3.24 MW. Note that the highest load times are in the afternoon on summer months, which is consistent with the observation that HVAC loads make up at least half of the peak load at most FOBs.

Likewise, the following plots illustrate the total load profile for the Cannon AFB, NM site⁶⁴.

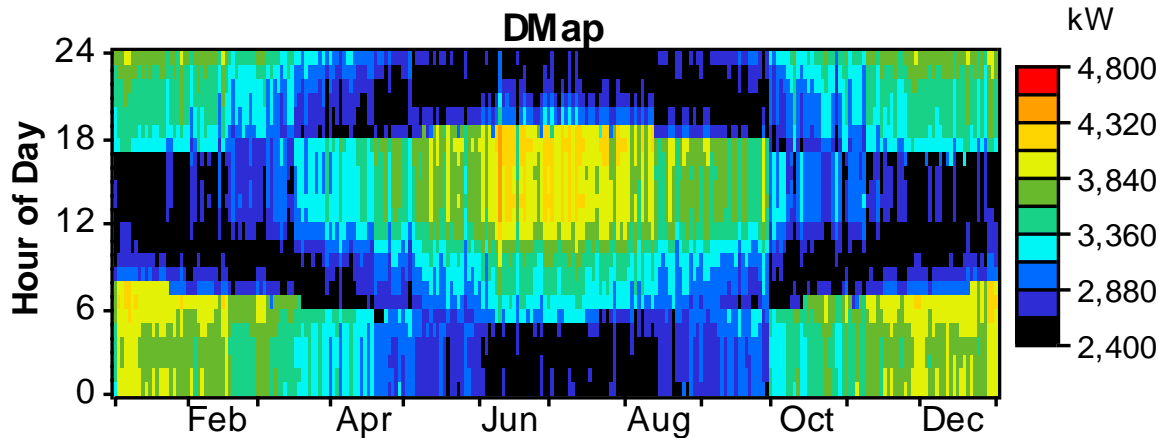


FIGURE B - 11: CANNON AFB YEARLY LOAD PROFILE

Figure B – 11 shows the load profile for each hour across the entire year. On the x-axis is the day of the year; on the y-axis is the hour of the day; and on the z-axis (color) is the load at that particular time. Figure B – 12 shows an average day's load profile for each month of the year with the hour of the day on the x-axis and the load on the y-axis. The Cannon AFB load profile peaks at 4.48 MW with an average load across the entire year of 3.16 MW. Note that although the peak load for the Cannon AFB site is significantly lower than that for Marjah, the average load is very similar. This is likely due to the fact that while HVAC load in the summer months is lower for cooler Cannon, significantly more heating in the winter months is required there than in Marjah.

⁶⁴ Plots generated by HOMER.

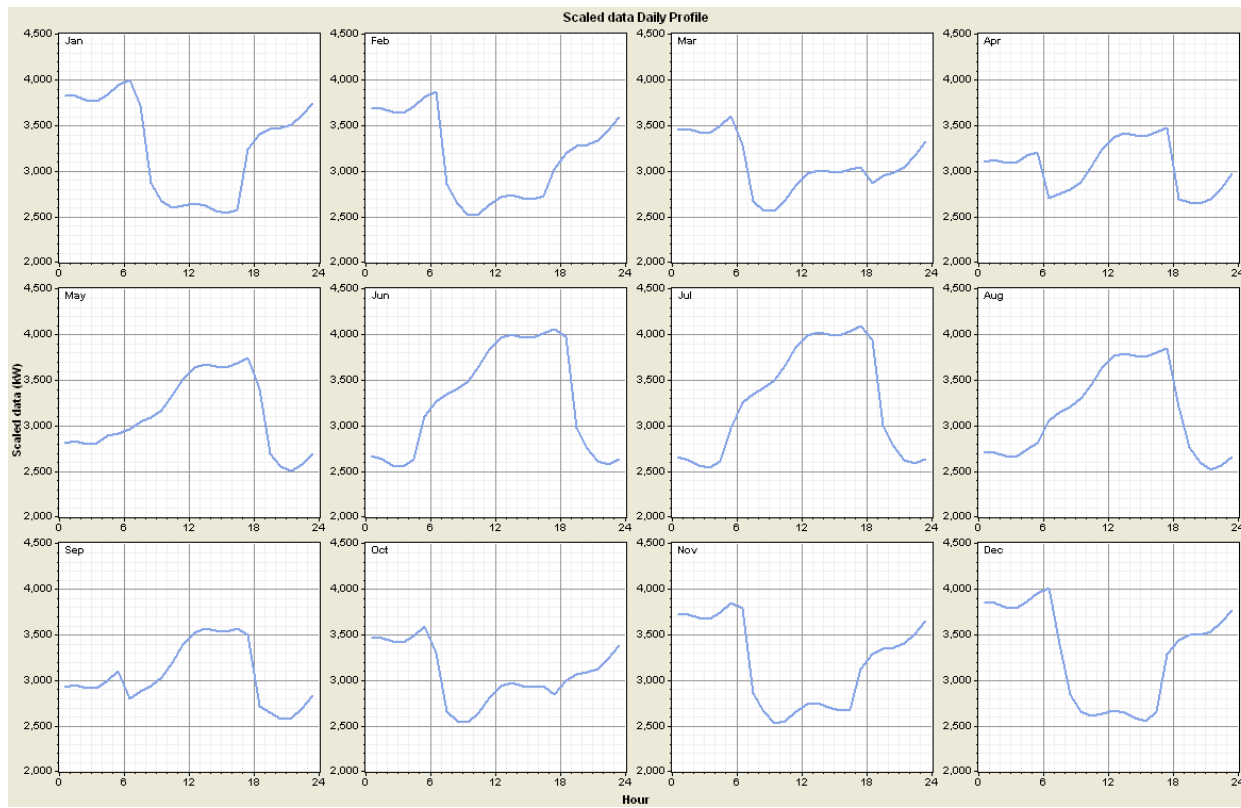


FIGURE B - 12: CANNON "AVERAGE DAY" LOAD PROFILE BY MONTH

[This Page Intentionally Left Blank]

APPENDIX C – EQUIPMENT MODELS

Models of all relevant pieces of equipment were needed to accurately simulate a BEAR base power generation system including renewable energy sources. Specifically, models were needed for the generators, wind turbines, PV panels, energy storage systems, and inverters used in this simulation. Since fuel consumption was an important result of the simulations, the focus in developing these models was on the energy generation and storage efficiency of each component.

GENERATOR MODEL

The following values were needed to populate the model for each of the eight main generators: generation capacity (kW), operational lifetime (hr), minimum load ratio (percent), and a fuel efficiency curve. These values were developed based on the following information.

The primary generator used by the USAF for BEAR base operations is the MEP-12A diesel generator. The MEP-12A produces 750 kW continuous, three phase power at 60 Hz and 4160 V (line-to-line) with a power factor of 0.8 lagging.⁶⁵ Therefore, the generation capacity was set to 750 kW in HOMER. Additionally, the generator must be overhauled approximately every 10,000 operational hours, which is used as the operational lifetime.⁶⁶ Note that it is assumed that the generators are never completely replaced over the two to eight year simulation timeframe – they are only overhauled every 10,000 hours. For the purposes of these simulations, the HOMER default value for minimum load ratio of 30% was used. This means that each MEP-12A can only provide power in the range of 225 – 750 kW.

⁶⁵ AFH 10-222 Vol. 5. 1 Jul 2008, 13.

⁶⁶ HQ AFCESA/CEXX.

The mechanical power source for the MEP-12A is the Cummins Engine Company KTA38-G3 turbocharged and aftercooled 12-cylinder diesel engine.⁶⁷ The diesel engine itself is rated for 776 kWm at 1800 rpm (60 Hz). Cummins Engine Company also provided the following (mechanical) output power versus fuel consumption curve for the KTA38-G3 at 1800 rpm (Figure C – 1). Note that this fuel curve is based on industry-standard diesel fuel rather than the JP-8 typically used by DoD in the field. For the purposes of this analysis, all generators are assumed to be equally fuel efficient on diesel and JP-8.

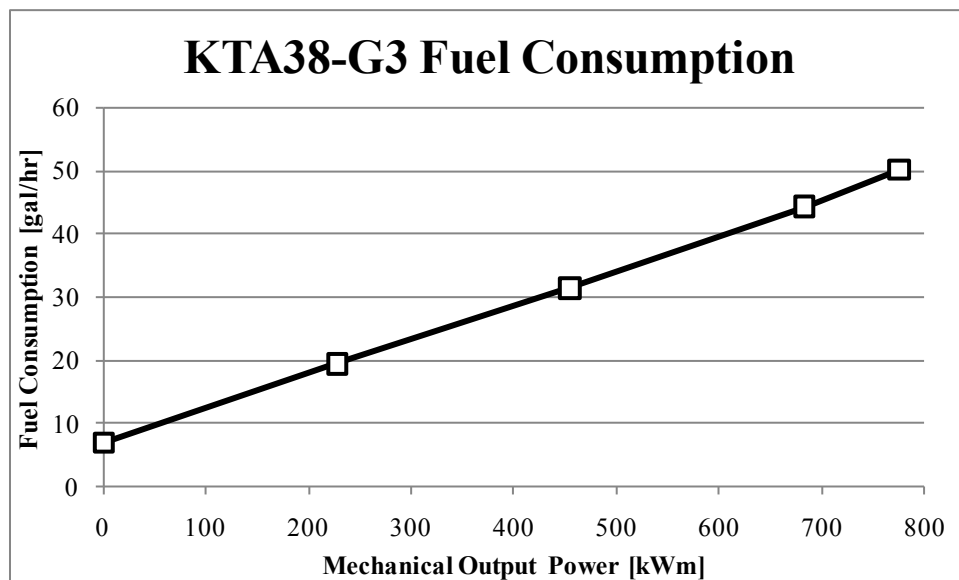


FIGURE C - 1: KTA38-G3 FUEL CONSUMPTION (1800 RPM)

What is of more importance in these simulations, however, is the relationship between electrical output power and fuel consumption. Since the engine is rated at 776 kWm and the generator is rated at 750 kW, it was assumed that mechanical and hysteresis losses are approximately 3.35% (i.e. generator efficiency is 96.65%). This 3.35% reduction was applied across the entire range of output power values to generate an electrical power versus fuel consumption curve, shown in Figure C – 2.

⁶⁷ Courtesy of Cummins Engine Company, Inc, Columbus, Indiana.

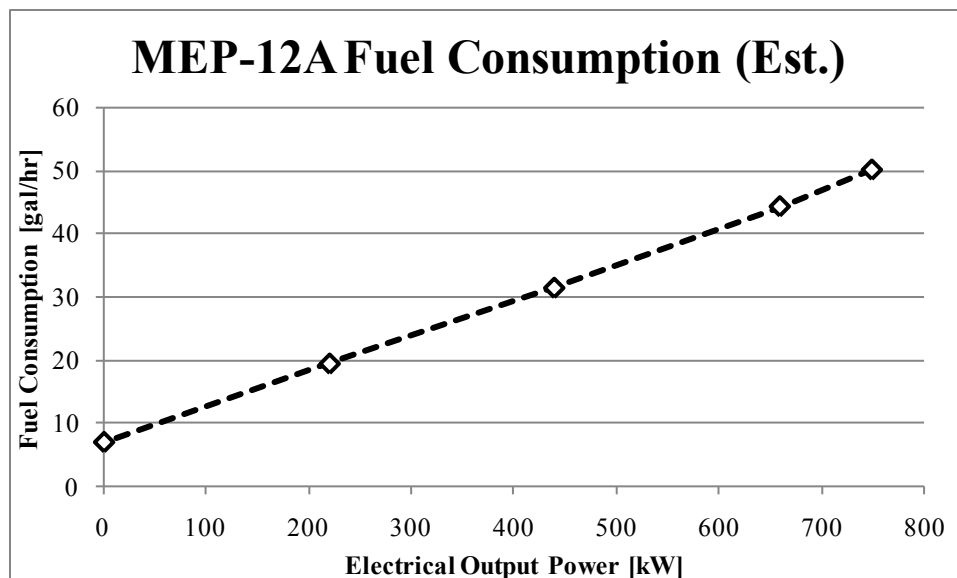


FIGURE C - 2: MEP-12A FUEL CONSUMPTION (ESTIMATE)

Using the fuel consumption curve in Figure C – 2, HOMER automatically calculates two parameters that fully describe the efficiency of the generator: the intercept coefficient (L/hr/kW rated) and the slope (L/hr/kW output). The estimates used for these values for the MEP-12A were 0.03425 and 0.2162, respectively. Figure C – 3 shows the estimated MEP-12A generator efficiency curve calculated by HOMER. Note that these generators are most fuel-efficient near 100% rated load with a rapid decrease in efficiency beginning below about 80% rated load.

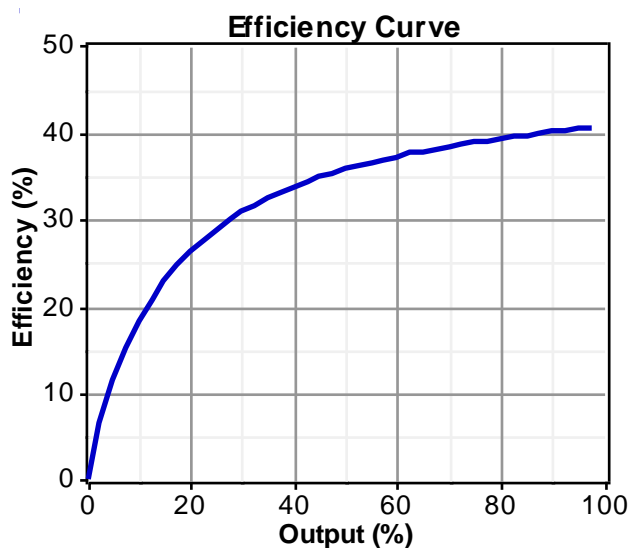


FIGURE C - 3: MEP-12A EFFICIENCY CURVE (ESTIMATE)

In summary, the following values were used for the HOMER model of the MEP-12A generator:

- Generation Capacity: 750 kW
- Operational Lifetime: 10,000 hr
- Minimum Load Ratio: 30%
- Fuel Efficiency Intercept Coefficient: 0.03425
- Fuel Efficiency Slope: 0.2162

WIND TURBINE MODEL

The following values were needed to populate the model for each wind turbine: operational lifetime (yr), hub height (m), and a power generation curve. These values were developed based on the information that follows.

The turbine used for these simulations was the community-scale Northern Power Northwind 100 turbine. Use of this particular turbine in simulation does not constitute endorsement of this model over other similar-sized turbines. This particular turbine was used because technical data needed for simulation was readily available. The Northwind 100 (NW100) is rated for 100 kW production at a wind speed of 14.5 m/s under standard conditions. It provides three phase power at 60 Hz and 480 VAC with a cut-in wind speed of 3.5 m/s and a cut-out wind speed of 25 m/s. The turbine is survivable to wind speeds of 59.5 m/s.⁶⁸ The NW100 can be installed on either a 30m or 37m tower, with a rotor diameter of 21m.⁶⁹ The 30m hub height was used for this simulation. The design life of this turbine is 20 years.⁷⁰ Table C – 1

⁶⁸ Northern Power. Northwind 100 Specifications, 2. Web. 21 Jul 2010. <<http://www.northernpower.com/pdf/specsheet-northwind100-us.pdf>>

⁶⁹ Northern Power. Northwind 100 Wind Turbine Logistics & Installation Guidelines, §1.2.1, 12 June 2008. Web. 21 July 2010. <<http://www.dcpower-systems.com/documents/Northwind100-InstallationGuidelines.pdf>>.

⁷⁰ Northwind 100 Specifications, 2.

and Figure C – 4 show the output power versus wind speed relationship for this turbine at standard conditions according to the specification sheet.

TABLE C - 1: NW100 OUTPUT POWER

Wind Speed (m/s)	Output Power (kW)
0	0
1	0
2	0
3	0
4	3.7
5	10.5
6	19
7	29.4
8	41
9	54.3
10	66.8
11	77.7
12	86.4
13	92.8
14	97.3
15	100
16	100.8
17	100.6
18	99.8
19	99.4
20	98.6
21	97.8
22	97.3
23	97.3
24	98
25	99.7
26	0

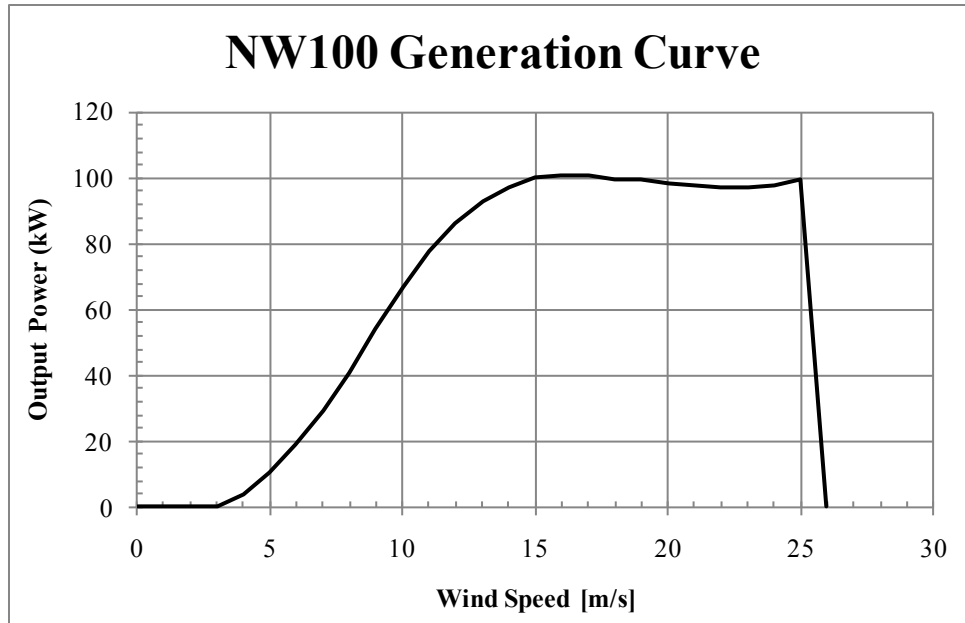


FIGURE C - 4: NW100 OUTPUT POWER CURVE

Note that HOMER automatically corrects for non-standard air density based upon the altitude of the site (775m for Marjah and 1300m for Cannon AFB).

In summary, the following values were used for the HOMER model of the NW100 turbine:

- Operational Lifetime: 20 yrs
- Hub Height: 30m
- Power Generation Curve: From Table C – 1

PV ARRAY MODEL

The following values were needed to populate the model for the PV array: output current (AC or DC), operational lifetime (yr), derating factor (percent), slope (degrees), azimuth (degrees W of S), ground reflectance (percent), and type of tracking system used. The model for the PV array in these simulations was a more generic model; that is, it was a model of a typical array rather than a specific array currently in production. This was relatively straightforward

since HOMER calculates PV power production based on the rated capacity of the array. In other words, values such as the relative efficiency were already rolled into the rated capacity figures.

HOMER also uses a derating factor to reduce the actual output of the solar array relative to its rated capacity. This factor is designed to account for “soiling of the panels, wiring losses, shading, snow cover, aging, and so on.”⁷¹ For these simulations, the derating factor was used to account primarily for aging. Efficiency of the PV array was modeled as a linear decay over time at a rate of 4% per year. For example, a solar array that would produce 100 kW in the lab was modeled at 100 kW for the first year, 96 kW for the second year, 92 kW for the third year, etc. The average of these values was taken to form the derating factor. For example, over a twenty year timeframe, the PV array was expected to shift from a derating factor of 100% to 60%, for an average factor of 80%. Based on these assumptions, derating factors of 98%, 96%, 94%, and 92% were used for the two, four, six, and eight year timeframes, respectively.

With the exception of derating factor, all of the default values for generic PV arrays were left untouched for these simulations. The values used were:

- Output Current: DC
- Operational Lifetime: 20 yrs
- Derating Factor: Simulation dependent (see above).
- Slope: Equal to the latitude of each location (31.50° for Marjah and 34.42° for Cannon AFB)
- Azimuth: 0°
- Ground Reflectance: 20%
- Tracking System Used: No Tracking

⁷¹ Lambert, Tom. *PV Derating Factor*. HOMER Help. 21 Nov 07.

ENERGY STORAGE MODELS

Two types of energy storage were compared in these simulations: lead-acid batteries and molten salt storage. For both types of storage systems, the cycle-charging dispatch strategy was used with a set point state of charge of 80%. In other words, storage systems were used in these simulations to attain generator efficiencies rather than load leveling. Since the instantaneous power generated by renewable sources rarely (if ever) exceeded the load for these simulations, cycle-charging is assumed to be the better dispatch strategy. For more information, see the HOMER help file on “Cycle Charging Strategy” by Tom Lambert. The development of the models for each type of storage system is described below.

LEAD-ACID BATTERIES

The lead-acid batteries used for these simulations were the Trojan L16P batteries from Trojan Battery Company. Again, use of these batteries for this project does not constitute an endorsement for this particular brand or model. These batteries were used because they are typical in technical specifications of those that might be used in the field and because a detailed model of these batteries was provided with HOMER. The Trojan L16P battery is a 6V, 360 Ah (2.16 kWh) battery with a roundtrip efficiency of 85%, float life of 10 years, and lifetime throughput of 1.075 MWh.⁷² For the purposes of these simulations, only two technical values were needed: the number of batteries per string and the initial state of charge (percent). The values used for this simulation were:

- Batteries per string: 80 (480V bus)
- Initial state of charge: 50%

⁷² Model included with HOMER.

The initial state of charge value was chosen to model a typical year that does not include installation of the batteries. Beginning each yearly simulation with an initial state of charge of 0% would have modeled a situation where the batteries are totally drained and recharged at the beginning and end of each year. This would not appear to be a realistic simulation. The value used is an approximation that should model a more realistic case.

MOLTEN SALT STORAGE

The molten salt storage system used for these simulations is a hypothetical system that could be developed in the near future (six months to two years). As a result, the values used are only estimates, but should be representative of a storage system that could be manufactured. The molten salt storage system is modeled with a bus voltage of 480V and capacity of 9 kAh (4.32 MWh). The roundtrip efficiency is 30% with a float life of 20 years and no lifetime throughput limitation. Max charge current is 2 kA (960 kW) with max discharge current of 1 kA (480 kW). The molten salt storage system also requires the same two values: number of batteries per string and initial state of charge. The values used for this simulation were:

- Batteries per string: 1 (480V bus)
- Initial state of charge: 80%

The initial state of charge used for the molten salt storage system is slightly higher than that used for the lead-acid battery system because the very high capacity of the molten salt system (4.32 MWh) will probably lead to a higher average charge (less draw-down). This assumption favors the molten salt storage system slightly (approximately 1.3 MWh of additional energy at the start of each year); however this author believes it to be a reasonable assumption.

INVERTER MODEL

Since the storage systems and PV array operate on a DC bus, inverters must be used to convert this electricity to AC (and in the case of the storage systems, rectifiers to convert AC to DC for storage). However, these simulations did not model the inverter/rectifier specifically. Cost values for both the PV array and storage systems were total installed costs which include the cost of inverters and rectifiers. The model for the converter was simply an overly large (e.g. 10 MW) inverter/rectifier that had zero cost. Therefore, the only relevant values needed for this simulation were: inverter efficiency (percent) and rectifier efficiency (percent). The following (default) values were used:

- Inverter Efficiency: 90%
- Rectifier Efficiency: 80%

APPENDIX D – ECONOMIC MODEL

The economic model for these simulations was developed in four steps. First, domestic installed costs for PV arrays, wind turbines, and storage systems were identified (no other factors are needed for the Cannon AFB simulation). Second, an additional factor was applied to account for the increased cost associated with installing renewable systems in a remote location. Third, a shipping cost factor was used to quantify the cost associated with shipping renewable components to Afghanistan. Finally, for the Marjah Leave-Behind Simulations only, the monetary benefit of the leave-behind strategy was quantified in terms of the value of leave behind energy (VLBE).

DOMESTIC COSTS

GENERATOR COST

A capital cost of \$240,000 per unit was used for the MEP-12A generators. Additionally, overhaul costs are expected to be \$70,000 per unit every 10,000 operating hours (this is used as the “replacement cost” in the HOMER simulation). Approximately \$600 per generator is needed for maintenance every 250 hours for filters, fluid, etc. A fixed maintenance cost of \$2.40/hr for each generator was used.⁷³

WIND TURBINE COST

To develop the cost model for wind turbines, an average installed cost of \$1,800/kW was used for the 20 turbine case (i.e. \$3.6 million to install 20 x 100 kW turbines).⁷⁴ A fixed cost of \$300,000 was assumed for crane use, site planning, etc. The cost of each additional turbine (after the first) was \$165,000. Maintenance costs were assumed to be approximately 1.5¢/kWh

⁷³ All generator cost estimates courtesy of HQ AFCEA/CEXX.

⁷⁴ Wisler, Ryan, and Mark Bolinger. Annual Report on U.S. Wind Power Installation, Cost, and Performance Trends. Rep. U.S. Department of Energy, May 2007, 15.

(approximately \$3,400/turbine-year for Cannon AFB). Figure D - 1 shows the cost curve for the wind turbines.

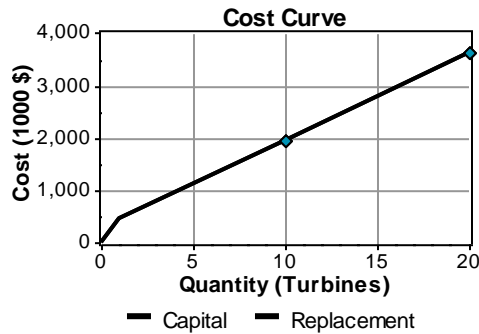


FIGURE D - 1: WIND TURBINE COST CURVE

PV ARRAY COST

Based on information provided by the Lawrence Berkeley National Laboratory, the following table was developed for PV array domestic installed costs for the year 2007.⁷⁵

TABLE D - 1: 2007 PV DOMESTIC INSTALLED COSTS

Rated Capacity (kW)	2007 Installed cost (\$/W)
7.5	\$8.00
20	\$7.80
65	\$7.60
175	\$7.40
375	\$7.00
625	\$6.60

Using the estimate that costs have historically decreased at a rate of approximately 30¢/W each year,⁷⁶ Table D – 2 was developed to estimate installed costs for the year 2010 (90¢/W lower for each cost). PV installations above 625 kW are assumed to also cost \$5.70/W. Note that these values are consistent with a PV array installation at Fort Carson, CO in 2007. Installed costs for

⁷⁵ Wisser, Ryan, Galen Barbose, and Carla Peterman. *Tracking the Sun: The Installed Cost of Photovoltaics in the U.S. from 1998-2007*. Rep. Lawrence Berkeley National Laboratory, February 2009. Figure 9, pg. 13.

⁷⁶ *Ibid*, 9.

that 2 MW array were approximately \$6.50/W.⁷⁷ When reduced by 90¢/W for the three year difference, the average cost would be \$5.60/W.

TABLE D - 2: 2010 PV DOMESTIC INSTALLED COSTS (ESTIMATE)

Rated Capacity (kW)	2010 Installed cost (\$/W)
7.5	\$7.10
20	\$6.90
65	\$6.70
175	\$6.50
375	\$6.10
625	\$5.70

Yearly maintenance costs were estimated at \$12/kW. This number is consistent with industry estimates.

STORAGE SYSTEM COST

LEAD-ACID BATTERIES

Although lead-acid batteries themselves are relatively inexpensive at about \$150/kWh,⁷⁸ a very conservative estimate of \$500/kWh was used for these simulations to encompass all installation costs, including connections, control infrastructure, and cooling. An additional \$130/kWh was added to cover the cost of inverters under the following assumptions:

- 50 kW of inverters needed for each string of batteries
- Approximately 37 ¢/W for inverter costs (above 200 kW)⁷⁹

The total domestic installed cost for lead-acid batteries was assumed to be \$630/kWh.

MOLTEN SALT STORAGE

Domestic installed cost for the molten salt storage system was estimated at \$1.2 million for a 4.3 MWh unit (\$280/kWh). Replacement cost was estimated at 80% of this value, or

⁷⁷ Ibid, 14.

⁷⁸ Ton, Dan T., Charles J. Hanley, Georgianne H. Peek, and John D. Boyes. Solar Energy Grid Integration Systems –Energy Storage (SEGIS-ES). Rep. Sandia National Laboratories, July 2008, 21.

⁷⁹ Based on PVP 260 kW inverter from www.affordable-solar.com for five battery strings.

\$960,000. Inverter costs for this storage system were assumed to be \$177,000 for a 500 kW inverter per molten salt storage unit (35 ¢/W).⁸⁰ Total capital cost was assumed to be \$1.377 million. Total maintenance cost was estimated at 2% of capital (\$24,000), or \$1,200/yr over a twenty year lifetime.

REMOTE INSTALLATION COSTS

In the absence of more accurate information, all installation and maintenance costs were increased by 20% for the Marjah simulations to account for installing components in a remote location. The costs subject to this increase were:

- Generator maintenance and “replacement” (overhaul) costs
- Wind turbine capital, replacement, and maintenance costs
- PV capital, replacement, and maintenance costs
- Molten salt storage maintenance costs

SHIPPING COSTS

GENERATOR SHIPPING

Since the MEP-12A generators are designed to fit in the cargo bay of a C-130 aircraft and are usually delivered in the first weeks of operations at a FOB, the assumption used here is that each generator will be shipped in a dedicated C-130 (each generator completely fills the cargo bay).⁸¹ Under the assumption that the C-130 must fly 7,500 miles at a cruise speed of 380 knots to reach the site at an aircraft operating cost of \$6,000/hr⁸², each generator costs \$103,000 to be shipped to the remote location. This cost is added to the capital cost for the Marjah simulations for a total of \$343,000 in capital cost per generator.

⁸⁰ Based on SMA 500 kW inverter from www.affordable-solar.com.

⁸¹ *AFH 10-222 Volume 5*, 14.

⁸² *FY2008 Reimbursable Rates: Fixed Wing*, <http://comptroller.defense.gov/rates/fy2008/2008_f.pdf>

WIND TURBINE SHIPPING

The primary components (nacelle, blades, hub, etc) of each Northwind 100 wind turbine ship in a 40-foot ISO container that weighs 26,400 lb.⁸³ The 30 m tower ships separately in three nested sections at a weight of 30,360 lbs.⁸⁴ The total shipping weight is 56,760 lbs or approximately 0.57 lb/W. This cost in terms of pounds per Watt is incorporated into the simulation using the shipping cost factors of \$1.00/lb, \$1.50/lb, and \$2.00/lb described in the body of the paper.

PV ARRAY SHIPPING

A survey of weights for PV modules and inverters from several manufacturers indicates a shipping weight of approximately 0.40 lb/W is reasonable for the arrays used for this simulation. This value was also incorporated into the simulation using the shipping cost factors described above.

STORAGE SHIPPING

Each lead-acid battery weighs approximately 113 lbs. The inverters needed to support these batteries weigh approximately 30 lbs/kW.⁸⁵ Based on the inverter size estimate of 50 kW per string of 80 batteries, the total weight of each string would be approximately 10,540 lbs. This value was multiplied by the shipping cost factors in \$/lb to calculate the shipping cost of each string of batteries.

The unit weight for the molten salt storage system was estimated at 40,000 lbs. A 500 kW inverter would be needed for this application, which adds an additional 6,725 lbs in weight⁸⁶ for

⁸³ *Northern Power*. Northwind 100 Wind Turbine Logistics & Installation Guidelines, §1.1, 12 June 2008. Web. 21 July 2010. <<http://www.dcpower-systems.com/documents/Northwind100-InstallationGuidelines.pdf>>.

⁸⁴ *Ibid*, §1.2.1.

⁸⁵ Based on PVP 100 kW inverters from www.affordable-solar.com.

⁸⁶ Based on SMA 500 kW inverter from www.affordable-solar.com.

a total of 46,725 lbs in shipping weight per molten salt unit. Again, this value was multiplied by the \$/lb shipping factors to calculate shipping cost per storage unit.

LEAVE-BEHIND ECONOMICS

HOMER does not natively handle the value of leave behind (VLBE) metric established in this paper; however, it does allow for a “capital cost multiplier” sensitivity parameter. This section discusses how the capital cost multiplier was used for each component to factor in the VLBE for the Marjah Leave-Behind Simulations only. This was accomplished by reducing the initial capital cost in HOMER by the total dollar amount of energy left behind, based on the VLBE. Equation D.1 calculates this value:

$$R_C = f_c \times h \times (VLBE/1000) \times D_1 \times D_2 \quad (D.1)$$

For this equation, f_c is the capacity factor in percent, h is the number of hours in a year (8,760), $VLBE$ is the value of leave behind energy in ϕ/kWh , D_1 is the discount factor associated with the leave behind term (e.g. discounting Year 5 – Year 20 annual revenue back to Year 4 for the four-year case), and D_2 is the discount factor associated with the US involved term (e.g. discounting Year 4 revenue back to Year 0 to compare with capital costs). The result, R_C , is equivalent capital cost reduction that the leave-behind strategy provides (in \$/W).

To complete the leave-behind model, the domestic installed costs were first input into the HOMER simulation. Then, the capital cost multiplier for each VLBE and shipping cost was calculated according to equation D.2.

$$CCM(VLBE, C_{shipping}) = \frac{1.2 \times C_{domestic} + C_{shipping} - R_C}{C_{domestic}} \quad (D.2)$$

For this equation, $C_{domestic}$ is the domestic installed cost in \$/W (the 20% remote install increase is added here), $C_{shipping}$ is the shipping cost for the component in \$/W, and R_C is the equivalent capital cost reduction in \$/W described by equation D.1. The result, CCM , is the capital cost

multiplier used for each combination of VLBE and shipping cost. For example, Tables D – 3 and D – 4 shows the capital cost multipliers (gray cells) for each VLBE and shipping cost for the four-year timeframe of US involvement for the PV array and wind turbines, respectively (D_1 and D_2 are 7.824 and 0.683 for this case).

TABLE D - 3: CAPITAL COST MULTIPLIERS FOR PV ARRAY (4 YEAR SCENARIO)

		Shipping Cost (per lb)		
		\$1.00	\$1.50	\$2.00
Value of Leave-Behind Energy (per kWh)	\$ -	1.27	1.31	1.34
	\$ 0.05	1.17	1.21	1.24
	\$ 0.10	1.07	1.11	1.14
	\$ 0.15	0.97	1.01	1.04
	\$ 0.20	0.87	0.91	0.94
	\$ 0.25	0.77	0.81	0.84
	\$ 0.30	0.67	0.71	0.74
	\$ 0.35	0.57	0.61	0.64
	\$ 0.40	0.47	0.51	0.54
	\$ 0.45	0.37	0.41	0.44
	\$ 0.50	0.27	0.31	0.34

TABLE D - 4: CAPITAL COST MULTIPLIERS FOR WIND TURBINES (4 YEAR SCENARIO)

		Shipping Cost (per lb)		
		\$1.00	\$1.50	\$2.00
Value of Leave-Behind Energy (per kWh)	\$ -	1.52	1.67	1.83
	\$ 0.05	1.38	1.53	1.69
	\$ 0.10	1.24	1.40	1.55
	\$ 0.15	1.10	1.26	1.41
	\$ 0.20	0.96	1.12	1.27
	\$ 0.25	0.82	0.98	1.14
	\$ 0.30	0.68	0.84	1.00
	\$ 0.35	0.54	0.70	0.86
	\$ 0.40	0.40	0.56	0.72
	\$ 0.45	0.26	0.42	0.58
	\$ 0.50	0.12	0.28	0.44

This analysis was used for the PV array and wind turbines. Also, to make this analysis accurate, the lifetime of both the PV array and wind turbines had to be set to the timeframe of US

involvement for each of the simulations. Otherwise, HOMER would automatically calculate a salvage value at the end of the project lifetime, assuming that the solar arrays and wind turbines would be scrapped. Since VLBE is difficult to quantify for energy storage systems, the salvage value at the end of the timeframe was left as the only benefit to the leave-behind term for both the molten salt storage system and the lead-acid batteries.

APPENDIX E – THERMAL STORAGE EXCURSION

For this paper, a hypothetical thermal (molten salt) storage system was also considered. Renewable system alternatives were considered with zero, one, and two molten salt systems, each with a capacity of 4.32 MWh. Each unit (including an appropriately-sized inverter) was estimated at \$1.38 million in capital cost (\$319/KWh). Additional information on the technical and economic values used for the thermal storage system can be found in Appendix C and Appendix D.

Under no simulation conditions did the molten salt system exceed the economic performance of the lead-acid battery systems, due to the large size, large capital cost, and relatively low roundtrip efficiency (30%) compared with the lead-acid batteries (85%), despite its longer lifetime (20 years versus 10 years). Therefore, molten salt storage was removed from the final simulations to reduce computation time. All results presented in the body of this paper are based on lead-acid battery storage. However, a brief table of results for alternatives including molten salt systems is shown in Tables E – 1 and E – 2 below. These results are for the four year timeframe, \$1.50/lb shipping cost case of the Marjah Actual Cost simulations with a FBCF of \$15/gal. Table E – 3 is shown for comparison with similar alternatives using 320 lead-acid batteries.

TABLE E - 1: SIMULATION RESULTS SUMMARY - ONE MOLTEN SALT UNIT

Molten Salt Units	PV Array Size (kW)	Wind Turbines	Net Present Cost (\$M)	Fuel Consumption (million gal)
1	0	0	95.6	1.91
1	0	10	96.1	1.85
1	0	20	96.2	1.80
1	1000	0	96.6	1.78
1	1000	10	97.2	1.73
1	1000	20	97.2	1.67
1	2000	0	97.2	1.66
1	2000	10	97.8	1.60
1	2000	20	97.8	1.54

TABLE E - 2: SIMULATION RESULTS SUMMARY - TWO MOLTEN SALT UNITS

Molten Salt Units	PV Array Size (kW)	Wind Turbines	Net Present Cost (\$M)	Fuel Consumption (million gal)
2	0	0	96.0	1.90
2	0	10	96.5	1.84
2	0	20	96.5	1.79
2	1000	0	97.0	1.77
2	1000	10	97.4	1.71
2	1000	20	97.4	1.66
2	2000	0	97.5	1.65
2	2000	10	98.0	1.59
2	2000	20	98.0	1.53

TABLE E - 3: SIMULATION RESULTS SUMMARY – 320 LEAD ACID BATTERIES

Lead-Acid Batteries	PV Array Size (kW)	Wind Turbines	Net Present Cost (\$M)	Fuel Consumption (million gal)
320	0	0	94.5	1.90
320	0	10	95.0	1.84
320	0	20	95.1	1.79
320	1000	0	95.6	1.77
320	1000	10	96.1	1.72
320	1000	20	96.1	1.66
320	2000	0	96.1	1.65
320	2000	10	96.6	1.59
320	2000	20	96.7	1.53

Note that the 320 lead-acid batteries provide fuel savings comparable with those provided by two thermal storage units; however, net present cost is lower. Increasing the amount of lead-acid batteries to 640 yields additional fuel savings at even lower net present costs (the additional capital cost is offset by the fuel savings).

It is important to remember that even though the lead-acid batteries economically outperformed the molten salt storage system for the situation and set of assumptions described in this paper, this is not a general result. There may be other cases (for larger bases, the domestic power grid, etc) where thermal storage systems are the better option.